

Detection of Block-Exchangeable Structure in Large-Scale Correlation Matrices

Samuel Perreault * Thierry Duchesne

Département de mathématiques et de statistique, Université Laval

Johanna G. Nešlehová

Department of Mathematics and Statistics, McGill University

May 5, 2022

Correspondence:

Samuel Perreault [samuel.perreault.3@ulaval.ca]
Département de mathématiques et de statistique
1045, avenue de la Médecine
Université Laval
Québec, QC, G1V 0A6
CANADA

*This work has been funded by individual operating grants from the Natural sciences and engineering research council of Canada to TD (RGPIN-2016-05883) and JN (RGPIN-2015-06801), team grants from the Fonds de recherche du Québec – Nature et technologies to TD and JN (2015-PR-183236) and from the Canadian Statistical Sciences Institutes to JGN and a graduate scholarship from the Fonds de recherche du Québec – Nature et technologie to SP.

Abstract

Correlation matrices are omnipresent in multivariate data analysis. When the number d of variables is large, the sample estimates of correlation matrices are typically noisy and conceal underlying dependence patterns. We consider the case when the variables can be grouped into K clusters with exchangeable dependence; an assumption often made in applications in finance and econometrics. Under this partial exchangeability condition, the corresponding correlation matrix has a block structure and the number of unknown parameters is reduced from $d(d-1)/2$ to at most $K(K+1)/2$. We propose a robust algorithm based on Kendall's rank correlation to identify the clusters without assuming the knowledge of K a priori or anything about the margins except continuity. The corresponding block-structured estimator performs considerably better than the sample Kendall rank correlation matrix when $K < d$. Even in the unstructured case $K = d$, though there is no gain asymptotically, the new estimator can be much more efficient in finite samples. When the data are elliptical, the results extend to linear correlation matrices and their inverses. The procedure is illustrated on financial stock returns.

Keywords: Agglomerative clustering; Constrained maximum likelihood; Copula; Kendall's tau; Parameter clustering; Shrinkage

1 INTRODUCTION

Relationships between the components of a random vector $\mathbf{X} = (X_1, \dots, X_d)$, say, are of prime interest in many fields where statistical methods are used. Traditionally, this dependence is summarized through a correlation matrix. When \mathbf{X} is multivariate Normal, the classical choice is the linear correlation matrix, which is omnipresent in inference. When multivariate Normality fails, however, as it frequently does in applications in econometrics, finance, insurance, and risk management, linear correlation can be grossly misleading and may not even exist (Embrechts et al., 2002). For this reason, it is safer to use a rank correlation matrix, such as the matrix of pair-wise Kendall’s taus or Spearman’s rhos.

In high dimensions, empirical correlation matrices typically conceal underlying dependence patterns. This is due to their sheer size, but also to the inherent imprecision of the estimates, especially when the sample size is small compared to dimension d . As an example, which we detail in Section 7, consider the log-returns of 106 stocks included in the NASDAQ100 index from the beginning of 2017 up to 2017/09/16, giving 177 observations. The empirical Kendall rank correlation matrix based on residuals from a fitted stochastic volatility model is displayed in the left panel of Figure 1. The darker the color, the larger the correlation. Hardly any dependence pattern is visible from this matrix.

Noisiness of sample correlation matrices is well documented. Several strategies have been proposed to remedy for it, most notably shrinkage (Ledoit and Wolf, 2003a,b, 2004; Schäfer and Strimmer, 2005). Alternative procedures developed in the context of graphical models consist of decomposing a noisy inverse covariance matrix into a low-rank matrix and a sparse matrix (Chandrasekaran et al., 2010; Ma et al., 2013; Agarwal et al., 2012).

We follow a different path in this article. Motivated by the above NASDAQ example and many others, we focus on applications in which it makes sense to assume that the

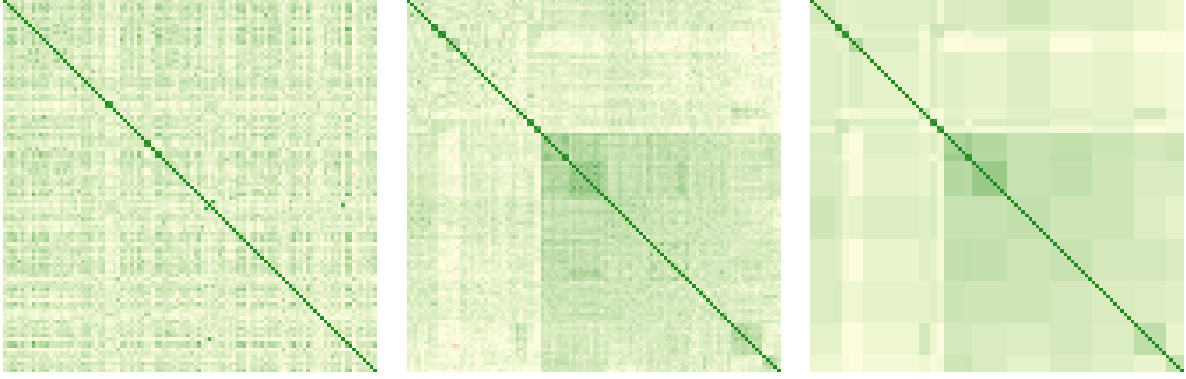


Figure 1: The matrix of pair-wise empirical Kendall's tau corresponding to the original labeling of the $d = 106$ stocks included in the NASDAQ100 index (left panel) and after relabeling (middle panel). The right panel shows the improved estimate obtained by applying Algorithm 1 to the stocks data and selecting a cluster structure with $\alpha = .95$.

correlation matrix has a block structure. This arises when the variables can be grouped into K disjoint clusters in such a way that for any two clusters A and B , and any $X_i \in A$ and $X_j \in B$, the correlation between X_i and X_j satisfies $\rho(X_i, X_j) = \rho_{AB}$. In other words, all variables within each cluster are equicorrelated and the between-cluster correlation depends only on the clusters but not the representatives. Assuming a block structure is a way to reduce dimensionality, for the number of unknown pairwise correlations decreases from $d(d-1)/2$ to at most $K(K+1)/2$. Prime examples are portfolio and credit risk modelling or more generally econometrics and finance, where variables can be grouped, e.g., by industry classifications or risk types; a model that makes explicit use of correlation matrices with a block structure is the block DECO model (Engle and Kelly, 2012). Correlation matrices with a block structure also arise in the modelling of categorical, clustered, or gene expression data, and in genomics studies. In the NASDAQ100 example, a block structure does indeed emerge upon relabeling of the variables, as shown in the middle panel of Figure 1. The

picture is still very noisy, however.

This article describes a technique for learning the cluster structure from data and shows how to use the latter to devise a more efficient estimator of the correlation matrix. No prior knowledge of the clusters, their number or composition is assumed. We only require that the underlying cluster structure satisfies a partial exchangeability condition, i.e., that the dependence within each cluster is exchangeable. To identify the clusters from the sample correlation matrix, we then devise an iterative algorithm that is similar to, but different from, agglomerative clustering. The knowledge of K is not assumed a priori. Though at first one might find this problem similar to the one tackled by model-based clustering, they are different. The latter attempts to cluster together observations that come from the same subpopulations of a multivariate mixture distribution, while the current proposal aims at identifying the elements of a correlation matrix that are equal. The partial exchangeability assumption imposes a particular set of constraints on the rows and columns of the correlation matrix, thus the need for a novel approach. The algorithm also outputs an improved estimate of the correlation matrix which has a block structure, and an estimate of its asymptotic covariance matrix. In the above example of stock returns, the relabeling in the middle panel was done using the clusters identified through the proposed algorithm; the improved estimate of the correlation matrix is displayed in the right panel. As we prove asymptotically and illustrate via simulations, the improvement of the estimator can be substantial, in particular for $K \ll d$. Even in the unstructured case when $K = d$ and there is no gain asymptotically, the new estimator can perform substantially better in finite samples due to a bias-variance tradeoff, particularly when n is small compared to d .

All procedures developed in this paper are based on the matrix \mathbf{T} of pair-wise Kendall rank correlations, which turned out to be slightly more convenient than Spearman's rank correlation matrix, for reasons stated in Section 2. A clear advantage of this approach

over the linear correlation matrix is that Kendall’s tau is margin-free, well-defined and well-behaved irrespective of the distribution of \mathbf{X} . This makes our methodology entirely nonparameteric and margin-free. No Normality assumption is required; the only assumption made throughout the paper is that the marginal distributions of X_1, \dots, X_d are continuous. As we explain in Section 2, the partial exchangeability assumption only concerns the dependence in \mathbf{X} and not its univariate marginals. In particular, it is not assumed that the variables in the same cluster are equally distributed. When \mathbf{X} is multivariate Normal, Student t , generalized hyperbolic or more generally elliptical, there is a one-to-one relationship between \mathbf{T} and the linear correlation matrix, provided the latter exists (Lindskog et al., 2002; Hult and Lindskog, 2002). This means that the linear correlation matrix or its inverse, often termed the precision matrix, may be obtained from an estimator of \mathbf{T} ; this idea has been exploited, e.g., in nonparanormal graphical models (Liu et al., 2012; Xue and Zou, 2012) and copula regression (Cai and Zhang, 2017; Zhao and Genest, 2017). The improved estimator of \mathbf{T} developed in this paper may thus be used to obtain more efficient estimators of the linear correlation matrix as well as the precision matrix.

Beyond the estimation of correlation itself, our procedure can be used as a first step in more complex dependence model constructions. When d is large, a model for the distribution of \mathbf{X} needs to be both flexible and parsimonious. Within the Normal or more generally elliptical model, this means that the number of free parameters in the correlation matrix needs to be reduced, and the block structure identified through our algorithm can serve precisely this purpose. Outside the Normal model, dependence in \mathbf{X} can be conveniently described through copulas. Due to the result of Sklar (1959), the joint distribution of \mathbf{X} can be rewritten, for all $x_1, \dots, x_d \in \mathbb{R}$, as

$$\mathbb{P}[X_1 \leq x_1, \dots, X_d \leq x_d] = C(F_1(x_1), \dots, F_d(x_d)), \quad (1)$$

where F_1, \dots, F_d are the univariate marginal distributions of \mathbf{X} and C is a copula, i.e., a

joint distribution function with standard uniform marginals. By combining an arbitrary copula with arbitrary univariate marginals, Sklar’s result can be used to construct a wide variety of distributions (Genest and Nešlehová, 2012; Joe, 2015). To achieve flexibility and parsimony when d is large, dimensionality reduction needs to take place through a clever construction of C ; examples are vines (Kurowicka and Joe, 2011), factor models (Krupskii and Joe, 2013; Hua and Joe, 2017), or hierarchical constructions (Mai and Scherer, 2012; Brechmann, 2014). The cluster algorithm proposed in this paper is particularly well suited for such approaches: Equicorrelated clusters can first be identified through it and modeled by exchangeable lower-dimensional copulas. Dependence between clusters can then be achieved subsequently through vines or factors.

The article is organized as follows. Section 2 specifies the partial exchangeability assumption and discusses its implications. In Section 3, we construct an improved estimator of \mathbf{T} when the cluster structure is known a priori, derive its asymptotic distribution, and show that it is superior to the empirical Kendall rank correlation matrix when $K < d$ in terms of asymptotic variance. The way this estimator is constructed is then used in Section 4 to derive an algorithm through which K and the cluster structure can be learned from data. The algorithm also returns an improved estimate of \mathbf{T} and an estimate of its finite-sample covariance matrix. In Section 5 we discuss the special case when \mathbf{X} is Normal or elliptical, and explain how the clustering algorithm and the improved estimate of \mathbf{T} can be used to estimate the linear correlation matrix. The performance of the algorithm and of the improved estimate of \mathbf{T} is studied through simulations in Section 6 and illustrated on NASDAQ100 stock returns in Section 7. Section 8 concludes the paper. Technical results and proofs are relegated to Appendices A and B. Additional simulation results and details about the clusters obtained for the application on stock returns are given in Appendices C and D, respectively. All appendices are available in the Online Supplement, as well as the

R-code to implement the clustering algorithm.

2 PARTIAL EXCHANGEABILITY ASSUMPTION

Throughout, let $\mathbf{X} = (X_1, \dots, X_d)$ be a random vector with continuous univariate marginals, denoted F_1, \dots, F_d . In this case, the copula C in Sklar's decomposition (1) is unique; in fact, it is the joint distribution of the vector $(F_1(X_1), \dots, F_d(X_d))$. The following partial exchangeability assumption plays a central role in this paper.

Partial Exchangeability Assumption (PEA). *For $j = 1, \dots, d$, let $U_j = F_j(X_j)$. A partition $\mathcal{G} := \{\mathcal{G}_1, \dots, \mathcal{G}_K\}$ of $\{1, \dots, d\}$ satisfies the Partial Exchangeability Assumption (PEA) if for any $u_1, \dots, u_d \in [0, 1]$ and any permutation π of $1, \dots, d$ such that for all $j \in \{1, \dots, d\}$ and all $k \in \{1, \dots, K\}$, $j \in \mathcal{G}_k$ if and only if $\pi(j) \in \mathcal{G}_k$, one has*

$$C(u_1, \dots, u_d) = C(u_{\pi(1)}, \dots, u_{\pi(d)})$$

or equivalently, $(U_1, \dots, U_d) \stackrel{\mathcal{L}}{=} (U_{\pi(1)}, \dots, U_{\pi(d)})$, where $\stackrel{\mathcal{L}}{=}$ denotes equality in distribution.

To understand the PEA, note first that the partition $\mathcal{G} = \{\{1, \dots, d\}\}$ with $K = 1$ satisfies the PEA only if C is fully exchangeable, meaning that for all $u_1, \dots, u_d \in [0, 1]$ and any permutation π of $1, \dots, d$, $C(u_1, \dots, u_d) = C(u_{\pi(1)}, \dots, u_{\pi(d)})$; examples of fully exchangeable copulas are Gaussian or Student t with an equicorrelation matrix, and all Archimedean copulas. When $K > 1$, the PEA is a weaker version of full exchangeability. A partition \mathcal{G} for which PEA holds divides X_1, \dots, X_d into clusters such that the copula C is invariant under within-cluster permutations. In particular, for any $k \in \{1, \dots, K\}$, the copula of $(X_j, j \in \mathcal{G}_k)$ is fully exchangeable. In contrast to many standard clustering contexts, the PEA does not imply that variables in the same cluster are equally distributed,

because it only concerns the copula C of \mathbf{X} and not the marginals F_1, \dots, F_d . Also note that the partition for which the PEA holds may not be unique; we discuss this point in greater detail in Section 4. Yet, the coarsest partition \mathcal{G} that satisfies the PEA is unique, viz.

$$\mathcal{G} = \arg \min_{\mathcal{G}^* \text{ satisfies the PEA}} (|\mathcal{G}^*|). \quad (2)$$

We should also emphasize that the PEA is not restrictive in any way. In the completely unstructured case, \mathcal{G} in (2) is $\{\{1\}, \dots, \{d\}\}$. However, as we demonstrate in Section 6, there may still be a substantial advantage in considering a coarser partition for inference purposes in finite samples. When the partition \mathcal{G} in (2) is such that $|\mathcal{G}| = K < d$, a dimension reduction from d to K takes place. Several commonly used models make an implicit or explicit use of this kind of dimension reduction; examples include latent variable models (e.g., frailty or random effects models), Markov random fields or graphical models, hierarchical copula models (Brechmann, 2014; Mai and Scherer, 2012), factor copulas (Gregory and Laurent, 2004; Krupskii and Joe, 2015), or nested Archimedean models (Joe, 2015).

Definition 1. *For a partition \mathcal{G} that satisfies the PEA, we write $X_i \sim X_j$ whenever $i, j \in \mathcal{G}_k$ for some $k \in \{1, \dots, K\}$. Furthermore, the cluster membership matrix Δ is a $d \times d$ matrix whose (i, j) th element is given, for all $i, j \in \{1, \dots, d\}$, by $\Delta_{ij} = \mathbb{1}(X_i \sim X_j)$.*

Next, let \mathbf{T} be the $d \times d$ matrix of pairwise Kendall correlation coefficients. Specifically, for all $i, j \in \{1, \dots, d\}$, the (i, j) th element of \mathbf{T} is $\mathbf{T}_{ij} = \tau(X_i, X_j)$, where

$$\tau(X_i, X_j) = \Pr((X_i - X_i^*)(X_j - X_j^*) > 0) - \Pr((X_i - X_i^*)(X_j - X_j^*) < 0)$$

is the population version of Kendall's tau between X_i and X_j , i.e. the difference between the probabilities of concordance and discordance of (X_i, X_j) and its independent copy (X_i^*, X_j^*) . Because $\tau(X_i, X_j)$ depends only on the copula C_{ij} of (X_i, X_j) , viz.

$$\tau(X_i, X_j) = -1 + 4 \int C_{ij}(u_i, u_j) \, dC_{ij}(u_i, u_j), \quad (3)$$

see, e.g., Nelsen (2006), it is not surprising that under the PEA, several entries in \mathbf{T} are identical. This is specified in the next result, which follows directly from the PEA and (3).

Proposition 1. *Suppose that the partition \mathcal{G} of $\{1, \dots, d\}$ satisfies the PEA and that $X_{i_1} \sim X_{i_2}$ and $X_{j_1} \sim X_{j_2}$ where $i_1 \neq j_1$ and $i_2 \neq j_2$. Then the copulas $C_{i_1 j_1}$ and $C_{i_2 j_2}$ are identical and, consequently, $\mathbf{T}_{i_1 j_1} = \mathbf{T}_{i_2 j_2}$.*

Remark 1. *It follows from Proposition 1 that whenever $X_{i_1} \sim X_{i_2}$ and $X_{j_1} \sim X_{j_2}$ where $i_1 \neq j_1$ and $i_2 \neq j_2$, any copula-based measure of association κ will satisfy $\kappa(X_{i_1}, X_{j_1}) = \kappa(X_{i_2}, X_{j_2})$; examples of such measures include Spearman's rho or Gini's gamma (Nelsen, 2006). The reason why we focus on Kendall's tau in this paper is that the asymptotic and finite-sample variance of the empirical Kendall's tau matrix have a tractable form, for example much more so than that of Spearman's rho (Borkowf, 2002). Having said that, the procedures proposed here could in principle be extended to other measures of association.*

Suppose now that a partition \mathcal{G} with $|\mathcal{G}| > 1$ satisfies the PEA. Proposition 1 then implies that when $X_i \sim X_j$ for some $i \neq j$, the i th and j th rows and columns in \mathbf{T} are identical, once the diagonal entries are aligned. Consequently, if the variables are relabeled so that the clusters are contiguous, then the cluster membership matrix $\mathbf{\Delta}$ is block-diagonal and \mathbf{T} becomes a block matrix. As an example, consider the following simple scenario, which is used throughout the paper to illustrate the main concepts.

Example 1. *Consider a random vector \mathbf{X}^* of dimension $d = 10$ such that the partition $\mathcal{G}^* = \{\mathcal{G}_1^*, \mathcal{G}_2^*, \mathcal{G}_3^*\}$ of size $K = 3$ given by $\mathcal{G}_1^* = \{1, 3, 6, 9\}$, $\mathcal{G}_2^* = \{5, 7, 8\}$ and $\mathcal{G}_3^* = \{2, 4, 10\}$ satisfies the PEA. The corresponding cluster membership matrix $\mathbf{\Delta}^*$ and the matrix \mathbf{T}^* of pairwise Kendall correlations are shown in Figure 2 (the exact distribution of \mathbf{X}^* does not matter at this point). In this case, the clusters are not contiguous, i.e., $\mathbf{\Delta}^*$ is not block diagonal, and the block structure of \mathbf{T}^* is not easily seen. Once the variables are relabeled as*

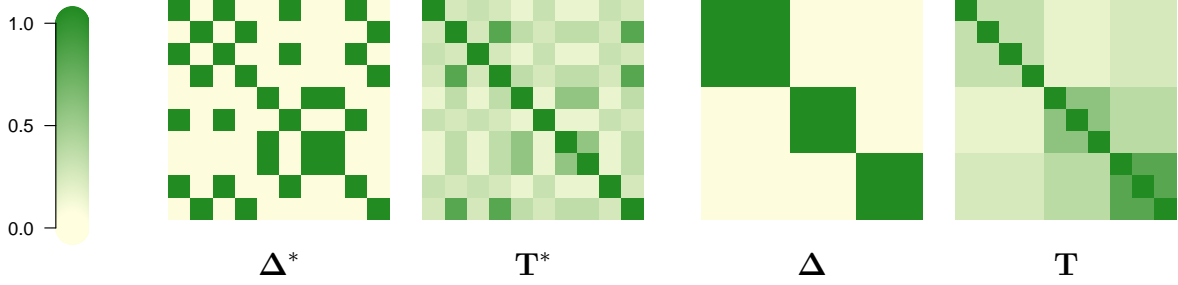


Figure 2: The Kendall correlation and cluster membership matrices corresponding to the vector \mathbf{X}^* in Example 1 before (\mathbf{T}^* and Δ^*) and after (\mathbf{T} and Δ) relabeling of the variables.

$\mathbf{X} = (X_1, \dots, X_{10}) = (X_1^*, X_3^*, X_6^*, X_9^*, X_5^*, X_7^*, X_8^*, X_2^*, X_4^*, X_{10}^*)$, the partition that satisfies the PEA becomes $\mathcal{G} := \{\mathcal{G}_1, \mathcal{G}_2, \mathcal{G}_3\}$, where

$$\mathcal{G}_1 := \{1, 2, 3, 4\}, \quad \mathcal{G}_2 := \{5, 6, 7\}, \quad \mathcal{G}_3 := \{8, 9, 10\}. \quad (4)$$

The clusters are now contiguous, Δ is block-diagonal and \mathbf{T} has an apparent block structure, viz. Figure 2. Every time we revisit this example, we work with the relabeled vector \mathbf{X} .

Although we use examples in which the matrix Δ is block-diagonal for illustrative purposes, contiguity of the clusters is not required. In fact, given that \mathcal{G} is unknown, the variables are unlikely to be labeled so that \mathbf{T} has an apparent block structure. To describe the latter, we first need additional notation. To this end, let \mathbf{R} be an arbitrary symmetric $d \times d$ matrix. The entries above the main diagonal can be stacked in a vector, say $\boldsymbol{\rho}$, of length $p = d(d-1)/2$. Note that the diagonal elements of \mathbf{R} play no role at this point. The particular way the vectorization is done is irrelevant, as long as it is the same throughout. For example, one may use the lexicographical ordering viz.

$$\boldsymbol{\rho} = (\mathbf{R}_{12}, \dots, \mathbf{R}_{1d}, \mathbf{R}_{23}, \dots, \mathbf{R}_{2d}, \dots, \mathbf{R}_{(d-1)d})^\top. \quad (5)$$

For arbitrary $r \in \{1, \dots, p\}$, (i_r, j_r) refers to the pair of indices $i_r < j_r$ such that $\boldsymbol{\rho}_r = \mathbf{R}_{i_r j_r}$. Now any partition $\mathcal{G} = \{\mathcal{G}_1, \dots, \mathcal{G}_K\}$ of $\{1, \dots, d\}$ induces a partition of the elements of $\boldsymbol{\rho}$, or, equivalently, of $\{1, \dots, p\}$. For any $k_1 \leq k_2 \in \{1, \dots, K\}$, let

$$\mathcal{B}_{k_1 k_2} = \{r \in \{1, \dots, p\} : (i_r, j_r) \in (\mathcal{G}_{k_1} \times \mathcal{G}_{k_2}) \cup (\mathcal{G}_{k_2} \times \mathcal{G}_{k_1})\}. \quad (6)$$

Note that the total number of nonempty blocks $\mathcal{B}_{k_1 k_2}$ is

$$L = K(K-1)/2 + \sum_{i=1}^K \mathbb{1}(|\mathcal{G}_i| > 1) \quad (7)$$

because when $k_1 = k_2$, $\mathcal{B}_{k_1 k_2}$ is nonempty only if $|\mathcal{G}_{k_1}| > 1$. Referring to the sets $\mathcal{B}_{k_1 k_2}$ using a single index, the partition of $\{1, \dots, p\}$ is then given by

$$\mathcal{B}_{\mathcal{G}} := \{\mathcal{B}_{\ell} : 1 \leq \ell \leq L\}. \quad (8)$$

In analogy to the cluster membership matrix $\boldsymbol{\Delta}$, we define a $p \times L$ block membership matrix \mathbf{B} ; for all $r \in \{1, \dots, p\}$ and $\ell \in \{1, \dots, L\}$, its (r, ℓ) th element is given by

$$\mathbf{B}_{r\ell} = \mathbb{1}(r \in \mathcal{B}_{\ell}). \quad (9)$$

Finally, define the set $\mathcal{T}_{\mathcal{G}}$ of all symmetric matrices with a block structure given by $\mathcal{B}_{\mathcal{G}}$, viz.

$$\mathcal{T}_{\mathcal{G}} := \{\mathbf{R} \in \mathbb{R}^{d \times d} : \mathbf{R} \text{ symmetric and } \forall \ell \in \{1, \dots, L\} \ r, s \in \mathcal{B}_{\ell} \Rightarrow \mathbf{R}_{i_r j_r} = \mathbf{R}_{i_s j_s}\}. \quad (10)$$

Note that only the elements of \mathbf{R} that are above the main diagonal enter the definition of $\mathcal{T}_{\mathcal{G}}$ in (10), so that the diagonal elements of \mathbf{R} play no role.

Now suppose that \mathcal{G} is a partition of $\{1, \dots, d\}$ such that the PEA holds and that the elements above the main diagonal of \mathbf{T} are stacked in $\boldsymbol{\tau}$. By Proposition 1, for any $\ell \in \{1, \dots, L\}$ and $r, s \in \mathcal{B}_{\ell}$, $\boldsymbol{\tau}_r = \boldsymbol{\tau}_s$, or, equivalently, $\mathbf{T}_{i_r j_r} = \mathbf{T}_{i_s j_s}$. This means that

$\mathbf{T} \in \mathcal{T}_{\mathcal{G}}$; when no confusion can arise, we will also write $\boldsymbol{\tau} \in \mathcal{T}_{\mathcal{G}}$. Consequently, there are only L distinct elements in $\boldsymbol{\tau}$. Storing these in a vector $\boldsymbol{\tau}^* \in [-1, 1]^L$, we thus have

$$\boldsymbol{\tau} = \mathbf{B}\boldsymbol{\tau}^*. \quad (11)$$

This means that when PEA holds, the number of free parameters in \mathbf{T} is reduced from $d(d-1)/2$ to L given in (7). We revisit Example 1 to illustrate.

Example 2. Consider the matrix \mathbf{T} corresponding to \mathbf{X} in Example 1, and stack it in a vector $\boldsymbol{\tau}$ of length $p = 45$ constructed as in (5). Given that there are $K = 3$ clusters given in (4), $L = 6$. Consequently, $\boldsymbol{\tau}^*$ is of length 6, i.e., the cluster structure \mathcal{G} reduces the number of free parameters in \mathbf{T} from 45 to 6. The 6 distinct blocks can be seen in Figure 2 or more clearly in the left panel of Figure 10 in the Online Supplement.

3 IMPROVED ESTIMATION OF \mathbf{T}

Suppose that $\mathbf{X}_i = (X_{i1}, \dots, X_{id})^\top$, $i = 1, \dots, n$, is a random sample from \mathbf{X} . The classical nonparametric estimator of \mathbf{T} is $\hat{\mathbf{T}}$; for $i, j \in \{1, \dots, d\}$, its (i, j) th element is given by

$$\hat{\mathbf{T}}_{ij} := -1 + \frac{4}{n(n-1)} \sum_{r \neq s} \mathbb{1}(X_{ri} \leq X_{si}) \mathbb{1}(X_{rj} \leq X_{sj}). \quad (12)$$

As we explained in Section 2, if the PEA holds for some partition \mathcal{G} with $|\mathcal{G}| < d$, \mathbf{T} has a block structure and the number of free parameters reduces from $d(d-1)/2$ to L . In this section, we show that an a priori knowledge of \mathcal{G} leads to a more efficient estimator of \mathbf{T} .

Recall first that for all $i \neq j \in \{1, \dots, d\}$, $\hat{\mathbf{T}}_{ij}$ is a U -statistic and thus unbiased and asymptotically Normal (Hoeffding, 1947, 1948). The behavior of $\hat{\mathbf{T}}$ was studied by El Maache and Lepage (2003) and Genest et al. (2011); results pertaining to the closely related coefficient of agreement appear in Ehrenberg (1952). If $\boldsymbol{\tau}$ and $\hat{\boldsymbol{\tau}}$ denote the vectorized

versions of \mathbf{T} and $\hat{\mathbf{T}}$ respectively, one has, as $n \rightarrow \infty$,

$$\sqrt{n}(\hat{\boldsymbol{\tau}} - \boldsymbol{\tau}) \rightsquigarrow \mathcal{N}(\mathbf{0}_p, \boldsymbol{\Sigma}_\infty), \quad (13)$$

where \rightsquigarrow denotes convergence in distribution and $\mathbf{0}_p$ is the p -dimensional vector of zeros. Genest et al. (2011) provide expressions for the asymptotic variance $\boldsymbol{\Sigma}_\infty$ as well as the finite sample variance $\boldsymbol{\Sigma}$ of $\hat{\boldsymbol{\tau}}$; the latter is also given in Part A of the Online Supplement.

The asymptotic Normality of $\hat{\boldsymbol{\tau}}$ specified in (13) suggests using the following loss function $\ell : [-1, 1]^d \rightarrow [0, \infty)$ as a basis for inference:

$$\ell(\mathbf{t}|\hat{\boldsymbol{\tau}}, \boldsymbol{\Sigma}) := (\hat{\boldsymbol{\tau}} - \mathbf{t})^\top \boldsymbol{\Sigma}^{-1}(\hat{\boldsymbol{\tau}} - \mathbf{t}). \quad (14)$$

This loss function is a (Mahalanobis) distance between \mathbf{t} and $\hat{\boldsymbol{\tau}}$, accounting for the heterogeneous variability of the entries of $\hat{\boldsymbol{\tau}}$. The fact that the finite sample variance $\boldsymbol{\Sigma}$ is unknown is irrelevant for now; it will only become a concern in Section 4.

Considering an arbitrary $\mathbf{t} \in [-1, 1]^d$, it is obvious that ℓ attains its minimum at $\hat{\boldsymbol{\tau}}$ since $\ell(\mathbf{t}|\hat{\boldsymbol{\tau}}, \boldsymbol{\Sigma}) \geq 0 = \ell(\hat{\boldsymbol{\tau}}|\hat{\boldsymbol{\tau}}, \boldsymbol{\Sigma})$. Now suppose that \mathcal{G} is a partition of $\{1, \dots, d\}$ such that the PEA holds. Unless $|\mathcal{G}| = d$, it is extremely unlikely that $\hat{\mathbf{T}}$ has the block structure implied by \mathcal{G} , i.e., $\hat{\mathbf{T}} \in \mathcal{T}_{\mathcal{G}}$. By transforming the loss function ℓ in (14) using (11), we can now introduce the structural constraints implied by \mathcal{G} into the estimation procedure.

Theorem 1. *Suppose that \mathcal{G} is a partition of $\{1, \dots, d\}$ such that the PEA holds. Then for $\ell(\mathbf{t}|\hat{\boldsymbol{\tau}}, \boldsymbol{\Sigma})$ as in (14) and the block membership matrix \mathbf{B} defined in (9),*

$$\tilde{\boldsymbol{\tau}}(\hat{\boldsymbol{\tau}}|\mathcal{G}) := \arg \min_{\mathbf{t} \in \mathcal{T}_{\mathcal{G}}} \ell(\mathbf{t}|\hat{\boldsymbol{\tau}}, \boldsymbol{\Sigma}) = \boldsymbol{\Gamma} \hat{\boldsymbol{\tau}}, \quad (15)$$

where $\boldsymbol{\Gamma} := \mathbf{B}\mathbf{B}^+$ and $^+$ denotes the Moore–Penrose generalized inverse. Furthermore, for any $\ell \in \{1, \dots, L\}$ and $r \in \mathcal{B}_\ell$,

$$\tilde{\boldsymbol{\tau}}(\hat{\boldsymbol{\tau}}|\mathcal{G})_r = \frac{1}{|\mathcal{B}_\ell|} \sum_{s \in \mathcal{B}_\ell} \hat{\boldsymbol{\tau}}_s.$$

Proof. Observe that any $\mathbf{t} \in \mathcal{T}_{\mathcal{G}}$ can be expressed as $\mathbf{B}\mathbf{t}^*$ for some $\mathbf{t}^* \in [-1, 1]^L$. Solving $\frac{\partial}{\partial \mathbf{t}^*} \ell(\mathbf{B}\mathbf{t}^* | \hat{\boldsymbol{\tau}}, \boldsymbol{\Sigma}) = \mathbf{0}$ for \mathbf{t}^* gives as the unique solution

$$\tilde{\boldsymbol{\tau}}^* = [\mathbf{B}^\top \boldsymbol{\Sigma}^{-1} \mathbf{B}]^{-1} \mathbf{B}^\top \boldsymbol{\Sigma}^{-1} \hat{\boldsymbol{\tau}}.$$

From Proposition 6 and Lemma 4 in the Online Supplement, we have that $\mathbf{B}^\top \boldsymbol{\Sigma}^{-1} = \mathbf{B}^\top \boldsymbol{\Sigma}^{-1} \mathbf{B} \mathbf{B}^+$. Consequently, $\tilde{\boldsymbol{\tau}}^* = \mathbf{B}^+ \hat{\boldsymbol{\tau}}$ and $\tilde{\boldsymbol{\tau}} = \boldsymbol{\Gamma} \hat{\boldsymbol{\tau}}$ given that $\tilde{\boldsymbol{\tau}} = \mathbf{B} \tilde{\boldsymbol{\tau}}^*$. The expression for $\tilde{\boldsymbol{\tau}}(\hat{\boldsymbol{\tau}} | \mathcal{G})_r$ follows immediately from (33) in the proof of Lemma 4. \square

Remark 2. *The block-wise averages that appear in $\tilde{\boldsymbol{\tau}}$ are akin to the pair-wise linear correlation averaging of Elton and Gruber (1973) and Ledoit and Wolf (2003a), and particularly the block DECO of Engle and Kelly (2012) which uses block-wise averages of linear correlations. Although $\tilde{\boldsymbol{\tau}}$ seems very natural, the PEA plays a crucial role in the proof of Theorem 1. It is needed to invoke Proposition 6 and Lemma 4 and get a $\boldsymbol{\Sigma}$ matrix with a structure that will lead to the required simplifications. In particular, it is not enough to assume that $\boldsymbol{\tau} \in \mathcal{T}_{\mathcal{G}}$ for some partition \mathcal{G} .*

When it introduces no confusion, we refer to $\tilde{\boldsymbol{\tau}}(\hat{\boldsymbol{\tau}} | \mathcal{G})$ as $\tilde{\boldsymbol{\tau}}$ and to its matrix version $\tilde{\mathbf{T}}(\hat{\mathbf{T}} | \mathcal{G})$ thereof as $\tilde{\mathbf{T}}$. What is crucial in Theorem 1 is that $\tilde{\boldsymbol{\tau}}$ consists of the cluster averages of the elements of $\hat{\boldsymbol{\tau}}$ and as such does not involve the unknown finite sample variance $\boldsymbol{\Sigma}$ of $\hat{\boldsymbol{\tau}}$, so an estimator of $\boldsymbol{\Sigma}$ is not needed to compute $\tilde{\boldsymbol{\tau}}$. The information contained in \mathcal{G} is introduced by projecting $\hat{\mathbf{T}}$ onto $\mathcal{T}_{\mathcal{G}}$. The resulting estimator $\tilde{\mathbf{T}}$ is expected to be closer to the original matrix \mathbf{T} because the entries that estimate a same value are averaged over, thus reducing the estimation variance. In fact, for any $r \in \{1, \dots, p\}$, the asymptotic variance of $\tilde{\boldsymbol{\tau}}_r$ is less than or equal to that of $\hat{\boldsymbol{\tau}}_r$ as a result of the following theorem.

Theorem 2. *Let \mathcal{G} be a partition of $\{1, \dots, d\}$ such that the PEA holds. For \mathbf{B} given by (9), let $\boldsymbol{\Gamma} = \mathbf{B} \mathbf{B}^+$ and $\tilde{\boldsymbol{\tau}} = \boldsymbol{\Gamma} \hat{\boldsymbol{\tau}}$ be as in Theorem 1. Then the following statements hold:*

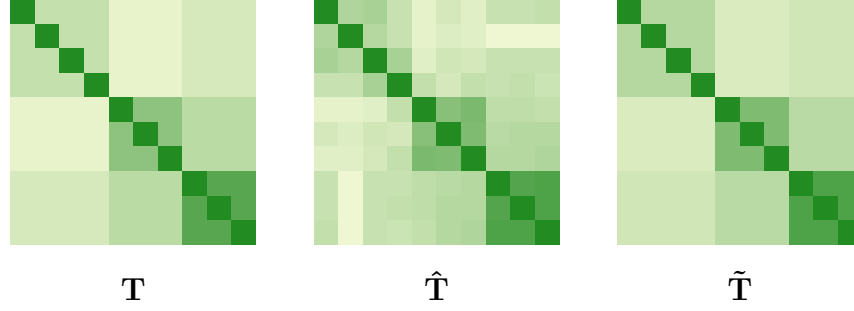


Figure 3: The matrices \mathbf{T} , $\hat{\mathbf{T}}$ and $\tilde{\mathbf{T}}$ in Example 3.

(i) As $n \rightarrow \infty$, $\sqrt{n}(\tilde{\boldsymbol{\tau}} - \boldsymbol{\tau}) \rightsquigarrow \mathcal{N}(\mathbf{0}, \boldsymbol{\Gamma}\boldsymbol{\Sigma}_{\infty})$.

(ii) The matrix $\boldsymbol{\Sigma}_{\infty} - \boldsymbol{\Gamma}\boldsymbol{\Sigma}_{\infty}$ is nonnegative definite.

Proof. Because $\tilde{\boldsymbol{\tau}} - \boldsymbol{\tau} = \boldsymbol{\Gamma}(\hat{\boldsymbol{\tau}} - \boldsymbol{\tau})$, (i) follows from (13) and the fact that $\boldsymbol{\Gamma}\boldsymbol{\Sigma}_{\infty}\boldsymbol{\Gamma} = \boldsymbol{\Gamma}\boldsymbol{\Sigma}_{\infty}$ by Lemma 5 in the Online Supplement. From Lemma 5 therein, $\boldsymbol{\Sigma}_{\infty} - \boldsymbol{\Gamma}\boldsymbol{\Sigma}_{\infty} = (\mathbf{I}_p - \boldsymbol{\Gamma})\boldsymbol{\Sigma}_{\infty} = (\mathbf{I}_p - \boldsymbol{\Gamma})^{\top}\boldsymbol{\Sigma}_{\infty}(\mathbf{I}_p - \boldsymbol{\Gamma})$, where \mathbf{I}_p denotes the $p \times p$ identity matrix. Consequently, (ii) follows from the fact that $\boldsymbol{\Sigma}_{\infty}$ is nonnegative definite. \square

To conclude this section, we illustrate $\tilde{\boldsymbol{\tau}}$ using the setup in Example 1.

Example 3. Consider a random sample of size $n = 70$ from the vector \mathbf{X} in Example 1; we used \mathbf{X} to be Normally distributed with Kendall correlation matrix \mathbf{T} displayed in Figure 2. Figure 3 displays \mathbf{T} , $\hat{\mathbf{T}}$ and $\tilde{\mathbf{T}}$. For this one simulated sample, it is clear that $\tilde{\mathbf{T}}$ is a better estimate of \mathbf{T} than $\hat{\mathbf{T}}$.

4 LEARNING THE STRUCTURE \mathcal{G}

Because the cluster structure \mathcal{G} is typically unknown, the improved estimator $\tilde{\boldsymbol{\tau}}$ derived in the previous section cannot be directly used. In this section, we propose a way to learn \mathcal{G} from data and to obtain an improved estimator of $\boldsymbol{\tau}$ as a by-product. The task of learning \mathcal{G} is split into two subtasks: we first identify d candidate structures in Section 4.1 and then choose one among them in Section 4.2.

4.1 Creating a set of candidate structures

The first observation to be made is that the cluster structure \mathcal{G} for which the PEA holds may not be unique. This is because if the PEA holds for some cluster structure \mathcal{G} , it holds for any refinement \mathcal{G}^* thereof defined as follows.

Definition 2. Let $\mathcal{G} = \{\mathcal{G}_1, \dots, \mathcal{G}_K\}$ be a partition of $\{1, \dots, d\}$. A refinement of \mathcal{G} is a partition $\mathcal{G}^* = \{\mathcal{G}_1, \dots, \mathcal{G}_{K^*}\}$ of $\{1, \dots, d\}$ such that $K^* > K$ and

$$\forall k^* \in \{1, \dots, K^*\} \exists k \in \{1, \dots, K\} \text{ such that } \mathcal{G}_{k^*} \subseteq \mathcal{G}_k.$$

The block structure implied by a refinement of \mathcal{G} is consistent with the the block structure implied by \mathcal{G} . This is formalized in the next proposition, which follows easily from (10).

Proposition 2. For two partitions \mathcal{G} and \mathcal{G}^* of $\{1, \dots, d\}$, \mathcal{G}^* is a refinement of \mathcal{G} if and only if $\mathcal{T}_{\mathcal{G}} \subseteq \mathcal{T}_{\mathcal{G}^*}$.

Proposition 2 implies in particular that if $\mathbf{T} \in \mathcal{T}_{\mathcal{G}}$ for some partition \mathcal{G} , then for any refinement \mathcal{G}^* thereof, $\mathbf{T} \in \mathcal{T}_{\mathcal{G}^*}$. This is illustrated in Example 4 below.

Example 4. Consider the partition \mathcal{G} given in (4) in Example 1. The partition $\mathcal{G}^* = \{\mathcal{G}_1^*, \dots, \mathcal{G}_5^*\}$ with $\mathcal{G}_1^* = \{1, 2\}$, $\mathcal{G}_2^* = \{3, 4\}$, $\mathcal{G}_3^* = \{5, 6, 7\}$, $\mathcal{G}_4^* = \{8, 9, 10\}$ is a refinement

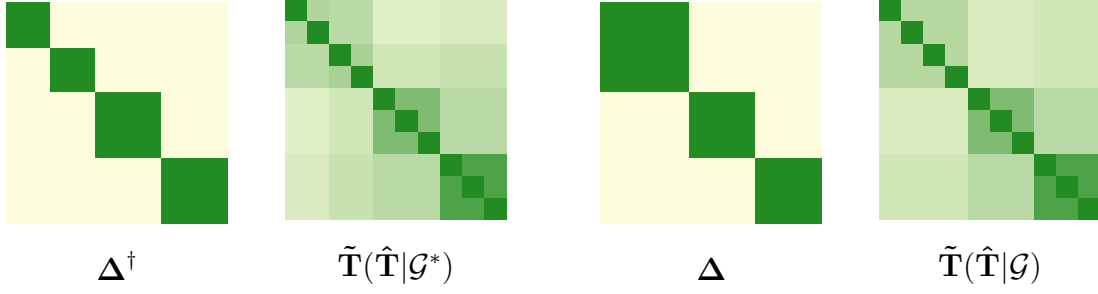


Figure 4: The estimates $\tilde{\mathbf{T}}(\hat{\mathbf{T}}|\mathcal{G}^*)$ and $\tilde{\mathbf{T}}(\hat{\mathbf{T}}|\mathcal{G})$ from Example 4, along with the cluster membership matrices Δ and Δ^* of the partitions \mathcal{G} and \mathcal{G}^* , respectively.

of \mathcal{G} since $\mathcal{G}_1^*, \mathcal{G}_2^* \subseteq \mathcal{G}_1$, $\mathcal{G}_3^* \subseteq \mathcal{G}_2$ and $\mathcal{G}_4^* \subseteq \mathcal{G}_3$. Consequently, \mathcal{G}^* satisfies the PEA as well. Figure 4 shows the cluster membership matrices Δ and Δ^* corresponding to \mathcal{G} and \mathcal{G}^* , respectively. Also displayed are the estimates $\tilde{\mathbf{T}}(\hat{\mathbf{T}}|\mathcal{G}^*)$ and $\tilde{\mathbf{T}}(\hat{\mathbf{T}}|\mathcal{G})$; one can see that the block structure of the former is embedded in the latter but not conversely.

While the partition for which the PEA holds may not be unique, the coarsest partition \mathcal{G} in (2) is. The fact that any refinement of \mathcal{G} in (2) also satisfies the PEA motivates us to start with the finest possible partition $\mathcal{G}^{(d)} := \{\{1\}, \dots, \{d\}\}$ for which the PEA always holds, and to merge the clusters one at a time in a way that resembles hierarchical agglomerative clustering. Specifically, we will create a path $\mathcal{P} = \{\mathcal{G}^{(d)}, \dots, \mathcal{G}^{(1)}\}$ through the set of all possible partitions of $\{1, \dots, d\}$ with $|\mathcal{G}^{(i)}| = i$ for $i = 1, \dots, d$, with the aim that \mathcal{G} given in (2) is an element of \mathcal{P} . The construction of \mathcal{P} is motivated by the following observation.

Proposition 3. *Let \mathcal{G} be an arbitrary partition of $\{1, \dots, d\}$, \mathbf{B} the associated block membership matrix (9) and $\mathbf{\Gamma} = \mathbf{B}\mathbf{B}^+$, where \mathbf{B}^+ is the generalized Moore–Penrose inverse of \mathbf{B} . Let also $\tilde{\boldsymbol{\tau}} = \mathbf{\Gamma}\hat{\boldsymbol{\tau}}$. If $\boldsymbol{\Sigma}_\infty$ is positive definite, and $\hat{\boldsymbol{\Sigma}}$ is an estimator of $\boldsymbol{\Sigma}$ such that $\hat{\boldsymbol{\Sigma}}^{-1}$ exists and, as $n \rightarrow \infty$, $n\hat{\boldsymbol{\Sigma}} \rightarrow \boldsymbol{\Sigma}_\infty$ element-wise in probability, the following holds.*

(i) If \mathcal{G} fulfils the PEA, $(\hat{\boldsymbol{\tau}} - \tilde{\boldsymbol{\tau}})^\top (\hat{\boldsymbol{\Sigma}}^{-1}/n)(\hat{\boldsymbol{\tau}} - \tilde{\boldsymbol{\tau}}) \rightarrow 0$ in probability.

(ii) If \mathcal{G} does not fulfill the PEA, $(\hat{\boldsymbol{\tau}} - \tilde{\boldsymbol{\tau}})^\top (\hat{\boldsymbol{\Sigma}}^{-1}/n)(\hat{\boldsymbol{\tau}} - \tilde{\boldsymbol{\tau}}) \rightarrow \boldsymbol{\tau}^\top (\mathbf{I}_p - \boldsymbol{\Gamma}) \boldsymbol{\Sigma}_\infty^{-1} (\mathbf{I}_p - \boldsymbol{\Gamma}) \boldsymbol{\tau}$ in probability; if $\boldsymbol{\Gamma} \boldsymbol{\tau} \neq \boldsymbol{\tau}$, the limit is strictly positive.

Proof. First, note that as $n \rightarrow \infty$, $\boldsymbol{\Sigma}^{-1}/n \rightarrow \boldsymbol{\Sigma}_\infty^{-1}$ in probability given that $A \mapsto A^{-1}$ is a continuous map for nonsingular matrices (Stewart, 1969). Now write

$$(\hat{\boldsymbol{\tau}} - \tilde{\boldsymbol{\tau}})^\top (\hat{\boldsymbol{\Sigma}}^{-1}/n)(\hat{\boldsymbol{\tau}} - \tilde{\boldsymbol{\tau}}) = \hat{\boldsymbol{\tau}}^\top (\mathbf{I}_p - \boldsymbol{\Gamma}) (\hat{\boldsymbol{\Sigma}}^{-1}/n) (\mathbf{I}_p - \boldsymbol{\Gamma}) \hat{\boldsymbol{\tau}}.$$

Because as $n \rightarrow \infty$, $\hat{\boldsymbol{\tau}} \rightarrow \boldsymbol{\tau}$ in probability by (13), $\hat{\boldsymbol{\tau}}^\top (\mathbf{I}_p - \boldsymbol{\Gamma}) (\hat{\boldsymbol{\Sigma}}^{-1}/n) (\mathbf{I}_p - \boldsymbol{\Gamma}) \hat{\boldsymbol{\tau}}$ converges to $\boldsymbol{\tau}^\top (\mathbf{I}_p - \boldsymbol{\Gamma}) \boldsymbol{\Sigma}_\infty^{-1} (\mathbf{I}_p - \boldsymbol{\Gamma}) \boldsymbol{\tau}$ in probability, proving the statement (ii). When \mathcal{G} fulfils the PEA, $\boldsymbol{\Gamma} \boldsymbol{\tau} = \boldsymbol{\tau}$ and hence $(\mathbf{I}_p - \boldsymbol{\Gamma}) \boldsymbol{\tau} = \mathbf{0}_p$, proving (i). \square

Remark 3. Note that in Proposition 3 (ii), $\boldsymbol{\Gamma} \boldsymbol{\tau} = \boldsymbol{\tau}$ could indeed occur even if \mathcal{G} does not satisfy the PEA. This is because Kendall's τ of two distinct copulas may be equal. However the PEA must be met in order for Theorems 1 and 2 to hold.

Motivated by Proposition 3, the construction of \mathcal{P} relies on slowly introducing information through constraints under which the loss function ℓ in (14) is minimized. Before proceeding with this idea however, the estimation of the unknown finite-sample variance $\boldsymbol{\Sigma}$ of $\hat{\boldsymbol{\tau}}$ needs to be considered. While $\boldsymbol{\Sigma}$ does not appear in the estimator $\tilde{\boldsymbol{\tau}}$ in Theorem 1, it is relevant for the construction of \mathcal{P} . In Appendix A in the Online Supplement, we explain how to obtain an estimator of $\boldsymbol{\Sigma}$ for a given partition \mathcal{G} . Because $\boldsymbol{\Sigma}$ inherits a certain block structure if the PEA holds for \mathcal{G} , this estimator is a function of an empirical estimator $\hat{\boldsymbol{\Sigma}}$ of $\boldsymbol{\Sigma}$, the structure \mathcal{G} and a shrinkage parameter w ; hence we denote it by $\tilde{\boldsymbol{\Sigma}}(\hat{\boldsymbol{\Sigma}} | \hat{\boldsymbol{\tau}}, \mathcal{G}, w)$. In Section A.3 of the Online Supplement it is shown that $n \tilde{\boldsymbol{\Sigma}}(\hat{\boldsymbol{\Sigma}} | \hat{\boldsymbol{\tau}}, \mathcal{G}, w) \rightarrow \boldsymbol{\Sigma}_\infty$ element-wise in probability if w shrinks to zero as $n \rightarrow \infty$.

Now suppose that the i th partition $\mathcal{G}^{(i)}$ has been selected; let $\tilde{\Sigma}_w^{(i)} := \tilde{\Sigma}(\hat{\Sigma} | \hat{\tau}, \mathcal{G}^{(i)}, w)$ denote the corresponding estimate of Σ . To select the $(i-1)$ -st cluster structure $\mathcal{G}^{(i-1)}$, merge two clusters at a time and choose the optimal merger, in the sense that

$$\mathcal{G}^{(i-1)} := \arg \min_{\mathcal{G}^*: \mathcal{T}_{\mathcal{G}^*} \subset \mathcal{T}_{\mathcal{G}^{(i)}}, |\mathcal{G}^*| = i-1} \ell \left(\tilde{\tau}(\hat{\tau} | \mathcal{G}^*) | \hat{\tau}, \tilde{\Sigma}_w^{(i)} \right). \quad (16)$$

The minimization in (16) is done by simply going through all $i(i-1)/2$ possible mergers; $\mathcal{T}_{\mathcal{G}^*} \subset \mathcal{T}_{\mathcal{G}^{(i)}}$ indicates that $\mathcal{G}^{(i)}$ must be a refinement of \mathcal{G}^* , so that the previously introduced equality constraints are carried. We then update the estimate of τ to $\tilde{\tau}(\hat{\tau} | \mathcal{G}^{(i-1)})$ as in Theorem 1, the estimate of Σ to $\tilde{\Sigma}_w^{(i-1)} = \tilde{\Sigma}(\hat{\Sigma} | \hat{\tau}, \mathcal{G}^{(i-1)}, w)$ and iterate the above steps until $i = 1$. The whole procedure is formalized in Algorithm 1 below.

Algorithm 1.

(0) Initialization. Fix $w \in [0, 1]$ and set

$$\mathcal{G}^{(d)} := \{\{1\}, \dots, \{d\}\} \quad \text{and} \quad \tilde{\Sigma}_w^{(d)} := \tilde{\Sigma}(\hat{\Sigma} | \hat{\tau}, \mathcal{G}^{(d)}, w).$$

(1) Iteration. For $i \in \{d-1, \dots, 1\}$,

(1a) Structure selection. Set $\mathcal{G}^{(i)} = \arg \min_{\mathcal{G}^*: \mathcal{T}_{\mathcal{G}^*} \subset \mathcal{T}_{\mathcal{G}^{(i+1)}}, |\mathcal{G}^*| = i} \ell \left(\tilde{\tau}(\hat{\tau} | \mathcal{G}^*) | \hat{\tau}, \tilde{\Sigma}_w^{(i+1)} \right);$

(1b) Update. Set $\tilde{\Sigma}_w^{(i)} = \tilde{\Sigma}(\hat{\Sigma} | \hat{\tau}, \mathcal{G}^{(i)}, w);$

(2) Output. Return $\mathcal{P} := \{\mathcal{G}^{(d)}, \dots, \mathcal{G}^{(1)}\}.$

Algorithm 1 returns a sequence $\mathcal{P} = \{\mathcal{G}^{(d)}, \dots, \mathcal{G}^{(1)}\}$ of decreasingly complex structures; note that $\mathcal{G}^{(i)}$ is a refinement of $\mathcal{G}^{(i-1)}$ for all $i = 2, \dots, d$. From each $\mathcal{G}^{(i)}$ in \mathcal{P} , we can then compute the cluster membership matrix $\Delta^{(i)}$, the improved estimate $\tilde{\tau}^{(i)} = \tilde{\tau}(\hat{\tau} | \mathcal{G}^{(i)})$ of τ defined as in Theorem 1, its matrix version $\tilde{\mathbf{T}}^{(i)}$, and an estimate $\tilde{\Sigma}^{(i)}$ of Σ (upon setting

$w = 0$). Furthermore, we may also construct the corresponding $\mathbf{\Gamma}$ matrix, say $\mathbf{\Gamma}^{(i)}$, and obtain a consistent estimator of the covariance matrix of $\tilde{\boldsymbol{\tau}}^{(i)}$, $\mathbf{\Gamma}^{(i)}\tilde{\boldsymbol{\Sigma}}^{(i)}\mathbf{\Gamma}^{(i)}$, which simplifies to $\mathbf{\Gamma}^{(i)}\tilde{\boldsymbol{\Sigma}}^{(i)}$ by Lemma 6.

If present on the path, the coarsest possible structure \mathcal{G} in (2) is always $\mathcal{G}^{(K)}$, where $K = |\mathcal{G}|$. Note that $\tilde{\mathbf{T}}^{(d)} = \hat{\mathbf{T}}$ and $\tilde{\mathbf{T}}^{(1)}$, the equicorrelation matrix corresponding to $\mathcal{G}^{(1)} = \{\{1, \dots, d\}\}$, are inevitable outputs of the algorithm. This is why we refer to \mathcal{P} as a *path*: in the space of all $d \times d$ matrices, it is the path we took to go from $\tilde{\mathbf{T}}^{(d)}$ to $\tilde{\mathbf{T}}^{(1)}$.

Example 5. Figure 5 depicts the application of Algorithm 1 on $\hat{\mathbf{T}}$ constructed from the random sample in Example 3 of \mathbf{X} from Example 1. Here, the true cluster structure \mathcal{G} in (2) is given by (4). It indeed lies on the path; it corresponds to $\boldsymbol{\Delta}^{(3)}$.

Remark 4. Consider a partition \mathcal{G} for which the PEA holds, and let \mathcal{G}^* be a refinement thereof. Let \mathbf{B} and \mathbf{B}^* be the block membership matrices given by (9) corresponding to \mathcal{G} and \mathcal{G}^* , respectively, and set $\mathbf{\Gamma} = \mathbf{B}\mathbf{B}^+$ and $\mathbf{\Gamma}^* = \mathbf{B}^*(\mathbf{B}^*)^+$. Then because $\boldsymbol{\Sigma}^{-1} \in \mathcal{S}_{\mathcal{G}} \subset \mathcal{S}_{\mathcal{G}^*}$, where $\mathcal{S}_{\mathcal{G}}$ and $\mathcal{S}_{\mathcal{G}^*}$ are as defined in Appendix A.2, Lemma 6 therein applies and $(\mathbf{I}_p - \mathbf{\Gamma}^*)^\top \boldsymbol{\Sigma} \mathbf{\Gamma}^* = \mathbf{0}$. Furthermore, for $\tilde{\boldsymbol{\tau}}^* = \mathbf{\Gamma}^* \hat{\boldsymbol{\tau}}$ and $\tilde{\boldsymbol{\tau}} = \mathbf{\Gamma} \hat{\boldsymbol{\tau}}$, $\mathbf{\Gamma}^* \tilde{\boldsymbol{\tau}} = \tilde{\boldsymbol{\tau}}$. Hence,

$$(\hat{\boldsymbol{\tau}} - \tilde{\boldsymbol{\tau}})^\top \boldsymbol{\Sigma}^{-1} (\hat{\boldsymbol{\tau}} - \tilde{\boldsymbol{\tau}}) = (\hat{\boldsymbol{\tau}} - \tilde{\boldsymbol{\tau}}^*)^\top \boldsymbol{\Sigma}^{-1} (\hat{\boldsymbol{\tau}} - \tilde{\boldsymbol{\tau}}^*) + (\tilde{\boldsymbol{\tau}}^* - \tilde{\boldsymbol{\tau}})^\top \boldsymbol{\Sigma}^{-1} (\tilde{\boldsymbol{\tau}}^* - \tilde{\boldsymbol{\tau}}). \quad (17)$$

Now set $K = |\mathcal{G}|$. If $\mathcal{G}^{(i)}$, $i = K, \dots, d$ is a sequence of partitions such that $\mathcal{G}^{(K)} = \mathcal{G}$, $\mathcal{G}^{(d)} = \{\{1\}, \dots, \{d\}\}$, and for each $i = K, \dots, d-1$, $\mathcal{G}^{(i+1)}$ is a refinement of $\mathcal{G}^{(i)}$. For all $i = K, \dots, d$, let $\mathbf{B}^{(i)}$ be as in (9), $\mathbf{\Gamma}^{(i)} = \mathbf{B}^{(i)}(\mathbf{B}^{(i)})^+$ and $\tilde{\boldsymbol{\tau}}^{(i)} = \mathbf{\Gamma}^{(i)} \hat{\boldsymbol{\tau}}$. A successive application of (17) then gives

$$(\hat{\boldsymbol{\tau}} - \tilde{\boldsymbol{\tau}}^{(K)})^\top \boldsymbol{\Sigma}^{-1} (\hat{\boldsymbol{\tau}} - \tilde{\boldsymbol{\tau}}^{(K)}) = \sum_{i=K+1}^d (\tilde{\boldsymbol{\tau}}^{(i)} - \tilde{\boldsymbol{\tau}}^{(i-1)})^\top \boldsymbol{\Sigma}^{-1} (\tilde{\boldsymbol{\tau}}^{(i)} - \tilde{\boldsymbol{\tau}}^{(i-1)}) \quad (18)$$

In particular, for any $i = K, \dots, d-1$, $\ell(\tilde{\boldsymbol{\tau}}^{(i)} | \hat{\boldsymbol{\tau}}, \boldsymbol{\Sigma}) \geq \ell(\tilde{\boldsymbol{\tau}}^{(i+1)} | \hat{\boldsymbol{\tau}}, \boldsymbol{\Sigma})$. This motivates that in the iteration Step (1a) of Algorithm 1, only two clusters are merged at a time.

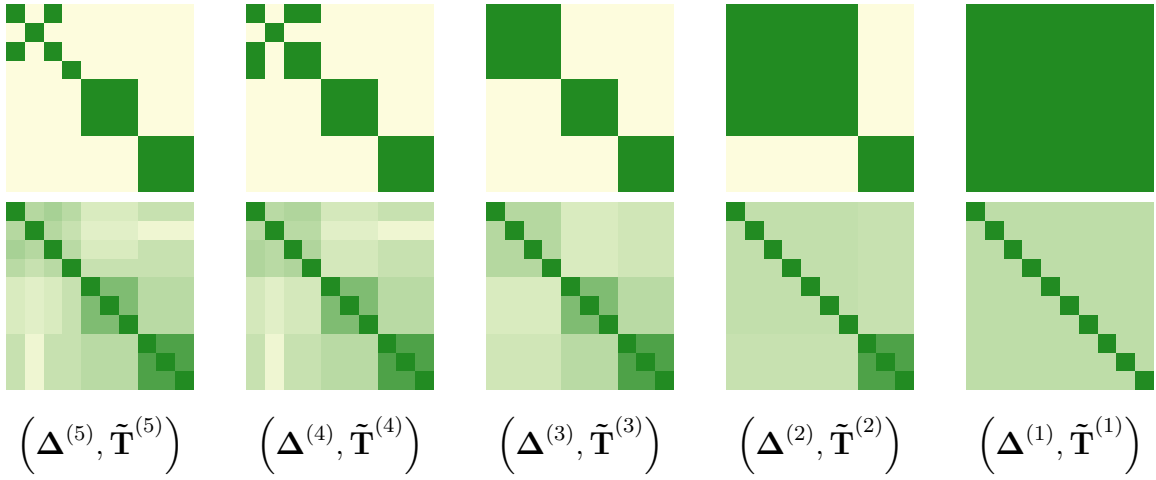
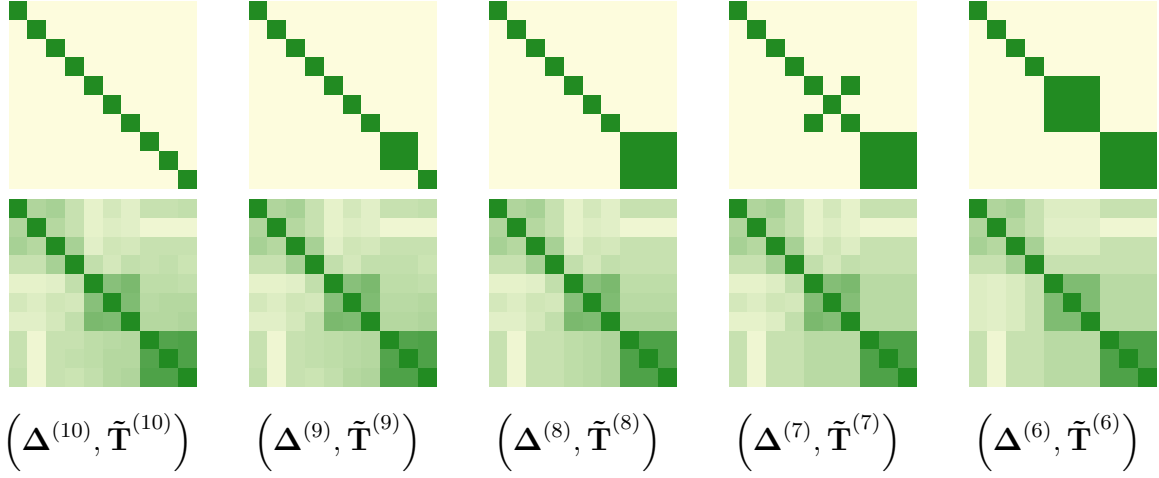


Figure 5: The pairs of matrices $(\Delta^{(i)}, \tilde{\mathbf{T}}^{(i)})$, $i = 1, \dots, d$ corresponding to the path \mathcal{P} obtained by applying Algorithm 1 in Example 5.

4.2 Structure selection

We need to identify a final estimate of \mathcal{G} among the d structures in \mathcal{P} . Proposition 3 suggests that the loss will increase sharply when the clustering has become too coarse. The

following result, whose proof can be found in Section B.2 of the Online Supplement, offers a way to determine when this sharp increase may have occurred.

Proposition 4. *Let $\mathcal{G} = \{\mathcal{G}_1, \dots, \mathcal{G}_K\}$ be a partition of $\{1, \dots, d\}$ satisfying the PEA, let \mathbf{B} be the corresponding block membership matrix (9), $\mathbf{\Gamma} = \mathbf{B}\mathbf{B}^+$ and $\tilde{\boldsymbol{\tau}} = \mathbf{\Gamma}\hat{\boldsymbol{\tau}}$. If $\boldsymbol{\Sigma}_\infty$ is positive definite, and $\hat{\boldsymbol{\Sigma}}$ is any estimator of $\boldsymbol{\Sigma}$ such that $\hat{\boldsymbol{\Sigma}}^{-1}$ exists and, as $n \rightarrow \infty$, $n\hat{\boldsymbol{\Sigma}} \rightarrow \boldsymbol{\Sigma}_\infty$ element-wise in probability, then, as $n \rightarrow \infty$,*

$$\ell(\tilde{\boldsymbol{\tau}}|\hat{\boldsymbol{\tau}}, \hat{\boldsymbol{\Sigma}}) = (\hat{\boldsymbol{\tau}} - \tilde{\boldsymbol{\tau}})^\top \hat{\boldsymbol{\Sigma}}^{-1} (\hat{\boldsymbol{\tau}} - \tilde{\boldsymbol{\tau}}) \rightsquigarrow \chi_{p-L}^2,$$

where L is the number of distinct blocks given in (7).

At each iteration of Algorithm 1, $\boldsymbol{\Sigma}$ is estimated by $\tilde{\boldsymbol{\Sigma}}_w^{(i)}$. Proposition 4 and Section A.3 of the Online Supplement suggests using $\ell(\tilde{\boldsymbol{\tau}}^{(i)}|\hat{\boldsymbol{\tau}}, \tilde{\boldsymbol{\Sigma}}_w^{(i)})$ to get a rough idea of when too much clustering has been applied through

$$\alpha^{(i)} := \mathbb{P} \left[\chi_{p-L_i}^2 > \ell(\tilde{\boldsymbol{\tau}}^{(i)}|\hat{\boldsymbol{\tau}}, \tilde{\boldsymbol{\Sigma}}_w^{(i)}) \right], \quad (19)$$

where L_i is the number of blocks given by (7) corresponding to the i th partition $\mathcal{G}^{(i)}$. For n large enough, we expect that a sharp decrease in $\alpha^{(i)}$ will occur at the first i such that $\mathcal{T}_{\mathcal{G}} \not\subseteq \mathcal{T}_{\mathcal{G}^{(i)}}$, that is, when the $\mathbf{\Gamma}$ matrix corresponding to $\mathcal{G}^{(i)}$ becomes inadmissible. We do not use the criterion (19) as a formal p -value, but rather as a tool that can help with structure selection. A naive automated selection procedure based on (19) is used in the simulations of Section 6, where it leads to good estimators of $\boldsymbol{\tau}$.

Example 6. *Consider again the random sample of size $n = 70$ from \mathbf{X} in Example 3. We computed $\alpha^{(i)}$, $i = 1, \dots, 10$, given by (19) for the path obtained with Algorithm 1 in Example 5. As can be seen in Figure 6, the gap between $\alpha^{(3)}$ and $\alpha^{(2)}$ strongly suggests that the best structure is $\mathcal{G}^{(3)}$, which is indeed the true structure in this case.*

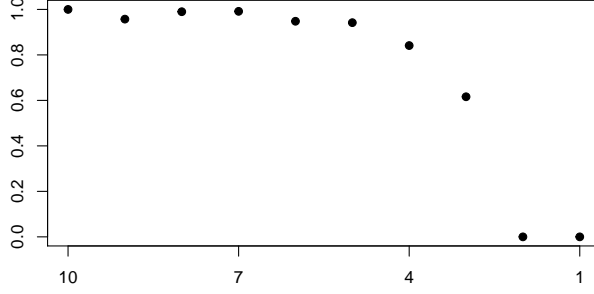


Figure 6: The pairs $(i, \alpha^{(i)})$, $i = 10 \dots, 1$, computed in Example 6.

5 ESTIMATION OF LINEAR CORRELATION

In this section, we show how the PEA can be used to obtain improved estimates of the classical linear correlation matrix \mathbf{P} with entries $\mathbf{P}_{ij} = \text{Cor}(X_i, X_j)$, $i, j = 1, \dots, d$ when \mathbf{X} is elliptical. Recall that an absolutely continuous random vector \mathbf{X} follows an elliptical distribution with mean vector $\boldsymbol{\mu} \in \mathbb{R}^d$, positive definite $d \times d$ dispersion matrix \mathbf{D} and density generator $g : [0, \infty) \rightarrow [0, \infty)$, in notation $\mathbf{X} \sim \mathcal{E}(\boldsymbol{\mu}, \mathbf{D}, g)$, if its density f satisfies, for all $\mathbf{x} \in \mathbb{R}^d$,

$$f(\mathbf{x}) = |\mathbf{D}|^{-1/2} g\left(\frac{(\mathbf{x} - \boldsymbol{\mu})' \mathbf{D}^{-1} (\mathbf{x} - \boldsymbol{\mu})}{2}\right), \quad (20)$$

where $|\mathbf{D}|$ denotes the determinant of \mathbf{D} . The equation (20) means that the level curves of f are concentric ellipses centred at $\boldsymbol{\mu}$. For a book treatment of elliptical distributions, see, e.g., Fang et al. (1990) or Fang and Zhang (1990). Well-known examples of elliptical distributions are the multivariate Normal, Student t or generalized hyperbolic distributions; for their use in finance and risk modelling, see McNeil et al. (2015).

Note that when $\mathbf{X} \sim \mathcal{E}(\boldsymbol{\mu}, \mathbf{D}, g)$, $\boldsymbol{\mu}$ and \mathbf{D} are not necessarily the mean and covariance matrix of \mathbf{X} , respectively; the former may not even exist. However, if $\mathbb{E}(X_i^2) < \infty$ for all $i \in \{1, \dots, d\}$, $\mathbb{E}(\mathbf{X}) = \boldsymbol{\mu}$ and there exists a constant $c > 0$ such that $\text{Cov}(\mathbf{X}) = c\mathbf{D}$

(Fang and Zhang, 1990, Theorem 2.6.4). Consequently, if the linear correlation matrix \mathbf{P} of \mathbf{X} exists, one has, for all $i, j \in \{1, \dots, d\}$, $\mathbf{P}_{ij} = \mathbf{D}_{ij} / \sqrt{\mathbf{D}_{ii}\mathbf{D}_{jj}}$. Surprisingly, for all $i \neq j \in \{1, \dots, d\}$, the correlation coefficient \mathbf{P}_{ij} is in one-to-one relationship with Kendall's correlation $\tau(X_i, X_j)$, viz.

$$\mathbf{P}_{ij} = \sin\left(\frac{\pi \mathbf{T}_{ij}}{2}\right), \quad (21)$$

as shown by Fang et al. (2002) and Lindskog et al. (2002). Because the map in (21) is a bijection, (21) can be used to construct an estimator of \mathbf{P} , given, for all $i \neq j \in \{1, \dots, d\}$, by $\hat{\mathbf{P}}_{ij} = \sin(\pi \hat{\mathbf{T}}_{ij}/2)$. As illustrated by Lindskog et al. (2002), the resulting estimator $\hat{\mathbf{P}}$ can be considerably more efficient than the sample correlation matrix, especially when the margins of \mathbf{X} are heavy-tailed. Recently, $\hat{\mathbf{P}}$ has been employed, e.g, in the context of nonparanormal graphical models (Liu et al., 2012; Xue and Zou, 2012) or Gaussian copula regression (Cai and Zhang, 2017).

Now suppose that \mathcal{G} is a partition of $\{1, \dots, d\}$ so that the PEA holds. Because \mathbf{X} is elliptical, this is equivalent to $\mathbf{T} \in \mathcal{T}_{\mathcal{G}}$, or, in view of (21), to $\mathbf{P} \in \mathcal{T}_{\mathcal{G}}$. Because $\tilde{\mathbf{T}}$ is a more efficient estimator of \mathbf{T} by Theorem 2, the delta method implies that $\tilde{\mathbf{P}} \in \mathcal{T}_{\mathcal{G}}$ obtained by using $\tilde{\mathbf{T}}_{ij}$ in (21) is a more efficient estimator of \mathbf{P} than $\hat{\mathbf{P}}$. Moreover, if \mathbf{P} is positive definite, it follows from Lemma 7 in the Online Supplement that the precision matrix $\mathbf{\Omega} = \mathbf{P}^{-1}$ has the same block structure as \mathbf{P} , that is, $\mathbf{\Omega} \in \mathcal{T}_{\mathcal{G}}$. As an estimator of $\mathbf{\Omega}$, one may thus use $\tilde{\mathbf{\Omega}} = \tilde{\mathbf{P}}^{-1}$ directly if the latter is positive definite; it then follows from Lemma 7 that $\tilde{\mathbf{\Omega}} \in \mathcal{T}_{\mathcal{G}}$. Otherwise, $\tilde{\mathbf{P}}$ can first be made positive definite using one of the shrinkage methods described, e.g., in Rousseeuw and Molenberghs (1993); its inverse can be further improved by averaging out the entries block-wise to obtain a matrix in $\mathcal{T}_{\mathcal{G}}$.

6 SIMULATION STUDY

6.1 Performance of the clustering algorithm

In this section, we first investigate whether the true cluster structure is on the path $\mathcal{P} = \{\mathcal{G}^{(d)}, \dots, \mathcal{G}^{(1)}\}$ returned by Algorithm 1 and how often does the criterion (19) select the true cluster structure given the latter is on the path. We only consider the case of a modest dimension $d = 20$ and focus on four different matrices \mathbf{T}_i , $i = 1, \dots, 4$ displayed in Figure 7 along with the corresponding cluster membership matrices Δ_i , $i = 1, \dots, 4$. The matrices \mathbf{T}_1 and \mathbf{T}_2 both have the same 4 clusters of 5 variables, but with entries of different magnitudes so that the blocks are less well separated in \mathbf{T}_2 . The entries of \mathbf{T}_2 are moreover smaller in absolute value, which implies more variability in $\hat{\mathbf{T}}$. We therefore expect its structure to be more difficult to identify. The structure of the matrices \mathbf{T}_3 and \mathbf{T}_4 is more complex and formed by 8 clusters of varying size. The clusters corresponding to \mathbf{T}_4 are the most difficult to identify.

For each of the four matrices \mathbf{T}_i , $i = 1, \dots, 4$, we generated 500 datasets from multivariate Normal distributions with standard Normal margins and Kendall's rank correlation matrix \mathbf{T}_i . This was replicated with three different sample sizes, $n = 125, 250, 500$. Examples of $\hat{\mathbf{T}}$ obtained with all 12 pairs (\mathbf{T}, n) are shown in Figure 12 of the Online Supplement. Note that since Algorithm 1 is ranked-based, different choices of the marginal distributions have no impact on the results so long as they are continuous. However, the dependence structure does matter. The simulations were thus repeated using samples from the Cauchy copula. The results were similar and are given in Appendix C of the Online Supplement.

For each simulated sample, we applied Algorithm 1 and computed the indicator of the presence of the true cluster membership matrix Δ on the path \mathcal{P} , viz.

$$\nu_1 := \mathbb{1}(\Delta \in \mathcal{P}).$$

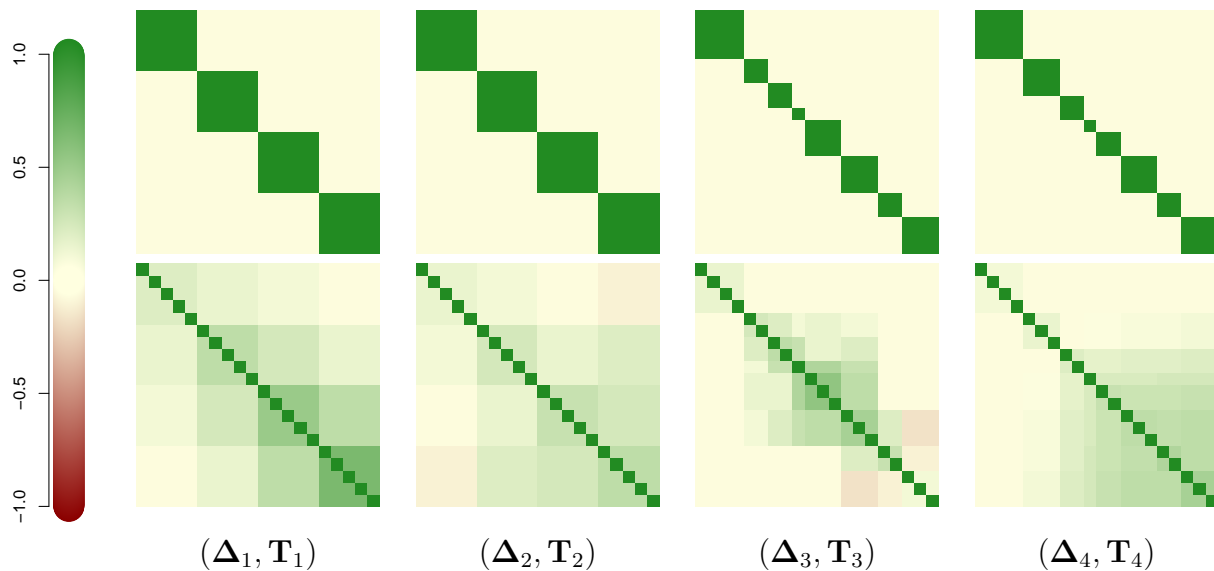


Figure 7: The matrices \mathbf{T}_i and Δ_i , $i = 1, 2, 3, 4$ used in simulations in Section 6.

The shrinkage parameter w was held fixed through all d iterations of Algorithm 1. We considered five values for w , 0, 0.25, 0.5, 0.75 and 1. The average value $\bar{\nu}_1$ when $w = 0.75$ is reported in Table 1. For all four matrices, the value of $\bar{\nu}_1$ increases with the sample size. For the matrices \mathbf{T}_1 , \mathbf{T}_2 and \mathbf{T}_3 with clearly distinct blocks, the path of Algorithm 1 very often goes through the true structure. For the matrix \mathbf{T}_4 , it is no surprise that this almost never happens, as the generated $\hat{\mathbf{T}}$ are very noisy and the clusters are hardly distinguishable. The results for the remaining values of w may be found in Table 5 in Appendix C of the Online Supplement. As expected, when the sample size is large ($n = 500$) the value of w has minor impact. When the sample size is small or moderate ($n = 125$ or 250), $w = 0$ leads to poorer results, but otherwise the value of w has little impact.

Our next objective was to check whether $\alpha^{(i)}$, defined in (19), is a reasonable structure identification tool. The selection was done with the following automated procedure.

Table 1: Average values of ν_1 over 500 simulations with $w = 0.75$.

| | \mathbf{T}_1 | | | \mathbf{T}_2 | | | \mathbf{T}_3 | | | \mathbf{T}_4 | | |
|---------------|----------------|------|------|----------------|------|------|----------------|------|------|----------------|------|------|
| n | 125 | 250 | 500 | 125 | 250 | 500 | 125 | 250 | 500 | 125 | 250 | 500 |
| $\bar{\nu}_1$ | 0.94 | 1.00 | 1.00 | 0.52 | 0.95 | 1.00 | 0.29 | 0.81 | 0.99 | 0.00 | 0.00 | 0.11 |

Algorithm 2.

(0) Fix $\alpha \in (0, 1)$ and set $i^\bullet \leftarrow d$.

For $i \in \{d-1, \dots, 1\}$:

(1) let $\tilde{\Sigma}_w^{(i)} = \tilde{\Sigma}(\hat{\Sigma}|\hat{\tau}, \mathcal{G}^{(i)}, w)$ and $L_i = |\mathcal{B}_{\mathcal{G}^{(i)}}|$;

(2) compute $\alpha^{(i)} := \mathbb{P} \left[\chi_{p-L_i}^2 > \ell \left(\tilde{\tau}^{(i)} | \hat{\tau}, \tilde{\Sigma}_w^{(i)} \right) \right]$;

(3) if $\alpha^{(i)} \geq \alpha$, set $i^\bullet \leftarrow i$.

This simple rule returns i^\bullet so that $\mathcal{G}^{(i^\bullet)}$ is the coarsest cluster structure such that $\alpha^{(i^\bullet)} \geq \alpha$. The parameter $\tilde{\Sigma}_w^{(i)}$ typically improves quickly after the first few steps. One could therefore monitor its behaviour and decrease w as i gets smaller. In this simulation study, we fix $w = 0$ through the whole process for simplicity. We run Algorithm 2 with $\alpha = 0.05, 0.1, 0.25, 0.5$, and look at the proportion of times Algorithm 2 identifies the true structure properly, given that it is present on the path obtained with Algorithm 1. Results for \mathbf{T}_1 , \mathbf{T}_2 and \mathbf{T}_3 are shown in Table 2; results for \mathbf{T}_4 are not shown because too few paths contained the true structure, viz. Table 1. As the sample size increases, the percentage gets closer to $1 - \alpha$, as one would expect. Hence, it is advantageous to choose a small value of α once n is sufficiently large. When $\mathbf{T} = \mathbf{T}_1$, $\mathbf{T} = \mathbf{T}_2$, and $\mathbf{T} = \mathbf{T}_3$, $\alpha = 0.05$ becomes the best option when $n = 125$, $n = 250$, and $n = 500$, respectively. For smaller sample

Table 2: Proportion of the 500 samples for which Algorithm 2 identified the true structure when it was present on the path returned by Algorithm 1.

| Level αn | \mathbf{T}_1 | | | \mathbf{T}_2 | | | \mathbf{T}_3 | | |
|------------------|----------------|------|------|----------------|------|------|----------------|------|------|
| | 125 | 250 | 500 | 125 | 250 | 500 | 125 | 250 | 500 |
| 0.05 | 0.94 | 0.96 | 0.96 | 0.67 | 0.94 | 0.95 | 0.04 | 0.51 | 0.96 |
| 0.10 | 0.90 | 0.90 | 0.92 | 0.78 | 0.93 | 0.90 | 0.14 | 0.63 | 0.92 |
| 0.25 | 0.77 | 0.77 | 0.77 | 0.79 | 0.80 | 0.76 | 0.37 | 0.69 | 0.77 |
| 0.50 | 0.54 | 0.53 | 0.50 | 0.60 | 0.54 | 0.51 | 0.53 | 0.61 | 0.59 |

sizes, it is advantageous to choose a larger value of α . This phenomenon is best visible when $\mathbf{T} = \mathbf{T}_3$ and $n = 125$; the best option in this setting is $\alpha = 0.5$.

6.2 Improved estimation of Kendall's rank correlation matrix

Even though Algorithm 1 in combination with Algorithm 2 may not identify the true coarsest cluster structure properly, the estimator $\tilde{\mathbf{T}}$ that it returns is still considerably more efficient than $\hat{\mathbf{T}}$. We explore this in this section by first calculating the statistic

$$\nu_2 := 1 - \min\{\|\tilde{\boldsymbol{\tau}}^{(j)} - \boldsymbol{\tau}\|_2^2 : \mathcal{G}^{(j)} \in \mathcal{P}\} / \|\hat{\boldsymbol{\tau}} - \boldsymbol{\tau}\|_2^2,$$

i.e., one minus the smallest squared error obtained among all members of the path \mathcal{P} returned by Algorithm 1, normalized by the squared error of $\hat{\boldsymbol{\tau}}$. To assess the performance of Algorithm 2, we also calculate

$$\xi(\alpha) := 1 - \|\boldsymbol{\tau}^\bullet - \boldsymbol{\tau}\|_2^2 / \|\hat{\boldsymbol{\tau}} - \boldsymbol{\tau}\|_2^2, \quad (22)$$

where $\boldsymbol{\Delta}^\bullet$ and $\boldsymbol{\tau}^\bullet$ are the outcomes of Algorithm 2 with level α . Note that ν_2 and $\xi(\alpha)$ are always between 0 (worst) and 1 (best).

Table 3: Average values of ν_2 and $\xi(\alpha)$ for $\alpha \in \{0.05, 0.1, 0.25, 0.5\}$ for 500 simulation runs with $w = 0.75$.

| Measure n | \mathbf{T}_1 | | | \mathbf{T}_2 | | | \mathbf{T}_3 | | | \mathbf{T}_4 | | |
|-------------------|----------------|------|------|----------------|------|------|----------------|------|------|----------------|------|------|
| | 125 | 250 | 500 | 125 | 250 | 500 | 125 | 250 | 500 | 125 | 250 | 500 |
| $\bar{\nu}_2$ | 0.63 | 0.65 | 0.65 | 0.68 | 0.79 | 0.79 | 0.50 | 0.59 | 0.63 | 0.50 | 0.51 | 0.56 |
| $\bar{\xi}(0.05)$ | 0.61 | 0.66 | 0.67 | 0.61 | 0.78 | 0.79 | 0.35 | 0.47 | 0.61 | 0.37 | 0.39 | 0.44 |
| $\bar{\xi}(0.10)$ | 0.61 | 0.65 | 0.66 | 0.63 | 0.78 | 0.78 | 0.38 | 0.50 | 0.61 | 0.39 | 0.41 | 0.46 |
| $\bar{\xi}(0.25)$ | 0.59 | 0.61 | 0.63 | 0.64 | 0.75 | 0.75 | 0.41 | 0.52 | 0.59 | 0.41 | 0.42 | 0.47 |
| $\bar{\xi}(0.50)$ | 0.53 | 0.55 | 0.54 | 0.61 | 0.70 | 0.69 | 0.43 | 0.51 | 0.53 | 0.41 | 0.42 | 0.45 |

The results for the simulation design from Section 6.1 are displayed in Table 3. First note that the results for distinct matrices \mathbf{T}_i are not directly comparable, because the maximum error reduction that can possibly be achieved depends on \mathbf{T}_i . By looking at the row pertaining to $\bar{\nu}_2$, we see that the mean squared error of $\hat{\tau}$ can be cut substantially by choosing the best structure on the path \mathcal{P} returned by Algorithm 1 in each of the scenarios considered. The values of $\bar{\xi}(\alpha)$ suggest that Algorithm 2 often selects a structure that does nearly as well in terms of error reduction. The reactivity to changes in α is low, which is a sign that the gap in $\alpha^{(i)}$ between reasonable and poor models is often large. Nonetheless, one can detect a similar phenomenon as in Table 2: Algorithm 2 performs best when α is small once the sample size is large enough. In summary, Table 3 illustrates that even if Algorithms 1 and 2 do not select the true coarsest partition \mathcal{G} that satisfies PEA, the resulting estimator $\tilde{\mathbf{T}}$ can considerably outperform $\hat{\mathbf{T}}$. This is particularly apparent in the last block pertaining to \mathbf{T}_4 . Even though hardly any path returned by Algorithm 1 goes through \mathcal{G} in this case, Table 3 shows that the structure selected by Algorithms 1 and 2 leads to a substantial reduction of mean squared error.

The above findings suggest that selecting a structure simpler than the true one might

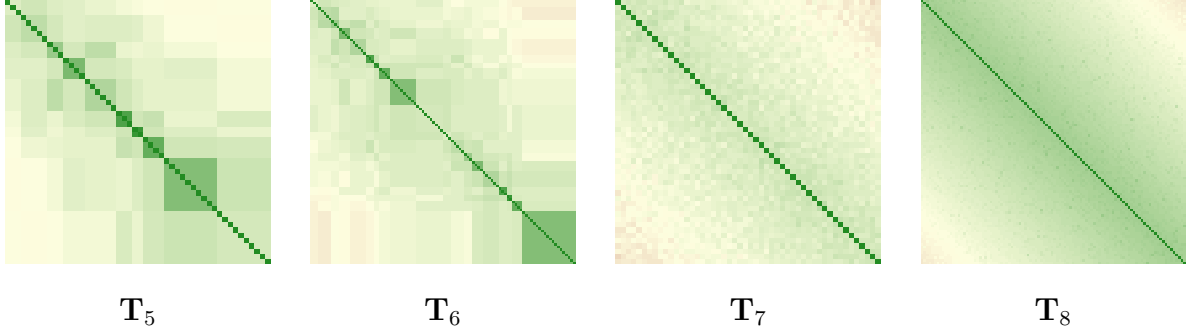


Figure 8: The matrices \mathbf{T}_i , $i = 5, 6, 7, 8$ used in simulations in Section 6.2.

be beneficial when $\hat{\mathbf{T}}$ is extremely noisy because even if it introduces a small bias, it reduces the variance considerably. To demonstrate this further, we challenge Algorithms 1 and 2 by considering $d \in \{50, 100\}$ and four additional matrices $\mathbf{T}_5, \dots, \mathbf{T}_8$ displayed in Figure 8. \mathbf{T}_5 and \mathbf{T}_6 correspond to 50 variables and have a block structure with 10 and 19 blocks, respectively. The matrices \mathbf{T}_7 and \mathbf{T}_8 are 100×100 noisy versions of Toeplitz matrices with a constant decay in their entries as one moves away from the diagonal. This means that \mathbf{T}_7 and \mathbf{T}_8 are unstructured, i.e., the only partition \mathcal{G} that satisfies PEA is $\{\{1\}, \dots, \{d\}\}$. We also consider rather small sample sizes, $n \in \{25, 50, 100\}$. Because better results are achieved for higher values of the shrinkage parameter w in small samples, we set $w = 1$.

The results for 500 simulation runs are summarized in Table 4. They suggest that the method still performs well in higher-dimensional settings, even when d is larger than n . As already observed in Tables 2 and 3, it is better to choose a more conservative value for α in small samples, although the sensitivity to α is small. The results are particularly interesting for \mathbf{T}_7 and \mathbf{T}_8 , which do not have a block structure. However, they still possess a certain structure that Algorithm 1 is able to capture and $\tilde{\mathbf{T}}$ performs better than $\hat{\mathbf{T}}$ due to a bias-variance tradeoff when n is small. Note that because $K = d$ in both cases, there is no gain asymptotically, so the improvement should decrease with the sample size. This

Table 4: Average values of ν_2 and $\xi(\alpha)$ for $\alpha \in \{0.05, 0.5, 0.95\}$ for 500 simulation runs with $w = 1$.

| Measure n | \mathbf{T}_5 | | | \mathbf{T}_6 | | | \mathbf{T}_7 | | | \mathbf{T}_8 | | |
|-------------------|----------------|------|------|----------------|------|------|----------------|------|------|----------------|------|------|
| | 25 | 50 | 100 | 25 | 50 | 100 | 25 | 50 | 100 | 25 | 50 | 100 |
| $\bar{\nu}_2$ | 0.47 | 0.52 | 0.54 | 0.48 | 0.46 | 0.48 | 0.66 | 0.51 | 0.37 | 0.42 | 0.38 | 0.34 |
| $\bar{\xi}(0.05)$ | 0.30 | 0.31 | 0.34 | 0.40 | 0.31 | 0.29 | 0.60 | 0.47 | 0.33 | 0.31 | 0.20 | 0.11 |
| $\bar{\xi}(0.50)$ | 0.34 | 0.37 | 0.38 | 0.40 | 0.33 | 0.31 | 0.59 | 0.48 | 0.34 | 0.32 | 0.22 | 0.13 |
| $\bar{\xi}(0.95)$ | 0.37 | 0.40 | 0.44 | 0.41 | 0.34 | 0.33 | 0.58 | 0.47 | 0.32 | 0.33 | 0.23 | 0.15 |

is already apparent for \mathbf{T}_8 for the sample sizes considered here.

7 APPLICATION TO STOCK RETURNS

We collected the daily value at close of all $d = 106$ stocks included in the NASDAQ100 index from the beginning of 2017 up to 2017/09/16 (as reported by Google Finance on 2017/09/17). The information on the components of the index (company name, sectors and industries) were taken from www.nasdaq.com. Our primary goal is not to cluster together stocks whose returns have a similar distribution, but rather to simplify their dependence structure by assuming partial exchangeability. Because the PEA is associated with a particular clustering of the variables, we can further verify if the clusters correspond to intuitive categories like business sectors.

As is the norm in joint modelling of financial time series, we compute the log returns for series of stocks and apply our methodology to the series of residuals from a fitted stochastic volatility model (Patton, 2006, 2012; Rémillard, 2013). The stochastic volatility model that yielded satisfactory results in this application was the GARCH (1, 1) model. This produced $n = 177$ residuals for each of the $d = 106$ stocks.

Note that even under the assumption that the stochastic volatility model is appropriate, the residuals are not i.i.d. However, as shown in Rémillard (2017, Corollary 2), the empirical copula process based on the residuals has the same asymptotic behavior as the empirical copula process for i.i.d. observations. As a result, (13) continues to hold with the very same asymptotic variance Σ_∞ . Even if Σ may not be the exact finite-sample variance of $\hat{\tau}$ based on the residuals, the result of Rémillard (2017) implies that (5) and (18) remain true. Consequently, the methodology developed here can be used as is.

For computational purposes and because the ratio $n/d = 1.67$ is small, we applied Algorithm 1 with $w = 1$. We then computed $\alpha^{(i)}$, $i = 106, \dots, 1$, as given by (19), again with $w = 1$. An excerpt of the plot is shown in Figure 9; $\alpha^{(i)}$ for $i > 20$ and $i < 10$ were essentially equal to 1 and 0, respectively. Among the 106 candidate structures produced by Algorithm 1, $\mathcal{G}^{(16)}$, $\mathcal{G}^{(15)}$ and $\mathcal{G}^{(14)}$ stand out as the most interesting, because they precede drops in $\alpha^{(i)}$ that are typical of questionable cluster mergers. As a matter of fact the selection procedure is not very sensitive to the arbitrary choice of the value of α : any value of α between 0.01 and 0.99 leads to one of $\mathcal{G}^{(16)}$, $\mathcal{G}^{(15)}$ and $\mathcal{G}^{(14)}$ among the 106 structures that were returned by Algorithm 1. The reduction in dimension is striking; for instance if we use $\mathcal{G}^{(15)}$ we go from $d(d-1)/2 = 5565$ parameters down to $K(K+1)/2 = 120$.

The left panel in Figure 1 shows the empirical Kendall's tau matrix $\hat{\mathbf{T}}$ when the variables are labeled consecutively as in the NASDAQ100 index. Clearly, any pattern is very hard to discern from this matrix. The middle panel of the same figure shows $\hat{\mathbf{T}}$ once the variables have been relabeled according to the clusters in $\mathcal{G}^{(15)}$, i.e., so that the cluster membership matrix is block-diagonal. Now a structure is beginning to emerge. The right panel displays the improved estimator $\tilde{\mathbf{T}}^{(15)}$ that takes the cluster structure into account. The benefit of using Algorithm 1 is clearly visible here.

The clusters in $\mathcal{G}^{(15)}$ are listed in Appendix D of the Online Supplement. It is comforting

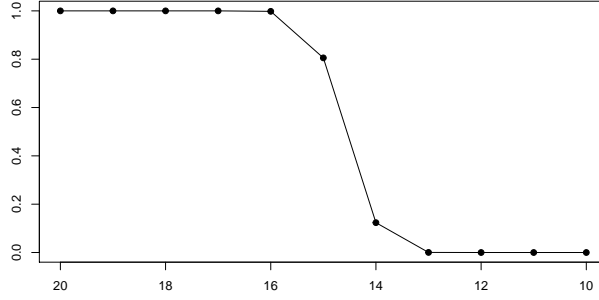


Figure 9: The pairs $(i, \alpha^{(i)})$, $i = 20, \dots, 10$ corresponding to the path returned by Algorithm 1 applied to the stock returns residuals.

that most of them have intuitive interpretations in terms of business sectors or known affiliations, particularly when the intra-cluster correlation is large. For example, cluster 4 is almost exclusively composed of stocks corresponding to semiconductor-related companies with intra-cluster correlation of 0.44; cluster 7 contains stocks from the biopharmaceutical industry only with intra-cluster correlation of 0.29. Furthermore, strongly related stocks are also clustered together: GOOG and GOOGL (.89); DISCA and DISCK (.88); FOX and FOXA (.87); LBTYK and LBTYA (.85); LILA and LILAK (.76).

8 CONCLUSION

We have developed a new approach to identify a block structure within the matrix of Kendall correlations. Aside from a mild partial exchangeability assumption, the method is completely nonparametric and does not require any additional assumption on the joint or marginal distributions of the variables (insofar as they are continuous). This contribution has the potential to be useful in all areas where the dependence between the variables is of interest. While goodness-of-fit tests can only be performed a posteriori, the proposed

method can serve as a model specification guide at the early stages of the data analysis.

We have formally shown that taking advantage of the block structure of the correlation matrix can lead to improved inference on the correlation coefficients. Not only are the new estimators consistent and asymptotically Normal, but their asymptotic variance is smaller than that of the empirical Kendall coefficients. This is important, as the latter tend to be extremely noisy when d gets large. But the improvements in the inference are not only true asymptotically when the correlation structure is known. Our simulations have shown that the new estimator has better mean squared error in finite samples even when the correlation structure is not known a priori and has to be estimated from the data.

The method that we propose to identify the blocks in the correlation matrix is an algorithm that performs an agglomerative clustering of the variables, not of observations. While this may still resemble model-based clustering, it differs from it in many aspects. Perhaps the most important difference is that the approach we use is independent of the distribution of the variables and concerns only $\hat{\tau}$, thus making the method model-free.

We have demonstrated that as the sample size gets large, this algorithm is based on a loss function that will assign negligible loss to merges that agree with the true block structure and large loss to merges that do not, which ensures that the agglomerative process will yield a set of d potential structures that includes the true one. We have also developed a tool that can help to identify the reasonable structures among the d proposed by the algorithm. The asymptotic properties of the loss function suggest that this tool will be adequate for large samples; our simulation study indicates good performance in finite samples as well. This suggests that block-exchangeable structures can be used as general-purpose shrinkage targets when n is small compared to d .

The loss function used in the agglomerative algorithm depends on a variance matrix Σ that must be estimated. We have shown under the Partial Exchangeability Assumption that

this matrix and its inverse share a common structure property. We exploit this property to improve the consistent plug-in estimator $\hat{\Sigma}$ of Σ . The new estimator $\tilde{\Sigma}_w$ is shown to possess the same structural properties as Σ .

Future work may follow from this proposal. The criterion $\alpha^{(i)}$ is intended as a guide and not as a formal test statistic or model selection criterion. Though such ad hoc selection tools are common in hierarchical clustering, perhaps a more formal statistic could be of value. For the shrinkage estimation of Σ , investigating adaptive weights w that would diminish with n and with each iteration of Algorithm 1 may also lead to slightly improved inference. Working with some, but not all, off-diagonal entries of $\hat{\Sigma}$ may also improve the performance of the procedure. Finally the already mild Partial Exchangeability Assumption could perhaps be relaxed to allow for more general hierarchical dependence structures.

Supplementary Material

The following material is available online.

Application code: R code to replicate the application on stocks. (.R)

Appendices: Supplementary theoretical and simulation results. (.pdf) This file contains:

Estimation of Σ (Appendix A), Outstanding proofs (Appendix B), Additional results of the simulation study (Appendix C), and Detailed clusters of the application to stock returns (Appendix D).

Web-based supporting materials for

Detection of Block-Exchangeable Structure in Large-Scale Correlation Matrices

Samuel Perreault Thierry Duchesne

Département de mathématiques et de statistique, Université Laval

Johanna G. Nešlehová

Department of Mathematics and Statistics, McGill University

May 5, 2022

A ESTIMATING Σ

Genest et al. (2011) traced back explicit formulas for the diagonal elements of Σ to Lindberg (1927, 1929). Extending the results of Ehrenberg (1952), they then provide a formula for the off-diagonal elements of Σ . Using this formula, given in (1) below, we define a plug-in estimator $\hat{\Sigma}$ of Σ . The estimator and its computation are presented in Subsection A.1. In most cases, it is not advisable to use $\hat{\Sigma}$ directly due to a high amount of noise in the estimation. More so because it needs to be inverted, which is known to amplify the estimation error when the original matrix is ill-conditioned. Fortunately, if \mathcal{G} satisfies the PEA, Σ has a block structure as well. The latter is described and explained in Subsection A.2. We then use this block structure to improve the estimation of Σ by averaging entries of $\hat{\Sigma}$ block-wise. The resulting estimate may still contain too much noise to be useful. Inspired by the work of Ledoit and Wolf (2004), we thus apply, in addition to the averaging just mentioned, a simple Stein-type shrinkage procedure which depends on a parameter w , often called the shrinkage intensity. The two shrinkage procedures are presented in Subsection A.3.

A.1 Plug-in estimator of Σ

Let \mathbf{X} be a random vector with continuous univariate marginals F_1, \dots, F_d and a unique copula C , as in Section 2. Let $\mathbf{U} = (F_1(X_1), \dots, F_d(X_d))$ and recall that \mathbf{U} has distribution function C . For any subset $\{i_1, \dots, i_k\} \subseteq \{1, \dots, d\}$ of indices, let C_{i_1, \dots, i_k} denote the unique copula of the marginal $(X_{i_1}, \dots, X_{i_k})$ of \mathbf{X} . As shown in Genest et al. (2011), for any $i_1 \neq j_1 \in \{1, \dots, d\}$ and $i_2 \neq j_2 \in \{1, \dots, d\}$,

$$\text{Cov}(\hat{\mathbf{T}}_{i_1 j_1}, \hat{\mathbf{T}}_{i_2 j_2}) = \left\{ \frac{4}{n(n-1)} \right\}^2 \{ n(n-1)(n-2)(\theta_1 + \theta_2 + \theta_3 + \theta_4) \} \quad (1)$$

$$+ n(n-1)(\vartheta_1 + \vartheta_2)\} - \frac{2(2n-3)}{n(n-1)}(\mathbf{T}_{i_1j_1} + 1)(\mathbf{T}_{i_2j_2} + 1),$$

where

$$\begin{aligned}\theta_1 &= \mathbb{E}(C_{i_1j_1}(U_{i_1}, U_{j_1})C_{i_2j_2}(U_{i_2}, U_{j_2})), & \theta_2 &= \mathbb{E}(\bar{C}_{i_1j_1}(U_{i_1}, U_{j_1})C_{i_2j_2}(U_{i_2}, U_{j_2})), \\ \theta_3 &= \mathbb{E}(C_{i_1j_1}(U_{i_1}, U_{j_1})\bar{C}_{i_2j_2}(U_{i_2}, U_{j_2})), & \theta_4 &= \mathbb{E}(\bar{C}_{i_1j_1}(U_{i_1}, U_{j_1})\bar{C}_{i_2j_2}(U_{i_2}, U_{j_2})), \\ \vartheta_1 &= \mathbb{E}(C_{i_1j_1i_2j_2}(U_{i_1}, U_{j_1}, U_{i_2}, U_{j_2})), & \vartheta_2 &= \mathbb{E}(\tilde{C}_{i_1j_1i_2j_2}(U_{i_1}, U_{j_1}, U_{i_2}, U_{j_2})),\end{aligned}\tag{2}$$

and \bar{C} denotes the survival function corresponding to C , while

$$\tilde{C}_{i_1j_1i_2j_2} = C_{i_1j_1} - C_{i_1j_1j_2} - C_{i_1j_1i_2} + C_{i_1j_1i_2j_2}.$$

For arbitrary $r, s \in \{1, \dots, p\}$, $\Sigma_{rs} = \text{Cov}(\hat{\mathbf{T}}_{i_rj_r}, \hat{\mathbf{T}}_{i_sj_s})$. From (1) and (2) and the fact that for all $i \neq j \in \{1, \dots, d\}$, $\mathbb{E}(C_{ij}(U_i, U_j)) = \mathbb{E}(\bar{C}_{ij}(U_i, U_j))$, we have, as $n \rightarrow \infty$, $n\Sigma \rightarrow \Sigma_\infty$, where for any $r, s \in \{1, \dots, p\}$, the (r, s) -th entry of Σ_∞ is given by

$$\begin{aligned}(\Sigma_\infty)_{rs} &= 16(\theta_1 + \theta_2 + \theta_3 + \theta_4) - 4(\mathbf{T}_{i_rj_r} + 1)(\mathbf{T}_{i_sj_s} + 1) \\ &= 16\text{Cov}\{C_{i_rj_r}(U_{i_r}, U_{j_r}) + \bar{C}_{i_rj_r}(U_{i_r}, U_{j_r}), C_{i_sj_s}(U_{i_s}, U_{j_s}) + \bar{C}_{i_sj_s}(U_{i_s}, U_{j_s})\}.\end{aligned}\tag{3}$$

For any $i_1 \neq j_1 \in \{1, \dots, d\}$ and $i_2 \neq j_2 \in \{1, \dots, d\}$, a plug-in estimator of $\text{Cov}(\hat{\mathbf{T}}_{i_1j_1}, \hat{\mathbf{T}}_{i_2j_2})$ can be defined by first replacing $\mathbf{T}_{i_1j_1}$ and $\mathbf{T}_{i_2j_2}$ by $\hat{\mathbf{T}}_{i_1j_1}$ and $\hat{\mathbf{T}}_{i_2j_2}$, respectively. Furthermore, the quantities in (2) can be estimated as follows. For $k = 1, 2$, let $\mathbf{I}^{(k)}$ be an $n \times n$ matrix with entries

$$\mathbf{I}_{rs}^{(k)} := \mathbb{1}(X_{ri_k} < X_{si_k}, X_{rj_k} < X_{sj_k}).\tag{4}$$

Similarly to the plug-in estimators considered in Ben Ghorbal et al. (2009), an unbiased estimator of θ_1 is then given by

$$\hat{\theta}_1 = \frac{1}{n(n-1)(n-2)} \sum_{r \neq s \neq t} \mathbb{1}(X_{ri_1} < X_{si_1}, X_{rj_1} < X_{sj_1}) \mathbb{1}(X_{ti_2} < X_{si_2}, X_{tj_2} < X_{sj_2})$$

$$= \frac{1}{n(n-1)(n-2)} \sum_{r \neq s \neq t} \mathbf{I}_{rs}^{(1)} \mathbf{I}_{ts}^{(2)}.$$

Similar formulas can be derived for the other parameters, viz.

$$\begin{aligned} \hat{\theta}_2 &= \frac{1}{n(n-1)(n-2)} \sum_{r \neq s \neq t} \mathbf{I}_{rs}^{(1)} \mathbf{I}_{tr}^{(2)}, & \hat{\theta}_3 &= \frac{1}{n(n-1)(n-2)} \sum_{r \neq s \neq t} \mathbf{I}_{rs}^{(1)} \mathbf{I}_{st}^{(2)}, \\ \hat{\theta}_4 &= \frac{1}{n(n-1)(n-2)} \sum_{r \neq s \neq t} \mathbf{I}_{rs}^{(1)} \mathbf{I}_{rt}^{(2)} \end{aligned}$$

and

$$\hat{\vartheta}_1 := \frac{1}{n(n-1)} \sum_{r \neq s} \mathbf{I}_{rs}^{(1)} \mathbf{I}_{rs}^{(2)}, \quad \hat{\vartheta}_2 := \frac{1}{n(n-1)} \sum_{r \neq s} \mathbf{I}_{rs}^{(1)} \mathbf{I}_{sr}^{(2)}.$$

Given that $\hat{\theta}_1, \dots, \hat{\theta}_4$ and $\hat{\vartheta}_1, \hat{\vartheta}_2$ are U -statistics with square integrable kernels, they are consistent and asymptotically Normal. These properties carry over to the resulting plug-in estimator $\hat{\Sigma}$ of Σ ; in particular,

$$n\hat{\Sigma} \rightarrow \Sigma_\infty \tag{5}$$

in probability, as $n \rightarrow \infty$. Similarly, one can define a consistent plug-in estimator of Σ_∞ by replacing $\theta_1, \dots, \theta_4$ and $\mathbf{T}_{i_1 j_1}$ and $\mathbf{T}_{i_2 j_2}$ by their estimators in (3).

Finally, note that $\hat{\Sigma}$ can be calculated efficiently using matrix products. To this end, consider again arbitrary $i_1 \neq j_1 \in \{1, \dots, d\}$ and $i_2 \neq j_2 \in \{1, \dots, d\}$, and for $k = 1, 2$, define $\mathbf{I}^{(k)}$ through (4) and set $\mathbf{J}^{(k)} = (\mathbf{I}^{(k)})^\top$. Furthermore, let $\mathbf{1}$ be the n -dimensional vector of ones and \circ denote the Hadamard product. Then because the diagonal entries of $\mathbf{I}^{(k)}$, $k = 1, 2$ are zero,

$$\begin{aligned} n(n-1)(n-2) \sum_{l=1}^4 \hat{\theta}_l &= \sum_{r \neq s \neq t} \left(\mathbf{I}_{rs}^{(1)} \mathbf{J}_{st}^{(2)} + \mathbf{J}_{rs}^{(1)} \mathbf{J}_{st}^{(2)} + \mathbf{I}_{rs}^{(1)} \mathbf{I}_{st}^{(2)} + \mathbf{J}_{rs}^{(1)} \mathbf{I}_{st}^{(2)} \right) \\ &= \sum_{r \neq t} \left[\left(\mathbf{I}^{(1)} + \mathbf{J}^{(1)} \right) \left(\mathbf{I}^{(2)} + \mathbf{J}^{(2)} \right) \right]_{rt} \end{aligned}$$

$$= \mathbf{1}^\top \left(\mathbf{I}^{(1)} + \mathbf{J}^{(1)} \right) \left(\mathbf{I}^{(2)} + \mathbf{J}^{(2)} \right) \mathbf{1} - \mathbf{1}^\top \left\{ \left(\mathbf{I}^{(1)} + \mathbf{J}^{(1)} \right) \circ \left(\mathbf{I}^{(2)} + \mathbf{J}^{(2)} \right) \right\} \mathbf{1}.$$

Similarly,

$$n(n-1)(\hat{v}_1 + \hat{v}_2) = \sum_{r \neq s} \mathbf{J}_{rs}^{(1)} \left[\mathbf{I}^{(2)} + \mathbf{J}^{(2)} \right]_{sr} = \mathbf{1}^\top \left\{ \mathbf{J}^{(1)} \circ \left(\mathbf{I}^{(2)} + \mathbf{J}^{(2)} \right) \right\} \mathbf{1},$$

so that

$$\begin{aligned} n(n-1)(n-2) \left(\sum_{l=1}^4 \hat{\theta}_l \right) + n(n-1)(\hat{v}_1 + \hat{v}_2) \\ = \mathbf{1}^\top \left(\mathbf{I}^{(1)} + \mathbf{J}^{(1)} \right) \left(\mathbf{I}^{(2)} + \mathbf{J}^{(2)} \right) \mathbf{1} - \mathbf{1}^\top \left\{ \mathbf{J}^{(1)} \circ \left(\mathbf{I}^{(2)} + \mathbf{J}^{(2)} \right) \right\} \mathbf{1}. \end{aligned}$$

A.2 Structure of Σ and Σ^{-1} implied by \mathcal{G}

Suppose that the Partial Exchangeability Assumption (PEA) holds for some partition \mathcal{G} . In this subsection, we describe the block structure of Σ and Σ^{-1} induced by the PEA. In Subsection A.3 we then exploit this structure to derive the improved estimator $\tilde{\Sigma}$ of Σ . To this end, let us first focus on a single entry Σ_{rs} for some arbitrary fixed $r, s \in \{1, \dots, p\}$. Recall that \mathcal{G} induces the partition $\mathcal{B}_{\mathcal{G}} = \{\mathcal{B}_1, \dots, \mathcal{B}_L\}$ of $\{1, \dots, p\}$, as given in (8). Equation (1) suggests that the value of Σ_{rs} depends on the blocks in $\mathcal{B}_{\mathcal{G}}$ to which r and s belong. To identify these blocks, let

$$\Phi_1 = \{(\ell_1, \ell_2) : 1 \leq \ell_1 \leq \ell_2 \leq L\}$$

be the set of all ordered pairs of block indices and define the function

$$\begin{aligned} \phi : \{1, \dots, p\}^2 &\rightarrow \Phi_1 \\ (r, s) &\mapsto (\ell_1 \wedge \ell_2, \ell_1 \vee \ell_2) \text{ such that } (r, s) \in \mathcal{B}_{\ell_1} \times \mathcal{B}_{\ell_2}, \end{aligned} \tag{6}$$

where for any $a, b \in \mathbb{R}$, $a \wedge b = \min(a, b)$ and $a \vee b = \max(a, b)$. Now recall from Section 2 that (i_r, j_r) is a pair of indices such that $\boldsymbol{\tau}_r = \mathbf{T}_{i_r j_r}$ and similarly for (i_s, j_s) . The value of $\boldsymbol{\Sigma}_{rs}$ does not depend only on $\phi(r, s)$, but also on the overlap between (i_r, j_r) and (i_s, j_s) . To account for the latter, let

$$\boldsymbol{\Phi}_2 = \{(k_1, k_2) : 0 \leq k_1 \leq k_2 \leq K\} \quad (7)$$

and define the function $\varphi : \{1, \dots, p\}^2 \rightarrow \boldsymbol{\Phi}_2$ given by

$$\varphi(r, s) = \begin{cases} (0, 0) & \text{if } \{i_r, j_r\} \cap \{i_s, j_s\} = \emptyset, \\ (0, k) & \text{if } \{i_r, j_r\} \cap \{i_s, j_s\} = \{i\}, i \in \mathcal{G}_k, \\ (k_1 \wedge k_2, k_1 \vee k_2) & \text{if } \{i_r, j_r\} \cap \{i_s, j_s\} = \{i, j\}, (i, j) \in (\mathcal{G}_{k_1} \times \mathcal{G}_{k_2}). \end{cases} \quad (8)$$

Using this notation, we introduce, for any $\boldsymbol{\ell} = (\ell_1, \ell_2) \in \boldsymbol{\Phi}_1$ and $\mathbf{k} = (k_1, k_2) \in \boldsymbol{\Phi}_2$,

$$\mathcal{C}_{\boldsymbol{\ell}\mathbf{k}} := \{(r, s) \in \{1, \dots, p\}^2 : r \leq s, \phi(r, s) = \boldsymbol{\ell}, \varphi(r, s) = \mathbf{k}\}, \quad (9)$$

and set $\mathcal{C}_{\mathcal{G}} := \{\mathcal{C}_{\boldsymbol{\ell}\mathbf{k}} : (\boldsymbol{\ell}, \mathbf{k}) \in \boldsymbol{\Phi}_1 \times \boldsymbol{\Phi}_2\}$. Similarly to $\mathcal{T}_{\mathcal{G}}$, we now define the set $\mathcal{S}_{\mathcal{G}}$ of matrices with a block structure given by $\mathcal{C}_{\mathcal{G}}$, i.e.,

$$\begin{aligned} \mathcal{S}_{\mathcal{G}} := \{ \mathbf{S} \in \mathbb{R}^{p \times p} : \mathbf{S} \text{ symmetric and } \forall (\boldsymbol{\ell}, \mathbf{k}) \in \boldsymbol{\Phi}_1 \times \boldsymbol{\Phi}_2 \\ (r_1, s_1), (r_2, s_2) \in \mathcal{C}_{\boldsymbol{\ell}\mathbf{k}} \Rightarrow \mathbf{S}_{r_1 s_1} = \mathbf{S}_{r_2 s_2} \}. \end{aligned} \quad (10)$$

Finally, for each $r \in \{1, \dots, p\}$, $\ell \in \{1, \dots, L\}$ and $\mathbf{k} \in \boldsymbol{\Phi}_2$, we shall also need the set

$$\mathcal{C}_{\boldsymbol{\ell}\mathbf{k}}^{(r)} := \{s \in \mathcal{B}_{\ell} : \varphi(r, s) = \mathbf{k}\}. \quad (11)$$

The next proposition confirms that $\boldsymbol{\Sigma}$ and $\boldsymbol{\Sigma}_{\infty}$ have the block structure induced by $\mathcal{C}_{\mathcal{G}}$.

Proposition 5. *Suppose that \mathcal{G} is such that the PEA holds. Then $\boldsymbol{\Sigma} \in \mathcal{S}_{\mathcal{G}}$ and $\boldsymbol{\Sigma}_{\infty} \in \mathcal{S}_{\mathcal{G}}$.*

Proof. Fix arbitrary $(\ell, \mathbf{k}) \in \Phi_1 \times \Phi_2$ and $(r_1, s_1), (r_2, s_2) \in \mathcal{C}_{\ell \mathbf{k}}$. To ease the notation, write $(i_1, j_1), (i_2, j_2), (i_3, j_3)$ and (i_4, j_4) instead of $(i_{r_1}, j_{r_1}), (i_{s_1}, j_{s_1}), (i_{r_2}, j_{r_2})$ and (i_{s_2}, j_{s_2}) , respectively. To prove the claim, it suffices to show all expectations in (1) are identical when (i_1, j_1) is changed to (i_3, i_3) and (i_2, j_2) to (i_4, j_4) , respectively. Focusing on θ_1 , we want to show

$$\mathbb{E}[C_{i_1 j_1}(U_{i_1}, U_{j_1}) C_{i_2 j_2}(U_{i_2}, U_{j_2})] = \mathbb{E}[C_{i_3 j_3}(U_{i_3}, U_{j_3}) C_{i_4 j_4}(U_{i_4}, U_{j_4})]. \quad (12)$$

Let \mathbf{I} be the set of unique indices from (i_1, j_1, i_2, j_2) and $\mathbf{I}^m = (i_m, j_m)$, $m = 1, 2$. The LHS of (12) can then be rewritten as

$$\begin{aligned} \mathbb{E}(C_{i_1 j_1}(U_{i_1}, U_{j_1}) C_{i_2 j_2}(U_{i_2}, U_{j_2})) &= \int C_{i_1 j_1}(u_{i_1}, u_{j_1}) C_{i_2 j_2}(u_{i_2}, u_{j_2}) \, dC_{i_1 j_1 i_2 j_2} \\ &= \int C_{\mathbf{I}^1}(\mathbf{u}_{\mathbf{I}^1}) C_{\mathbf{I}^2}(\mathbf{u}_{\mathbf{I}^2}) \, dC_{\mathbf{I}}. \end{aligned} \quad (13)$$

Now define \mathbf{J} to be the set of distinct indices from (i_3, j_3, i_4, j_4) and $\mathbf{J}^m = (i_{m+2}, j_{m+2})$, $m = 1, 2$. Combining the facts that $\phi(r_1, s_1) = \phi(r_2, s_2)$ and $\varphi(r_1, s_1) = \varphi(r_2, s_2)$, we deduce that for any $k \in \{1, \dots, K\}$, \mathbf{I} and \mathbf{J} have the same number of entries coming from \mathcal{G}_k , with no repetition. The same can be deduced for \mathbf{I}^m and \mathbf{J}^m , $m = 1, 2$. We can therefore use the PEA to replace $C_{\mathbf{I}}$ by $C_{\mathbf{J}}$ and $C_{\mathbf{I}^m}$ by $C_{\mathbf{J}^m}$ for $m = 1, 2$. Consequently,

$$\int C_{\mathbf{I}^1}(\mathbf{u}_{\mathbf{I}^1}) C_{\mathbf{I}^2}(\mathbf{u}_{\mathbf{I}^2}) \, dC_{\mathbf{I}} = \int C_{\mathbf{J}^1}(\mathbf{u}_{\mathbf{J}^1}) C_{\mathbf{J}^2}(\mathbf{u}_{\mathbf{J}^2}) \, dC_{\mathbf{J}},$$

thus showing that (13) is indeed equal to the RHS of (12). Equalities for the other quantities $\theta_2, \dots, \theta_4$ and ϑ_1, ϑ_2 can be shown using the same technique. \square

Example 7. For \mathcal{G} as given in (4) in Example 1, there are $L = 6$ sets in $\mathcal{B}_{\mathcal{G}}$, viz.

$$\mathcal{B}_{\mathcal{G}} = \{\mathcal{B}_{11}, \mathcal{B}_{12}, \mathcal{B}_{13}, \mathcal{B}_{22}, \mathcal{B}_{23}, \mathcal{B}_{33}\} \equiv \{\mathcal{B}_1, \dots, \mathcal{B}_6\}, \quad (14)$$

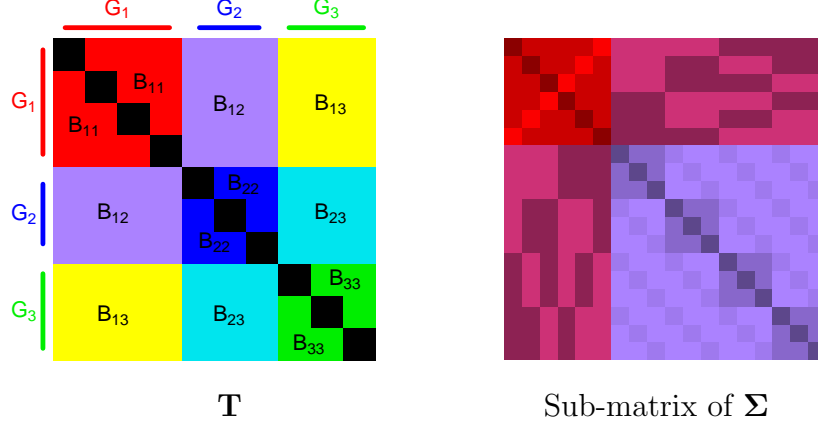


Figure 10: The matrix \mathbf{T} (left) and a sub-matrix of Σ (right) from Example 7. The cells are tinted so that, in each matrix, all entries sharing the same value are of the same colour and colour intensity.

where for $k_1, k_2 \in \{1, \dots, 3\}$, $\mathcal{B}_{k_1 k_2}$ is as in (6). The blocks in $\mathcal{B}_{\mathcal{G}}$ are displayed in left panel of Figure 10. In this picture, for each $k_1, k_2 \in \{1, 2, 3\}$, the cells (i_r, j_r) and (j_r, i_r) for $r \in \mathcal{B}_{k_1 k_2}$ are tinted with the same colour, emphasizing that the entries are equal.

Given that $p = d(d+1)/2 = 9(10)/2 = 45$, the 45×45 matrix Σ is more cumbersome to visualize. To see its structure more clearly, we vectorize \mathbf{T} not as in (5), but rather block by block. For instance the first 18 entries of $\boldsymbol{\tau}$ are the 6 entries in \mathbf{T} corresponding to $\mathcal{B}_{11} \equiv \mathcal{B}_1 = \{1, \dots, 6\}$ followed by the 12 entries in \mathbf{T} corresponding to $\mathcal{B}_{12} \equiv \mathcal{B}_2 = \{7, \dots, 18\}$, i.e. $(\boldsymbol{\tau}_1, \dots, \boldsymbol{\tau}_{18}) = (\mathbf{T}_{1,2}, \mathbf{T}_{1,3}, \mathbf{T}_{1,4}, \mathbf{T}_{2,3}, \mathbf{T}_{2,4}, \mathbf{T}_{3,4}, \mathbf{T}_{1,5}, \dots, \mathbf{T}_{4,7})$. The 18×18 dimensional sub-matrix of Σ displaying the pair-wise covariances of $\hat{\boldsymbol{\tau}}_1, \dots, \hat{\boldsymbol{\tau}}_{18}$ is showed in the right panel of Figure 10. Distinct values are depicted using different colour and colour intensity. The colours represent distinct values of ϕ : for all $r, s \in \{1, \dots, 18\}$, the cell (r, s) is tinted red, magenta and violet if $\phi(r, s)$ equals $(1, 1)$, $(1, 2)$ and $(2, 2)$, respectively. In other words, the coloured blocks are induced by \mathcal{B}_{11} and \mathcal{B}_{12} . Next, notice

that in each coloured block, the values of Σ can differ, and this is depicted through different colour intensity. This is because for any $r, s \in \{1, \dots, p\}$, the value of Σ_{rs} also depends on $\varphi(r, s)$. For example, the red block in the top left corner contains three distinct values, for if $r, s \in \{1, \dots, 6\}$, $\{i_r, j_r\} \cap \{i_s, j_s\}$ is either empty (red), contains one element from \mathcal{G}_1 (light red), or contains two elements from \mathcal{G}_1 (dark red). To illustrate, consider $r = 1, 2, 6$. Then $(i_1, j_1) = (1, 2)$, $(i_2, j_2) = (1, 3)$, and $(i_6, j_6) = (3, 4)$. Consequently, $\phi(1, 1) = \phi(1, 2) = \phi(1, 6) = (1, 1)$, and indeed the entries Σ_{11} , Σ_{12} and Σ_{16} are tinted red. However, $\varphi(1, 1) = (1, 1)$, $\varphi(1, 2) = (0, 1)$ and $\varphi(1, 6) = (0, 0)$, which is why Σ_{11} , Σ_{12} and Σ_{16} are dark red, red and light red, respectively. One can indeed verify that $\Sigma_{11} \neq \Sigma_{12} \neq \Sigma_{16}$. This shows that the block structure Σ is described by both ϕ and φ ; the sets in $\mathcal{C}_{\mathcal{G}}$ correspond to the cells above the main diagonal of Σ with the same colour and intensity.

Finally, the right panel in Figure 10 can be used to visualize the sets $\mathcal{C}_{\ell \mathbf{k}}^{(r)}$ defined in (11). For a given $r \in \{1, \dots, p\}$, the union of the sets $\mathcal{C}_{\ell \mathbf{k}}^{(r)}$, $\ell \in \{1, \dots, L\}$, $\mathbf{k} \in \Phi_2$ may be identified with the r -th row (or equivalently the r -th column) of Σ : the index ℓ determines the colour and \mathbf{k} the intensity in that row (column). To illustrate in the context of this example, pick $r = 1$ and $\ell = 1$, say. Then

$$\mathcal{C}_{1(1,1)}^{(1)} = \{1\}, \quad \mathcal{C}_{1(0,1)}^{(1)} = \{2, 3, 4, 5\}, \quad \mathcal{C}_{1(0,0)}^{(1)} = \{6\},$$

while $\mathcal{C}_{1\mathbf{k}}^{(1)} = \emptyset$ for any other $\mathbf{k} \in \Phi_2$. Note that $\{\mathcal{C}_{1(1,1)}^{(1)}, \mathcal{C}_{1(0,1)}^{(1)}, \mathcal{C}_{1(0,0)}^{(1)}\}$ is a partition of \mathcal{B}_{11} .

The loss function ℓ depends on Σ through its inverse Σ^{-1} . The following proposition establishes that the structure of Σ^{-1} is the same as that of Σ .

Proposition 6. *Suppose that \mathcal{G} is a partition for which the PEA holds. An invertible matrix \mathbf{S} is an element of $\mathcal{S}_{\mathcal{G}}$ if and only if $\mathbf{S}^{-1} \in \mathcal{S}_{\mathcal{G}}$. That is, $\mathcal{S}_{\mathcal{G}}$ is closed under inversion.*

Proof. From the Cayley-Hamilton Theorem (Harville, 2008, p.583) \mathbf{S} satisfies its characteristic equation

$$\mathbf{S}^p + \sum_{s=1}^{p-1} c_s \mathbf{S}^s + (-1)^p |\mathbf{S}| \mathbf{I}_p = 0,$$

for some known coefficients c_s , $s = 1, \dots, p-1$. As a consequence, the inverse of a $p \times p$ matrix \mathbf{S} can be represented by a linear function of its $p-1$ first powers:

$$\mathbf{S}^{-1} = \frac{1}{|\mathbf{S}|} \sum_{s=1}^p c_s \mathbf{S}^{s-1}.$$

Therefore, it suffices to show that if $\mathbf{S}, \mathbf{Q} \in \mathcal{S}_{\mathcal{G}}$ and $\mathbf{S}\mathbf{Q}$ is symmetric, $\mathbf{S}\mathbf{Q} \in \mathcal{S}_{\mathcal{G}}$. To this end, fix an arbitrary $\boldsymbol{\ell} = (\ell_1, \ell_2) \in \boldsymbol{\Phi}_1$, $\mathbf{k} = (k_1, k_2) \in \boldsymbol{\Phi}_2$, and arbitrary pairs $(r_1, s_1), (r_2, s_2) \in \mathcal{C}_{\boldsymbol{\ell}\mathbf{k}}$. To show that $[\mathbf{S}\mathbf{Q}]_{r_1 s_1} = [\mathbf{S}\mathbf{Q}]_{r_2 s_2}$, first note that because $\mathbf{S}\mathbf{Q}$ is symmetric by assumption, it can be assumed, without loss of generality, that $r_1, r_2 \in \mathcal{B}_{\ell_1}$ and $s_1, s_2 \in \mathcal{B}_{\ell_2}$. For any $\boldsymbol{\ell}^* \in \boldsymbol{\Phi}_1$ and any $\mathbf{k}^* \in \boldsymbol{\Phi}_2$, let $\mathbf{S}^{\boldsymbol{\ell}^* \mathbf{k}^*}$ and $\mathbf{Q}^{\boldsymbol{\ell}^* \mathbf{k}^*}$ denote the unique values such that $\mathbf{S}_{rs} = \mathbf{S}^{\boldsymbol{\ell}^* \mathbf{k}^*}$ and $\mathbf{Q}_{rs} = \mathbf{Q}^{\boldsymbol{\ell}^* \mathbf{k}^*}$ whenever $(r, s) \in \mathcal{C}_{\boldsymbol{\ell}^* \mathbf{k}^*}$. Because $\mathcal{B}_{\mathcal{G}}$ given by (8) is a partition of $\{1, \dots, p\}$, we can write

$$[\mathbf{S}\mathbf{Q}]_{r_1 s_1} = \sum_{t=1}^p \mathbf{S}_{r_1 t} \mathbf{Q}_{t s_1} = \sum_{\ell=1}^L \sum_{t \in \mathcal{B}_{\ell}} \mathbf{S}_{r_1 t} \mathbf{Q}_{t s_1}. \quad (15)$$

For any fixed $\ell \in \{1, \dots, d\}$ and $t \in \mathcal{B}_{\ell}$, $\phi(r_1, t) = (\ell \wedge \ell_1, \ell \vee \ell_1) \equiv \boldsymbol{\ell}_{1\ell}$ and $\phi(s_1, t) = (\ell \wedge \ell_2, \ell \vee \ell_2) \equiv \boldsymbol{\ell}_{2\ell}$. However, $\mathbf{S}_{r_1 t}$ and $\mathbf{Q}_{t s_1}$ also depend on $\varphi(r_1, t)$ and $\varphi(s_1, t)$, and this requires further partitioning of \mathcal{B}_{ℓ} by means of the sets defined in (11). Specifically,

$$\mathcal{B}_{\ell} = \bigcup_{\mathbf{k}_1, \mathbf{k}_2 \in \boldsymbol{\Phi}_2} (\mathcal{C}_{\boldsymbol{\ell}\mathbf{k}_1}^{(r_1)} \cap \mathcal{C}_{\boldsymbol{\ell}\mathbf{k}_2}^{(s_1)}).$$

Clearly, the sets $(\mathcal{C}_{\boldsymbol{\ell}\mathbf{k}_1}^{(r_1)} \cap \mathcal{C}_{\boldsymbol{\ell}\mathbf{k}_2}^{(s_1)})$ are disjoint for distinct $\mathbf{k}_1, \mathbf{k}_2 \in \boldsymbol{\Phi}_2$, and for any given $\mathbf{k}_1, \mathbf{k}_2 \in \boldsymbol{\Phi}_2$ and $t \in \mathcal{C}_{\boldsymbol{\ell}\mathbf{k}_1}^{(r_1)} \cap \mathcal{C}_{\boldsymbol{\ell}\mathbf{k}_2}^{(s_1)}$, $\varphi(r_1, t) = \mathbf{k}_1$ and $\varphi(t, s_1) = \mathbf{k}_2$ so that $\mathbf{S}_{r_1 t} = \mathbf{S}^{\boldsymbol{\ell}_{1\ell} \mathbf{k}_1}$ and

$\mathbf{Q}_{ts_1} = \mathbf{Q}^{\ell_{2t}\mathbf{k}_2}$. Consequently, the last expression in (15) can be rewritten as

$$\sum_{\ell=1}^L \sum_{\mathbf{k}_1, \mathbf{k}_2 \in \Phi_2} \sum_{t \in \mathcal{C}_{\ell\mathbf{k}_1}^{(r_1)} \cap \mathcal{C}_{\ell\mathbf{k}_2}^{(s_1)}} \mathbf{S}^{\ell_{1t}\mathbf{k}_1} \mathbf{Q}^{\ell_{2t}\mathbf{k}_2} = \sum_{\ell=1}^L \sum_{\mathbf{k}_1, \mathbf{k}_2 \in \Phi_2} \left| \mathcal{C}_{\ell\mathbf{k}_1}^{(r_1)} \cap \mathcal{C}_{\ell\mathbf{k}_2}^{(s_1)} \right| \mathbf{S}^{\ell_{1t}\mathbf{k}_1} \mathbf{Q}^{\ell_{2t}\mathbf{k}_2}. \quad (16)$$

Now for any $\ell \in \{1, \dots, L\}$ and any $\mathbf{k}_1, \mathbf{k}_2 \in \Phi_2$, Lemma 3 gives that $|\mathcal{C}_{\ell\mathbf{k}_1}^{(r_1)} \cap \mathcal{C}_{\ell\mathbf{k}_2}^{(s_1)}| = |\mathcal{C}_{\ell\mathbf{k}_1}^{(r_2)} \cap \mathcal{C}_{\ell\mathbf{k}_2}^{(s_2)}|$. Furthermore, for any $t \in \mathcal{C}_{\ell\mathbf{k}_1}^{(r_2)} \cap \mathcal{C}_{\ell\mathbf{k}_2}^{(s_2)}$, $\phi(r_2, t) = \ell_{1t}$, $\phi(t, s_2) = \ell_{2t}$ and $\varphi(r_2, t) = \mathbf{k}_1$, $\varphi(t, s_2) = \mathbf{k}_2$, so that $\mathbf{S}_{r_2t} = \mathbf{S}^{\ell_{1t}\mathbf{k}_1}$, and $\mathbf{Q}_{ts_2} = \mathbf{Q}^{\ell_{2t}\mathbf{k}_2}$. Consequently, the RHS in (16) equals

$$\sum_{\ell=1}^L \sum_{\mathbf{k}_1, \mathbf{k}_2 \in \Phi_2} \left| \mathcal{C}_{\ell\mathbf{k}_1}^{(r_2)} \cap \mathcal{C}_{\ell\mathbf{k}_2}^{(s_2)} \right| \mathbf{S}^{\ell_{1t}\mathbf{k}_1} \mathbf{Q}^{\ell_{2t}\mathbf{k}_2} = \sum_{\ell=1}^L \sum_{\mathbf{k}_1, \mathbf{k}_2 \in \Phi_2} \sum_{t \in \mathcal{C}_{\ell\mathbf{k}_1}^{(r_2)} \cap \mathcal{C}_{\ell\mathbf{k}_2}^{(s_2)}} \mathbf{S}_{r_2t} \mathbf{Q}_{ts_2} = [\mathbf{S}\mathbf{Q}]_{r_2s_2},$$

as claimed. \square

In view of Proposition 5, the following result follows directly from Proposition 6.

Corollary 1. *Suppose that \mathcal{G} is such that the PEA holds. If Σ is invertible, then $\Sigma^{-1} \in \mathcal{S}_{\mathcal{G}}$. Similarly, if Σ_{∞} is invertible, then $\Sigma_{\infty}^{-1} \in \mathcal{S}_{\mathcal{G}}$.*

A.3 An improved estimator of Σ

Throughout this section, assume that \mathcal{G} is a partition of $\{1, \dots, d\}$ such that the PEA holds. The empirical estimator $\hat{\Sigma}$ defined in Section A.1 does not exploit the structural information provided by $\mathcal{C}_{\mathcal{G}}$. It is natural to think that, as was the case for τ , we can improve the estimation of Σ by averaging its entries with respect to the sets in $\mathcal{C}_{\mathcal{G}}$. But we can do even better by exploiting the following decomposition of Σ . To this end, write

$$\Sigma = \Theta - \frac{2(2n-3)}{n(n-1)}(\tau + \mathbf{1})(\tau + \mathbf{1})^{\top} \quad (17)$$

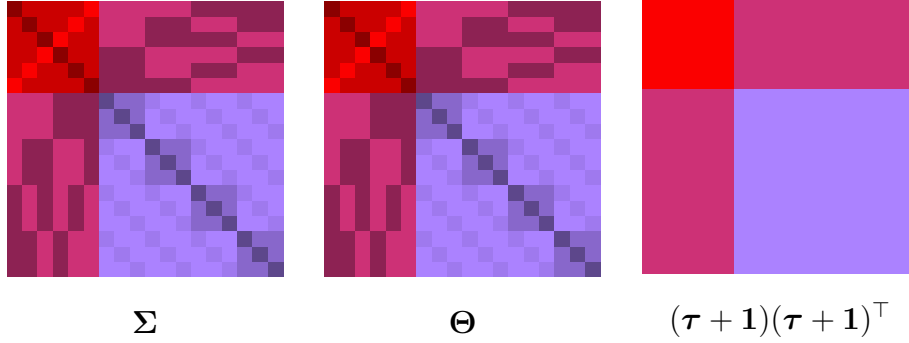


Figure 11: Submatrices of Σ , Θ and $(\boldsymbol{\tau} + \mathbf{1})(\boldsymbol{\tau} + \mathbf{1})^\top$ from Example 8. The same vectorization of \mathbf{T} as in Example 7 is used.

where $\mathbf{1}$ is the p -dimensional vector of ones and Θ is a $p \times p$ matrix gathering the terms involving $\theta_1, \dots, \theta_4$ and ϑ_1, ϑ_2 in (1). It easily follows from the proof of Proposition 5 that $\Theta \in \mathcal{S}_{\mathcal{G}}$ as well as $(\boldsymbol{\tau} + \mathbf{1})(\boldsymbol{\tau} + \mathbf{1})^\top \in \mathcal{S}_{\mathcal{G}}$. However, the structure of $(\boldsymbol{\tau} + \mathbf{1})(\boldsymbol{\tau} + \mathbf{1})^\top$ is even simpler, because the overlaps between pairs of indices described by the function φ need not be taken into account. Specifically, $(\boldsymbol{\tau} + \mathbf{1})(\boldsymbol{\tau} + \mathbf{1})^\top \in \mathcal{T}_{\mathcal{B}_{\mathcal{G}}} \subset \mathcal{S}_{\mathcal{G}}$, where

$$\mathcal{T}_{\mathcal{B}_{\mathcal{G}}} = \{\mathbf{R} \in \mathbb{R}^{p \times p} : \forall \ell_1, \ell_2 \in \{1, \dots, L\}, r_1, r_2 \in \mathcal{B}_{\ell_1} \text{ and } s_1, s_2 \in \mathcal{B}_{\ell_2} \Rightarrow \mathbf{R}_{r_1 s_1} = \mathbf{R}_{r_2 s_2}\}.$$

That is, $(\boldsymbol{\tau} + \mathbf{1})(\boldsymbol{\tau} + \mathbf{1})^\top$ possesses a block structure similar to \mathbf{T} , but defined in accordance with the clustering $\mathcal{B}_{\mathcal{G}}$ instead of \mathcal{G} . In particular, $(\boldsymbol{\tau} + \mathbf{1})(\boldsymbol{\tau} + \mathbf{1})^\top$ possesses L diagonal blocks, as opposed to K diagonal blocks for \mathbf{T} (counting the diagonal blocks that correspond to clusters in \mathcal{G} of size 1 as well). The decomposition (17) of Σ is illustrated next.

Example 8. *The decomposition of Σ from Example 1 according to (17) is depicted in Figure 11. The matrix Σ clearly inherits its structure from $\Theta \in \mathcal{S}_{\mathcal{G}}$ and the structure of $(\boldsymbol{\tau} + \mathbf{1})(\boldsymbol{\tau} + \mathbf{1})^\top$ is considerably simpler.*

Let $\hat{\Theta}$ be the plug-in empirical estimator of Θ , defined by replacing, for each $(r, s) \in$

$\{1, \dots, p\}^2$, the parameters $\theta_1, \dots, \theta_4$ and ϑ_1, ϑ_2 by their empirical estimates given in Section A.1. Because $\Theta \in \mathcal{S}_{\mathcal{G}}$, we now define the improved estimator $\tilde{\Theta}$, which is in $\mathcal{S}_{\mathcal{G}}$ by construction. First, the upper triangular (including the diagonal) entries of $\tilde{\Theta}$ are simply the entries of $\hat{\Theta}$ averaged out over each block in $\mathcal{C}_{\mathcal{G}}$. Second, because $\tilde{\Theta}$ is symmetric its lower triangular entries are obtained by symmetry. Furthermore, let $\tilde{\tau} = \tilde{\tau}(\hat{\tau}|\mathcal{G})$ be as in (15) and estimate $(\tau + \mathbf{1})(\tau + \mathbf{1})^\top$ by $(\tilde{\tau} + \mathbf{1})(\tilde{\tau} + \mathbf{1})^\top \in \mathcal{T}_{\mathcal{B}_{\mathcal{G}}}$, so that even more averaging is employed. The resulting estimator $\tilde{\Sigma}$ is then

$$\tilde{\Sigma} = \tilde{\Theta} - \frac{2(2n-3)}{n(n-1)}(\tilde{\tau} + \mathbf{1})(\tilde{\tau} + \mathbf{1})^\top.$$

Clearly, $\tilde{\Sigma} \in \mathcal{S}_{\mathcal{G}}$. Using (3), write $\Sigma_\infty = \Theta_\infty - 4(\tau + \mathbf{1})(\tau + \mathbf{1})^\top$, where Θ_∞ has entries $16(\theta_1 + \dots + \theta_4)$. Note that from the proof of Proposition 5, $\Theta_\infty \in \mathcal{S}_{\mathcal{G}}$. Hence, as $n \rightarrow \infty$, $n\tilde{\Theta} \rightarrow \Theta_\infty$ element-wise in probability. Furthermore, given that $\tilde{\tau}$ is a consistent estimator of τ as per Theorem 2, $(\tilde{\tau} + \mathbf{1})(\tilde{\tau} + \mathbf{1})^\top \rightarrow (\tau + \mathbf{1})(\tau + \mathbf{1})^\top$. Put together,

$$n\tilde{\Sigma} \rightarrow \Sigma_\infty \tag{18}$$

element-wise in probability.

When n is small compared to d , and $|\mathcal{G}|$ is large, not enough averaging is operated and $\tilde{\Sigma}$ may be too noisy to be useful. We therefore apply (Steinian) shrinkage and consider

$$\tilde{\Sigma}_w := \tilde{\Sigma}(\hat{\Sigma}|\hat{\tau}, \mathcal{G}, w) := (1-w)\tilde{\Sigma} + w\tilde{\Sigma}_{\text{diag}}, \tag{19}$$

where $\tilde{\Sigma}_{\text{diag}}$ is the diagonal matrix whose non zero elements are the elements on the diagonal of $\tilde{\Sigma}$ and $w \in [0, 1]$ is the shrinkage intensity parameter. This type of “linear shrinkage” follows the proposal in Devlin et al. (1975). It is easy to show that $\tilde{\Sigma}_w \in \mathcal{S}_{\mathcal{G}}$. Because $\tilde{\Sigma}$ is consistent, so is $\tilde{\Sigma}_w$, as long as $w \rightarrow 0$ as $n \rightarrow \infty$.

Finally, note that the estimators $\hat{\Sigma}$, $\tilde{\Sigma}$, and $\tilde{\Sigma}_w$ may not be positive definite, in particular when n is small. For the methodology presented in this paper, $\tilde{\Sigma}_w$ needs to be invertible,

and this is often easily achieved by a larger value of the shrinkage parameter w when n is small; in the data illustration and simulation study conducted in this paper no problems with invertibility were encountered. If the estimator of Σ further needs to be positive semi-definite, one can project any of the estimators $\hat{\Sigma}$, $\tilde{\Sigma}$, and $\tilde{\Sigma}_w$ to the cone of positive semi-definite matrices; this projection, say $\bar{\Sigma}$, can be computed using the alternative direction of multipliers algorithm as described, e.g., in Appendix A of Datta and Zou (2017). Since the projection onto the cone of positive semidefinite matrices is a continuous mapping, $\bar{\Sigma}$ will be consistent.

B OUTSTANDING PROOFS

This section is divided as follows. Subsection B.1 contains six auxiliary lemmas that pertain to the structure of $\mathcal{S}_{\mathcal{G}}$ and that are invoked in the proofs of Theorem 1, Theorem 2 and Proposition 4. The proof of Proposition 4 is detailed in Subsection B.2 while Subsection B.3 contains additional results on the structural properties of the inverse of correlation matrices used in Section 5 of the paper.

B.1 Description of $\mathcal{S}_{\mathcal{G}}$

We first present three auxiliary lemmas that pertain to the cardinality of the sets $\mathcal{C}_{\ell\mathbf{k}}^{(r)}$ defined in (11).

Lemma 1. *Let \mathcal{G} be an arbitrary partition of $\{1, \dots, d\}$ and $\mathcal{B}_{\mathcal{G}}$ as in (8). Assume that $r, s \in \mathcal{B}_{\ell}$ for some $\ell \in \{1, \dots, L\}$. Then for all $\lambda \in \{1, \dots, L\}$, and all $\mathbf{k} \in \Phi_2$, $|\mathcal{C}_{\lambda\mathbf{k}}^{(r)}| = |\mathcal{C}_{\lambda\mathbf{k}}^{(s)}|$.*

Remark 5. *Before proceeding with the proof of Lemma 1, let us illustrate the claim on the*

right panel of Figure 10. Because $\Sigma \in \mathcal{S}_{\mathcal{G}}$, the sets $\mathcal{C}_{\ell \mathbf{k}}^{(r)}$ for a fixed r can be identified with the r -th row of Σ ; different colours and intensities correspond to different values of ℓ and \mathbf{k} , respectively; see also Example 7. Lemma 1 implies that, for example, the number of cells with the same colour and intensity in the first six rows (corresponding to \mathcal{B}_1) is the same.

Proof. Fix arbitrary \mathcal{G} , $\ell \in \{1, \dots, L\}$ and $r, s \in \mathcal{B}_{\ell}$. We will prove the assertion by showing that there exists a bijective function $h : \{1, \dots, p\} \rightarrow \{1, \dots, p\}$ such that for all $\lambda \in \{1, \dots, L\}$ and $\kappa \in \Phi_2$,

$$t \in \mathcal{C}_{\lambda \kappa}^{(r)} \Leftrightarrow h(t) \in \mathcal{C}_{\lambda \kappa}^{(s)}, \quad (20)$$

for then obviously $|\mathcal{C}_{\lambda \kappa}^{(r)}| = |\mathcal{C}_{\lambda \kappa}^{(s)}|$. To this end, first identify $k_1, k_2 \in \{1, \dots, K\}$ such that $(i_r, j_r) \in \mathcal{G}_{k_1} \times \mathcal{G}_{k_2}$. Note that then $\mathcal{B}_{\ell} = \mathcal{B}_{(k_1 \wedge k_2)(k_1 \vee k_2)}$. Because $s \in \mathcal{B}_{\ell}$ by assumption, either $(i_s, j_s) \in \mathcal{G}_{k_1} \times \mathcal{G}_{k_2}$ or $(i_s, j_s) \in \mathcal{G}_{k_2} \times \mathcal{G}_{k_1}$.

First assume that $(i_s, j_s) \in \mathcal{G}_{k_1} \times \mathcal{G}_{k_2}$. Let π be any permutation such that

$$\forall i \in \{1, \dots, d\} \forall k \in \{1, \dots, K\}, \quad i \in \mathcal{G}_k \Leftrightarrow \pi(i) \in \mathcal{G}_k, \quad (21)$$

and further such that

$$\pi(i_r) = i_s, \quad \pi(j_r) = j_s. \quad (22)$$

Because $i_r \neq j_r$ and $i_s \neq j_s$, and $i_r, i_s \in \mathcal{G}_{k_1}$, $j_r, j_s \in \mathcal{G}_{k_2}$, such a permutation always exists, although it is generally not unique. Now define h by

$$h : \{1, \dots, p\} \rightarrow \{1, \dots, p\} \quad (23)$$

$$t \mapsto t^* \text{ such that } i_{t^*} = \pi(i_t) \wedge \pi(j_t) \text{ and } j_{t^*} = \pi(i_t) \vee \pi(j_t).$$

First, observe that h is well defined because for any $t \in \{1, \dots, p\}$, $i_t < j_t$, $\pi(i_t) \neq \pi(j_t)$ and hence $i_{t^*} < j_{t^*}$, so that t^* indeed exists. Furthermore, h is a bijection. This is because,

for any $t^* \in \{1, \dots, p\}$ and t such that $i_t = \pi^{-1}(i_{t^*}) \wedge \pi^{-1}(j_{t^*})$ and $j_t = \pi^{-1}(i_{t^*}) \vee \pi^{-1}(j_{t^*})$, $h(t) = t^*$. Furthermore, (21) implies that for any $\lambda \in \{1, \dots, L\}$, $t \in \mathcal{B}_\lambda$ if and only if $h(t) \in \mathcal{B}_\lambda$. To prove that h satisfies (20), it thus remains to show that for any $\kappa \in \Phi_2$, $\varphi(r, t) = \kappa$ if and only if $\varphi(s, h(t)) = \kappa$. This follows from the following facts, each of which is an immediate consequence of (22):

- (i) For any $i \in \{1, \dots, d\}$, $\{i\} \cap \{i_r, j_r\} = \emptyset$ if and only if $\{\pi(i)\} \cap \{i_s, j_s\} = \emptyset$.
- (ii) For any $i \in \{1, \dots, d\}$, $\{i\} \cap \{i_r, j_r\} = \{i_r\}$ if and only if $\{\pi(i)\} \cap \{i_s, j_s\} = \{i_s\}$; i_r and i_s are elements of the same cluster \mathcal{G}_{k_1} .
- (iii) For any $i \in \{1, \dots, d\}$, $\{i\} \cap \{i_r, j_r\} = \{j_r\}$ if and only if $\{\pi(i)\} \cap \{i_s, j_s\} = \{j_s\}$; j_r and j_s are elements of the same cluster \mathcal{G}_{k_2} .

This concludes the proof in the case when $(i_s, j_s) \in \mathcal{G}_{k_1} \times \mathcal{G}_{k_2}$. When $(i_s, j_s) \in \mathcal{G}_{k_2} \times \mathcal{G}_{k_1}$, one can proceed analogously by constructing h from an arbitrary fixed permutation π satisfying (21) and such that $\pi(i_r) = j_s$ and $\pi(j_r) = i_s$. \square

Lemma 2. *Let \mathcal{G} be an arbitrary partition of $\{1, \dots, d\}$ and $\mathcal{B}_\mathcal{G}$ as in (8). Then for any $\ell_1, \ell_2 \in \{1, \dots, L\}$, $r \in \mathcal{B}_{\ell_1}$, $s \in \mathcal{B}_{\ell_2}$, and $\mathbf{k} \in \Phi_2$,*

$$\frac{|\mathcal{C}_{\ell_2 \mathbf{k}}^{(r)}|}{|\mathcal{B}_{\ell_2}|} = \frac{|\mathcal{C}_{\ell_1 \mathbf{k}}^{(s)}|}{|\mathcal{B}_{\ell_1}|}.$$

Proof. To prove the claim, fix arbitrary $\ell_1, \ell_2 \in \{1, \dots, L\}$, $r \in \mathcal{B}_{\ell_1}$, $s \in \mathcal{B}_{\ell_2}$, and $\mathbf{k} \in \Phi_2$. The case $\ell_1 = \ell_2$ trivially follows from Lemma 1. For $\ell_1 \neq \ell_2$, set $\ell = (\ell_1 \wedge \ell_2, \ell_1 \vee \ell_2)$. Using Lemma 1 again, we then have that

$$|\mathcal{C}_{\ell \mathbf{k}}| = \sum_{t \in \mathcal{B}_{\ell_1}} |\mathcal{C}_{\ell_2 \mathbf{k}}^{(t)}| = \sum_{t \in \mathcal{B}_{\ell_1}} |\mathcal{C}_{\ell_2 \mathbf{k}}^{(r)}| = |\mathcal{C}_{\ell_2 \mathbf{k}}^{(r)}| |\mathcal{B}_{\ell_1}|.$$

Similarly, summing over elements in \mathcal{B}_{ℓ_2} , $|\mathcal{C}_{\ell \mathbf{k}}| = |\mathcal{C}_{\ell_1 \mathbf{k}}^{(s)}| |\mathcal{B}_{\ell_2}|$, which proves the claim. \square

Lemma 3. *Let \mathcal{G} be an arbitrary partition of $\{1, \dots, d\}$ and $\mathcal{B}_{\mathcal{G}}$ as in (8). Assume that $r_1, r_2 \in \mathcal{B}_{\ell_1}$ and $s_1, s_2 \in \mathcal{B}_{\ell_2}$ for some $\ell = (\ell_1, \ell_2) \in \Phi_1$. Further assume that $(r_1, s_1), (r_2, s_2) \in \mathcal{C}_{\ell \mathbf{k}}$ for some $\mathbf{k} \in \Phi_2$. Then for all $\lambda \in \{1, \dots, L\}$, and all $\kappa_1, \kappa_2 \in \Phi_2$, one has $|\mathcal{C}_{\lambda \kappa_1}^{(r_1)} \cap \mathcal{C}_{\lambda \kappa_2}^{(s_1)}| = |\mathcal{C}_{\lambda \kappa_1}^{(r_2)} \cap \mathcal{C}_{\lambda \kappa_2}^{(s_2)}|$, i.e.,*

$$|\{t \in \mathcal{B}_{\lambda} : \varphi(r_1, t) = \kappa_1, \varphi(s_1, t) = \kappa_2\}| = |\{t \in \mathcal{B}_{\lambda} : \varphi(r_2, t) = \kappa_1, \varphi(s_2, t) = \kappa_2\}|.$$

Proof. To show this claim, we can proceed similarly as in the proof of Lemma 1. We will again define a function h through (23) from a certain permutation π of $(1, \dots, d)$ satisfying (21). As argued in the proof of Lemma 1, h is then a well-defined bijection such that for all $\lambda \in \{1, \dots, L\}$, $t \in \mathcal{B}_{\lambda}$ if and only if $h(t) \in \mathcal{B}_{\lambda}$. If h is further such that for each $t \in \{1, \dots, p\}$ and $\kappa_1, \kappa_2 \in \Phi_2$,

$$\varphi(r_1, t) = \kappa_1 \Leftrightarrow \varphi(r_2, h(t)) = \kappa_1 \quad \text{and} \quad \varphi(s_1, t) = \kappa_2 \Leftrightarrow \varphi(s_2, h(t)) = \kappa_2, \quad (24)$$

then it holds that for all $t \in \{1, \dots, p\}$, $t \in \mathcal{C}_{\lambda \kappa_1}^{(r_1)} \cap \mathcal{C}_{\lambda \kappa_2}^{(s_1)}$ if and only if $h(t) \in \mathcal{C}_{\lambda \kappa_1}^{(r_2)} \cap \mathcal{C}_{\lambda \kappa_2}^{(s_2)}$, and consequently that $|\mathcal{C}_{\lambda \kappa_1}^{(r_1)} \cap \mathcal{C}_{\lambda \kappa_2}^{(s_1)}| = |\mathcal{C}_{\lambda \kappa_1}^{(r_2)} \cap \mathcal{C}_{\lambda \kappa_2}^{(s_2)}|$, as claimed.

In contrast to the proof of Lemma 1, the properties of the permutation π require a more cumbersome case distinction. To this end, fix $\ell = (\ell_1, \ell_2) \in \Phi_1$, $\mathbf{k} \in \Phi_2$, and $(r_1, s_1), (r_2, s_2) \in \mathcal{C}_{\ell \mathbf{k}}$ such that $r_1, r_2 \in \mathcal{B}_{\ell_1}$ and $s_1, s_2 \in \mathcal{B}_{\ell_2}$. Now let $k_{11}, k_{12}, k_{21}, k_{22} \in \{1, \dots, K\}$ be such $\mathcal{B}_{\ell_1} = \mathcal{B}_{k_{11}k_{12}}$ and $\mathcal{B}_{\ell_2} = \mathcal{B}_{k_{21}k_{22}}$. Without loss of generality, assume that

$$(i_{r_1}, j_{r_1}), (i_{r_2}, j_{r_2}) \in \mathcal{G}_{k_{11}} \times \mathcal{G}_{k_{12}} \quad \text{and} \quad (i_{s_1}, j_{s_1}), (i_{s_2}, j_{s_2}) \in \mathcal{G}_{k_{21}} \times \mathcal{G}_{k_{22}}. \quad (25)$$

Case I. $\mathbf{k} = \varphi(r_1, s_1) = \varphi(r_2, s_2) = (0, 0)$. Here,

$$|\{i_{r_1}, j_{r_1}, i_{s_1}, j_{s_1}\}| = |\{i_{r_2}, j_{r_2}, i_{s_2}, j_{s_2}\}| = 4, \quad (26)$$

and π is an arbitrary fixed permutation with the property (21) and such that

$$\pi(i_{r_1}) = i_{r_2}, \quad \pi(j_{r_1}) = j_{r_2}, \quad \pi(i_{s_1}) = i_{s_2}, \quad \pi(j_{s_1}) = j_{s_2}. \quad (27)$$

Such a permutation exists because of (25) and (26), although it is generally not unique. Because of (27), it holds that, for any $i \in \{1, \dots, d\}$,

- (i) $\{i\} \cap \{i_{r_1}, j_{r_1}\} = \emptyset$ if and only if $\{\pi(i)\} \cap \{i_{r_2}, j_{r_2}\} = \emptyset$, and $\{i\} \cap \{i_{s_1}, j_{s_1}\} = \emptyset$ if and only if $\{\pi(i)\} \cap \{i_{s_2}, j_{s_2}\} = \emptyset$;
- (ii) $\{i\} \cap \{i_{r_1}, j_{r_1}\} = \{i_{r_1}\}$ if and only if $\{\pi(i)\} \cap \{i_{r_2}, j_{r_2}\} = \{i_{r_2}\}$; i_{r_1} and i_{r_2} are elements of the same cluster $\mathcal{G}_{k_{11}}$.
- (iii) $\{i\} \cap \{i_{r_1}, j_{r_1}\} = \{j_{r_1}\}$ if and only if $\{\pi(i)\} \cap \{i_{r_2}, j_{r_2}\} = \{j_{r_2}\}$; j_{r_1} and j_{r_2} are elements of the same cluster $\mathcal{G}_{k_{12}}$.
- (iv) $\{i\} \cap \{i_{s_1}, j_{s_1}\} = \{i_{s_1}\}$ if and only if $\{\pi(i)\} \cap \{i_{s_2}, j_{s_2}\} = \{i_{s_2}\}$; i_{s_1} and i_{s_2} are elements of the same cluster $\mathcal{G}_{k_{21}}$.
- (v) $\{i\} \cap \{i_{s_1}, j_{s_1}\} = \{j_{s_1}\}$ if and only if $\{\pi(i)\} \cap \{i_{s_2}, j_{s_2}\} = \{j_{s_2}\}$; j_{s_1} and j_{s_2} are elements of the same cluster $\mathcal{G}_{k_{22}}$.

Hence h fulfills (24) and the proof is complete in this case.

Case II. $\mathbf{k} = \varphi(r_1, s_1) = \varphi(r_2, s_2) = (0, k)$ for some $k \in \{1, \dots, K\}$. In this case,

$$|\{i_{r_1}, j_{r_1}, i_{s_1}, j_{s_1}\}| = |\{i_{r_2}, j_{r_2}, i_{s_2}, j_{s_2}\}| = 3. \quad (28)$$

Observe that the three distinct elements of $\{i_{r_1}, j_{r_1}, i_{s_1}, j_{s_1}\}$ are $\{a_1, a_2, a_3\}$, say, such that $a_1 \in \{i_{r_1}, j_{r_1}\} \cap \{i_{s_1}, j_{s_1}\}$, $a_2 \in \{i_{r_1}, j_{r_1}\} \setminus \{a_1\}$, and $a_3 \in \{i_{s_1}, j_{s_1}\} \setminus \{a_1\}$. Similarly, $\{i_{r_2}, j_{r_2}, i_{s_2}, j_{s_2}\} = \{b_1, b_2, b_3\}$ such that $b_1 \in \{i_{r_2}, j_{r_2}\} \cap \{i_{s_2}, j_{s_2}\}$, $b_2 \in \{i_{r_2}, j_{r_2}\} \setminus \{b_1\}$, and $b_3 \in \{i_{s_2}, j_{s_2}\} \setminus \{b_1\}$. Note that then necessarily

$$\{i_{r_1}, j_{r_1}\} = \{a_1, a_2\}, \{i_{s_1}, j_{s_1}\} = \{a_1, a_3\}, \{i_{r_2}, j_{r_2}\} = \{b_1, b_2\}, \{i_{s_2}, j_{s_2}\} = \{b_1, b_3\}.$$

Furthermore, for $m \in \{1, 2, 3\}$, a_m and b_m are members of the same cluster. Indeed, given that $\mathbf{k} = (0, k)$, $a_1, b_1 \in \mathcal{G}_k$. From (25) it further follows that a_2, b_2 are in $\mathcal{G}_{k_{11}}$ and $\mathcal{G}_{k_{12}}$, respectively, if $a_2 = i_{r_1}$, $b_2 = i_{r_2}$, and $a_2 = j_{r_1}$, $b_2 = j_{r_2}$, respectively. If $a_2 = i_{r_1}$ and $b_2 = j_{r_2}$, then $a_1 = j_{r_1}$ and $b_1 = i_{r_2}$ and (25) together with the fact that $a_1, b_1 \in \mathcal{G}_k$ imply that $k = k_{11} = k_{12}$. Hence, $a_2, b_2 \in \mathcal{G}_k$. Similarly, if $a_2 = j_{r_1}$ and $b_2 = i_{r_2}$, we also have that $a_2, b_2 \in \mathcal{G}_k$. The verification of the fact that a_3 and b_3 are in the same cluster is analogous.

Now let π be any permutation with the property (21) and such that

$$\pi(a_1) = b_1, \quad \pi(a_2) = b_2, \quad \pi(a_3) = b_3. \quad (29)$$

Such a permutation indeed exists, although it is again generally not unique; existence is guaranteed because the a_m 's are all distinct and for $m \in \{1, 2, 3\}$, a_m and b_m are members of the same cluster. Because of (29), it holds that, for any $i \in \{1, \dots, d\}$,

- (i) $\{i\} \cap \{i_{r_1}, j_{r_1}\} = \emptyset$ if and only if $\{\pi(i)\} \cap \{i_{r_2}, j_{r_2}\} = \emptyset$, and $\{i\} \cap \{i_{s_1}, j_{s_1}\} = \emptyset$ if and only if $\{\pi(i)\} \cap \{i_{s_2}, j_{s_2}\} = \emptyset$;
- (ii) $\{i\} \cap \{i_{r_1}, j_{r_1}\} = \{a_1\}$ if and only if $\{\pi(i)\} \cap \{i_{r_2}, j_{r_2}\} = \{b_1\}$; a_1 and b_1 are elements of the same cluster \mathcal{G}_k .
- (iii) $\{i\} \cap \{i_{r_1}, j_{r_1}\} = \{a_2\}$ if and only if $\{\pi(i)\} \cap \{i_{r_2}, j_{r_2}\} = \{b_2\}$; a_2 and b_2 are elements of the same cluster $\mathcal{G}_{k_{11}}$, $\mathcal{G}_{k_{12}}$ or \mathcal{G}_k , as the case may be.
- (iv) $\{i\} \cap \{i_{s_1}, j_{s_1}\} = \{a_1\}$ if and only if $\{\pi(i)\} \cap \{i_{s_2}, j_{s_2}\} = \{b_1\}$; a_1 and b_1 are elements of the same cluster \mathcal{G}_k .
- (v) $\{i\} \cap \{i_{s_1}, j_{s_1}\} = \{a_3\}$ if and only if $\{\pi(i)\} \cap \{i_{s_2}, j_{s_2}\} = \{b_3\}$; a_3 and b_3 are elements of the same cluster $\mathcal{G}_{k_{21}}$, $\mathcal{G}_{k_{22}}$ or \mathcal{G}_k , as the case may be.

Hence h fulfills (24) and the proof is complete in this case.

Case III. $\mathbf{k} = \varphi(r_1, s_1) = \varphi(r_2, s_2) = (k_1, k_2)$ where $k_1, k_2 > 0$. In this case,

$$|\{i_{r_1}, j_{r_1}, i_{s_1}, j_{s_1}\}| = |\{i_{r_2}, j_{r_2}, i_{s_2}, j_{s_2}\}| = 2. \quad (30)$$

Write $\{i_{r_1}, j_{r_1}, i_{s_1}, j_{s_1}\} = \{a_1, a_2\}$, and $\{i_{r_2}, j_{r_2}, i_{s_2}, j_{s_2}\} = \{b_1, b_2\}$, with $a_1, b_1 \in \mathcal{G}_{k_1}$ and $a_2, b_2 \in \mathcal{G}_{k_2}$. Now let π be any permutation with the property (21) and such that

$$\pi(a_1) = b_1 \quad \pi(a_2) = b_2. \quad (31)$$

Because of (31) and the fact that $\{a_1, a_2\} = \{i_{r_1}, j_{r_1}\} \cap \{i_{s_1}, j_{s_1}\}$, and $\{b_1, b_2\} = \{i_{r_2}, j_{r_2}\} \cap \{i_{s_2}, j_{s_2}\}$, it holds that, for any $i \in \{1, \dots, d\}$,

- (i) $\{i\} \cap \{i_{r_1}, j_{r_1}\} = \emptyset$ if and only if $\{\pi(i)\} \cap \{i_{r_2}, j_{r_2}\} = \emptyset$, and $\{i\} \cap \{i_{s_1}, j_{s_1}\} = \emptyset$ if and only if $\{\pi(i)\} \cap \{i_{s_2}, j_{s_2}\} = \emptyset$;
- (ii) $\{i\} \cap \{i_{r_1}, j_{r_1}\} = \{a_1\}$ if and only if $\{\pi(i)\} \cap \{i_{r_2}, j_{r_2}\} = \{b_1\}$; a_1 and b_1 are elements of the same cluster \mathcal{G}_{k_1} .
- (iii) $\{i\} \cap \{i_{r_1}, j_{r_1}\} = \{a_2\}$ if and only if $\{\pi(i)\} \cap \{i_{r_2}, j_{r_2}\} = \{b_2\}$; a_2 and b_2 are elements of the same cluster \mathcal{G}_{k_2} .
- (iv) $\{i\} \cap \{i_{s_1}, j_{s_1}\} = \{a_1\}$ if and only if $\{\pi(i)\} \cap \{i_{s_2}, j_{s_2}\} = \{b_1\}$; a_1 and b_1 are elements of the same cluster \mathcal{G}_{k_1} .
- (v) $\{i\} \cap \{i_{s_1}, j_{s_1}\} = \{a_2\}$ if and only if $\{\pi(i)\} \cap \{i_{s_2}, j_{s_2}\} = \{b_2\}$; a_2 and b_2 are elements of the same cluster \mathcal{G}_{k_2} .

Hence h fulfills (24) and the proof is complete in this case as well. \square

The following lemma is the cornerstone of the proof of Theorem 1.

Lemma 4. *Let \mathcal{G} be an arbitrary partition of $\{1, \dots, d\}$. If $\mathbf{S} \in \mathcal{S}_{\mathcal{G}}$ and \mathbf{B} is as in (9), then $\mathbf{B}^\top \mathbf{S} = \mathbf{B}^\top \mathbf{S} \mathbf{B} \mathbf{B}^+$.*

Proof. First note that for any $\ell \in \{1, \dots, L\}$ and $r \in \{1, \dots, p\}$,

$$[\mathbf{B}^\top \mathbf{S}]_{\ell r} = \sum_{s=1}^p \mathbf{B}_{s\ell} \mathbf{S}_{sr} = \sum_{s \in \mathcal{B}_\ell} \mathbf{S}_{sr} \quad (32)$$

and that $[\mathbf{B}^+]_{\ell r} = \mathbb{1}(r \in \mathcal{B}_\ell) |\mathcal{B}_\ell|^{-1}$. Also, for any $s \in \mathcal{B}_\ell$,

$$[\mathbf{B} \mathbf{B}^+]_{rs} = \mathbb{1}(r \in \mathcal{B}_\ell) |\mathcal{B}_\ell|^{-1}. \quad (33)$$

Now fix an arbitrary $\ell \in \{1, \dots, L\}$ and $r \in \{1, \dots, p\}$ and find ℓ^* so that $r \in \mathcal{B}_{\ell^*}$. Then from (32) and (33),

$$\begin{aligned} [\mathbf{B}^\top \mathbf{S} \mathbf{B} \mathbf{B}^+]_{\ell r} &= \sum_{s=1}^p [\mathbf{B}^\top \mathbf{S}]_{\ell s} [\mathbf{B} \mathbf{B}^+]_{sr} = \sum_{s=1}^p \left(\sum_{t \in \mathcal{B}_\ell} \mathbf{S}_{ts} \right) \frac{\mathbb{1}(s \in \mathcal{B}_{\ell^*})}{|\mathcal{B}_{\ell^*}|} \\ &= \sum_{s \in \mathcal{B}_{\ell^*}} \sum_{t \in \mathcal{B}_\ell} \frac{\mathbf{S}_{ts}}{|\mathcal{B}_{\ell^*}|} = \sum_{t \in \mathcal{B}_\ell} \frac{1}{|\mathcal{B}_{\ell^*}|} \sum_{s \in \mathcal{B}_{\ell^*}} \mathbf{S}_{ts}. \end{aligned} \quad (34)$$

Now set $\ell = (\ell \wedge \ell^*, \ell \vee \ell^*)$ and for any $\mathbf{k} \in \Phi_2$, let $\mathbf{S}^{\ell \mathbf{k}}$ denote the unique value such that $\mathbf{S}_{ts} = \mathbf{S}^{\ell \mathbf{k}}$ whenever $(t, s) \in \mathcal{C}_{\ell \mathbf{k}}$. Because $\mathcal{B}_{\ell^*} = \cup_{\mathbf{k} \in \Phi_2} \mathcal{C}_{\ell^* \mathbf{k}}^{(t)}$ for any $t \in \mathcal{B}_\ell$ and $\mathbf{S} \in \mathcal{S}_{\mathcal{G}}$ by assumption,

$$\sum_{s \in \mathcal{B}_{\ell^*}} \mathbf{S}_{ts} = \sum_{\mathbf{k} \in \Phi_2} \sum_{s \in \mathcal{C}_{\ell^* \mathbf{k}}^{(t)}} \mathbf{S}_{ts} = \sum_{\mathbf{k} \in \Phi_2} \sum_{s \in \mathcal{C}_{\ell^* \mathbf{k}}^{(t)}} \mathbf{S}^{\ell \mathbf{k}} = \sum_{\mathbf{k} \in \Phi_2} |\mathcal{C}_{\ell^* \mathbf{k}}^{(t)}| \mathbf{S}^{\ell \mathbf{k}}.$$

Using this and Lemma 2, the RHS in (34) equals

$$\sum_{t \in \mathcal{B}_\ell} \sum_{\mathbf{k} \in \Phi_2} \frac{|\mathcal{C}_{\ell^* \mathbf{k}}^{(t)}|}{|\mathcal{B}_{\ell^*}|} \mathbf{S}^{\ell \mathbf{k}} = \sum_{t \in \mathcal{B}_\ell} \sum_{\mathbf{k} \in \Phi_2} \frac{|\mathcal{C}_{\ell \mathbf{k}}^{(r)}|}{|\mathcal{B}_\ell|} \mathbf{S}^{\ell \mathbf{k}} = \sum_{\mathbf{k} \in \Phi_2} |\mathcal{C}_{\ell \mathbf{k}}^{(r)}| \mathbf{S}^{\ell \mathbf{k}}.$$

Now use the fact that $\mathcal{B}_\ell = \cup_{\mathbf{k} \in \Phi_2} \mathcal{C}_{\ell \mathbf{k}}^{(r)}$ and that $\mathbf{S} \in \mathcal{S}_\mathcal{G}$ to rewrite the RHS as

$$\sum_{\mathbf{k} \in \Phi_2} \sum_{t \in \mathcal{C}_{\ell \mathbf{k}}^{(r)}} \mathbf{S}^{\ell \mathbf{k}} = \sum_{t \in \mathcal{B}_\ell} \mathbf{S}_{tr},$$

which is equal to the RHS in (32), as claimed. \square

Next, note the following result, which is an immediate consequence of the properties of the Moore-Penrose pseudo-inverse.

Lemma 5. *Let \mathcal{G} be an arbitrary partition of $\{1, \dots, d\}$, \mathbf{B} as in (9) and $\mathbf{\Gamma} = \mathbf{B}\mathbf{B}^+$. Then $\mathbf{\Gamma}$ and $(\mathbf{I}_p - \mathbf{\Gamma})$ are idempotent, i.e., $\mathbf{\Gamma}\mathbf{\Gamma} = \mathbf{\Gamma}$ and $(\mathbf{I}_p - \mathbf{\Gamma})(\mathbf{I}_p - \mathbf{\Gamma}) = (\mathbf{I}_p - \mathbf{\Gamma})$.*

Lemma 6. *Let \mathcal{G} be an arbitrary partition of $\{1, \dots, d\}$, \mathbf{B} as in (9) and $\mathbf{\Gamma} = \mathbf{B}\mathbf{B}^+$. Then for any $\mathbf{S} \in \mathcal{S}_\mathcal{G}$, $\mathbf{\Gamma}\mathbf{S} = \mathbf{\Gamma}\mathbf{S}\mathbf{\Gamma} = \mathbf{S}\mathbf{\Gamma}$.*

Proof. For arbitrary $\ell \in \Phi_1$ and $\mathbf{k} \in \Phi_2$, let $\mathbf{S}^{\ell \mathbf{k}}$ denote the unique value such that $\mathbf{S}_{rs} = \mathbf{S}^{\ell \mathbf{k}}$ whenever $(r, s) \in \mathcal{C}_{\ell \mathbf{k}}$. Now fix arbitrary $r, s \in \{1, \dots, p\}$ and let ℓ_1, ℓ_2 be such that $r \in \mathcal{B}_{\ell_1}$ and $s \in \mathcal{B}_{\ell_2}$. Set $\ell = (\ell_1 \wedge \ell_2, \ell_1 \vee \ell_2)$. From (33) and Lemma 2 we can conclude that

$$[\mathbf{\Gamma}\mathbf{S}]_{rs} = \sum_{t \in \mathcal{B}_{\ell_1}} \frac{\mathbf{S}_{ts}}{|\mathcal{B}_{\ell_1}|} = \sum_{\mathbf{k} \in \Phi_2} \sum_{t \in \mathcal{C}_{\ell_1 \mathbf{k}}^{(s)}} \frac{\mathbf{S}^{\ell \mathbf{k}}}{|\mathcal{B}_{\ell_1}|} = \sum_{\mathbf{k} \in \Phi_2} \frac{|\mathcal{C}_{\ell_1 \mathbf{k}}^{(s)}|}{|\mathcal{B}_{\ell_1}|} \mathbf{S}^{\ell \mathbf{k}} = \sum_{\mathbf{k} \in \Phi_2} \frac{|\mathcal{C}_{\ell_2 \mathbf{k}}^{(r)}|}{|\mathcal{B}_{\ell_2}|} \mathbf{S}^{\ell \mathbf{k}} = [\mathbf{S}\mathbf{\Gamma}]_{rs},$$

proving that $\mathbf{\Gamma}\mathbf{S} = \mathbf{S}\mathbf{\Gamma}$. Furthermore, $\mathbf{\Gamma}\mathbf{S} = \mathbf{S}\mathbf{\Gamma}$ and Lemma 5 together imply that $\mathbf{\Gamma}\mathbf{\Gamma}\mathbf{S} = \mathbf{\Gamma}\mathbf{S}\mathbf{\Gamma}$. Using the idempotence of $\mathbf{\Gamma}$ again, this simplifies to $\mathbf{\Gamma}\mathbf{S} = \mathbf{\Gamma}\mathbf{S}\mathbf{\Gamma}$. \square

Remark 6. *Suppose that \mathcal{G} satisfies the PEA. Proposition 5 and Corollary 1 along with Lemma 5 imply that $(\mathbf{I}_p - \mathbf{\Gamma})\mathbf{S} = (\mathbf{I}_p - \mathbf{\Gamma})\mathbf{S}(\mathbf{I}_p - \mathbf{\Gamma}) = \mathbf{S}(\mathbf{I}_p - \mathbf{\Gamma})$ holds for both $\mathbf{S} = \mathbf{\Sigma}$ and $\mathbf{S} = \mathbf{\Sigma}^{-1}$.*

B.2 Proof of Proposition 4

Because \mathcal{G} satisfies the PEA, $\mathbf{\Gamma}\boldsymbol{\tau} = \boldsymbol{\tau}$. Therefore,

$$\begin{aligned} (\hat{\boldsymbol{\tau}} - \tilde{\boldsymbol{\tau}})^\top \hat{\boldsymbol{\Sigma}}^{-1} (\hat{\boldsymbol{\tau}} - \tilde{\boldsymbol{\tau}}) &= (\hat{\boldsymbol{\tau}} - \boldsymbol{\tau} - \mathbf{\Gamma}(\hat{\boldsymbol{\tau}} - \boldsymbol{\tau}))^\top \hat{\boldsymbol{\Sigma}}^{-1} (\hat{\boldsymbol{\tau}} - \boldsymbol{\tau} - \mathbf{\Gamma}(\hat{\boldsymbol{\tau}} - \boldsymbol{\tau})) \\ &= (\hat{\boldsymbol{\tau}} - \boldsymbol{\tau})^\top (\mathbf{I}_p - \mathbf{\Gamma}) \hat{\boldsymbol{\Sigma}}^{-1} (\mathbf{I}_p - \mathbf{\Gamma}) (\hat{\boldsymbol{\tau}} - \boldsymbol{\tau}). \end{aligned}$$

Because $\mathbf{A} \mapsto \mathbf{A}^{-1}$ is a continuous mapping on the space of nonsingular matrices (Stewart, 1969), $\hat{\boldsymbol{\Sigma}}^{-1}/n$ converges element-wise to $\boldsymbol{\Sigma}_\infty^{-1}$ in probability as $n \rightarrow \infty$. The asymptotic Normality (13) implies along with Slutsky's lemma that

$$(\hat{\boldsymbol{\tau}} - \tilde{\boldsymbol{\tau}})^\top \hat{\boldsymbol{\Sigma}}^{-1} (\hat{\boldsymbol{\tau}} - \tilde{\boldsymbol{\tau}}) \rightsquigarrow \mathbf{V}^\top \boldsymbol{\Sigma}_\infty^{-1} \mathbf{V},$$

where $\mathbf{V} \sim \mathcal{N}(\mathbf{0}_p, (\mathbf{I}_p - \mathbf{\Gamma})\boldsymbol{\Sigma}_\infty(\mathbf{I}_p - \mathbf{\Gamma}))$. Now set $\mathbf{M} := (\mathbf{I}_p - \mathbf{\Gamma})\boldsymbol{\Sigma}_\infty(\mathbf{I}_p - \mathbf{\Gamma})$ and $\mathbf{A} := \boldsymbol{\Sigma}_\infty^{-1}$. Following Lemma 5 and Remark 6, we easily get that

$$\mathbf{M}\mathbf{A} = (\mathbf{I}_p - \mathbf{\Gamma})\boldsymbol{\Sigma}_\infty(\mathbf{I}_p - \mathbf{\Gamma})\boldsymbol{\Sigma}_\infty^{-1} = (\mathbf{I}_p - \mathbf{\Gamma})$$

is idempotent and has trace $\text{tr}(\mathbf{I}_p - \mathbf{\Gamma}) = p - \text{tr}(\mathbf{\Gamma})$. An application of Theorem 8.6 in Severini (2005) thus yields that $\mathbf{V}^\top \boldsymbol{\Sigma}_\infty^{-1} \mathbf{V}$ is $\chi_{p-\text{tr}(\mathbf{\Gamma})}^2$. The claim now follows from

$$\text{tr}(\mathbf{\Gamma}) = \sum_{r=1}^p \mathbf{\Gamma}_{rr} = \sum_{\ell=1}^L \sum_{r \in \mathcal{B}_\ell} \frac{1}{|\mathcal{B}_\ell|} = L.$$

B.3 Additional results for Section 5 of the paper

In this section, we consider inverses of matrices in $\mathcal{T}_\mathcal{G}$. To this end, consider an arbitrary partition \mathcal{G} of $\{1, \dots, d\}$ and introduce constraints on the diagonal entries of the matrices in $\mathcal{T}_\mathcal{G}$ through the set

$$\mathcal{T}_\mathcal{G}^\dagger := \{\mathbf{R} \in \mathcal{T}_\mathcal{G} : \text{for any } i, j \text{ such that } \boldsymbol{\Delta}_{ij} = 1, \mathbf{R}_{ii} = \mathbf{R}_{jj}\}.$$

A direct consequence of this definition is that $\mathcal{T}_{\mathcal{G}}^{\dagger} \subset \mathcal{T}_{\mathcal{G}}$. Furthermore, $\mathbf{T} \in \mathcal{T}_{\mathcal{G}}^{\dagger}$ since $\mathbf{T}_{ii} = 1$ for all $i \in \{1, \dots, d\}$.

Lemma 7. *If $\mathbf{R} \in \mathcal{T}_{\mathcal{G}}^{\dagger}$ is invertible, $\mathbf{R}^{-1} \in \mathcal{T}_{\mathcal{G}}^{\dagger}$.*

Proof. Invoking once again the Cayley-Hamilton Theorem as in the proof of Proposition 6, it suffices to show $\mathbf{R}, \mathbf{Q} \in \mathcal{T}_{\mathcal{G}}^{\dagger}$ implies that $\mathbf{RQ} \in \mathcal{T}_{\mathcal{G}}^{\dagger}$. To this end, fix arbitrary $k_1, k_2 \in \{1, \dots, K\}$ and let $(i_1, j_1), (i_2, j_2) \in \mathcal{G}_{k_1} \times \mathcal{G}_{k_2}$ be such that $i_1 = j_1$ if and only if $i_2 = j_2$. Then for any $k \in \{1, \dots, K\}$,

$$\sum_{s \in \mathcal{G}_k} \mathbf{R}_{i_1 s} \mathbf{Q}_{s j_1} = \sum_{s \in \mathcal{G}_k} \mathbf{R}_{i_2 s} \mathbf{Q}_{s j_2}.$$

Therefore,

$$[\mathbf{RQ}]_{i_1 j_1} = \sum_{s=1}^d \mathbf{R}_{i_1 s} \mathbf{Q}_{s j_1} = \sum_{k=1}^K \sum_{s \in \mathcal{G}_k} \mathbf{R}_{i_1 s} \mathbf{Q}_{s j_1} = \sum_{k=1}^K \sum_{s \in \mathcal{G}_k} \mathbf{R}_{i_2 s} \mathbf{Q}_{s j_2} = [\mathbf{RQ}]_{i_2 j_2},$$

which proves the claim. \square

C ADDITIONAL RESULTS OF THE SIMULATION STUDY

In this section, we provide the omitted results for the statistics ν_1 and ν_2 defined in Section 6 of the paper. The results obtained with the Normal copula are given in Table 5. Figure 12 provides examples of matrices $\hat{\mathbf{T}}$ obtained with the different combinations of the factors (\mathbf{T}, n) . The results obtained with the Cauchy copula are given in Table 6.

Table 5: Average values of ν_1 and ν_2 over the 500 simulations, as defined in Section 6, from multivariate Normal distribution for all combinations of factors (\mathbf{T}, n) and shrinkage intensities $w \in \{0, 0.25, 0.5, 0.75, 1\}$.

| \mathbf{T} | n | w | | | | | w | | | | |
|----------------|-----|------|------|------|------|------|------|------|------|------|------|
| | | 0 | .25 | .5 | .75 | 1 | 0 | .25 | .5 | .75 | 1 |
| \mathbf{T}_1 | 125 | 0.00 | 0.94 | 0.95 | 0.94 | 0.92 | 0.00 | 0.63 | 0.63 | 0.63 | 0.62 |
| | 250 | 0.02 | 1.00 | 1.00 | 1.00 | 0.99 | 0.01 | 0.65 | 0.65 | 0.65 | 0.65 |
| | 500 | 1.00 | 1.00 | 1.00 | 1.00 | 1.00 | 0.65 | 0.65 | 0.65 | 0.65 | 0.65 |
| \mathbf{T}_2 | 125 | 0.00 | 0.41 | 0.50 | 0.52 | 0.50 | 0.00 | 0.64 | 0.67 | 0.68 | 0.68 |
| | 250 | 0.20 | 0.94 | 0.95 | 0.95 | 0.95 | 0.27 | 0.78 | 0.79 | 0.79 | 0.79 |
| | 500 | 1.00 | 1.00 | 1.00 | 1.00 | 1.00 | 0.79 | 0.79 | 0.79 | 0.79 | 0.79 |
| \mathbf{T}_3 | 125 | 0.00 | 0.21 | 0.26 | 0.29 | 0.23 | 0.00 | 0.47 | 0.49 | 0.50 | 0.48 |
| | 250 | 0.07 | 0.76 | 0.81 | 0.81 | 0.75 | 0.08 | 0.58 | 0.59 | 0.59 | 0.57 |
| | 500 | 0.98 | 0.99 | 0.99 | 0.99 | 0.98 | 0.62 | 0.62 | 0.62 | 0.63 | 0.62 |
| \mathbf{T}_4 | 125 | 0.00 | 0.00 | 0.00 | 0.00 | 0.00 | 0.00 | 0.43 | 0.48 | 0.50 | 0.51 |
| | 250 | 0.00 | 0.00 | 0.01 | 0.00 | 0.00 | 0.10 | 0.47 | 0.50 | 0.51 | 0.50 |
| | 500 | 0.03 | 0.08 | 0.10 | 0.11 | 0.08 | 0.49 | 0.53 | 0.55 | 0.56 | 0.53 |

$\bar{\nu}_1$

$\bar{\nu}_2$

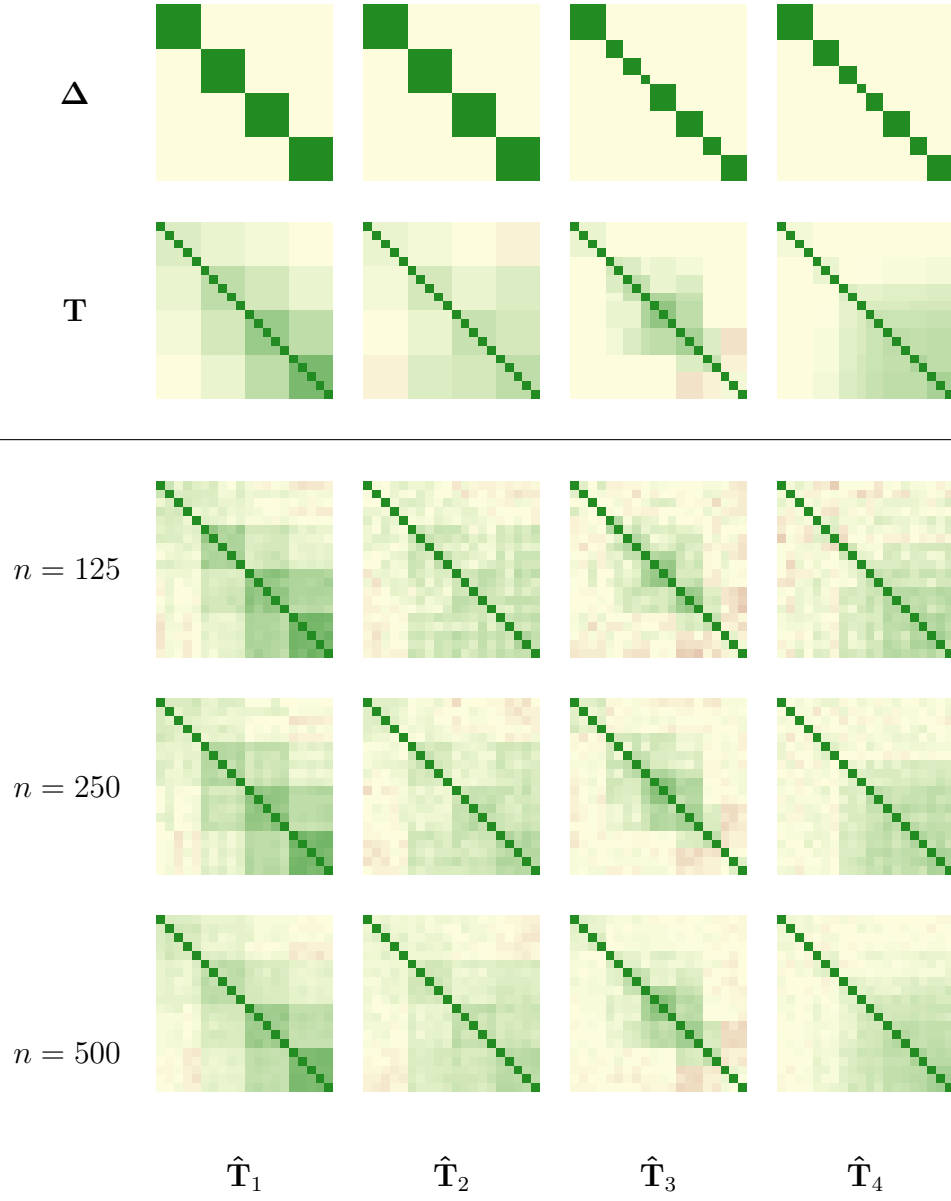


Figure 12: Examples of matrices $\hat{\mathbf{T}}$ obtained from data generated using the 12 different combinations (\mathbf{T}, n) and the Normal copula.

Table 6: Average values of ν_1 and ν_2 over the 500 simulations, as defined in Section 6, from a Cauchy copula with uniform $(0, 1)$ margins for all combinations of factors (\mathbf{T}, n) and shrinkage intensities $w \in \{0, 0.25, 0.5, 0.75, 1\}$.

| \mathbf{T} | n | w | | | | | w | | | | |
|----------------|-----|------|------|------|------|------|------|------|------|------|------|
| | | 0 | .25 | .5 | .75 | 1 | 0 | .25 | .5 | .75 | 1 |
| \mathbf{T}_1 | 125 | 0.00 | 0.68 | 0.75 | 0.73 | 0.71 | 0.00 | 0.62 | 0.63 | 0.63 | 0.62 |
| | 250 | 0.00 | 0.96 | 0.97 | 0.97 | 0.96 | 0.00 | 0.67 | 0.68 | 0.68 | 0.68 |
| | 500 | 1.00 | 1.00 | 1.00 | 1.00 | 1.00 | 0.70 | 0.70 | 0.70 | 0.70 | 0.70 |
| \mathbf{T}_2 | 125 | 0.00 | 0.09 | 0.12 | 0.16 | 0.13 | 0.01 | 0.57 | 0.61 | 0.63 | 0.63 |
| | 250 | 0.02 | 0.57 | 0.61 | 0.61 | 0.61 | 0.19 | 0.73 | 0.74 | 0.74 | 0.74 |
| | 500 | 0.91 | 0.96 | 0.96 | 0.97 | 0.97 | 0.80 | 0.81 | 0.81 | 0.81 | 0.81 |
| \mathbf{T}_3 | 125 | 0.00 | 0.05 | 0.04 | 0.04 | 0.03 | 0.00 | 0.44 | 0.46 | 0.47 | 0.45 |
| | 250 | 0.00 | 0.32 | 0.38 | 0.39 | 0.35 | 0.06 | 0.52 | 0.54 | 0.54 | 0.52 |
| | 500 | 0.78 | 0.88 | 0.89 | 0.89 | 0.86 | 0.61 | 0.63 | 0.63 | 0.63 | 0.62 |
| \mathbf{T}_4 | 125 | 0.00 | 0.00 | 0.00 | 0.00 | 0.00 | 0.00 | 0.49 | 0.53 | 0.54 | 0.55 |
| | 250 | 0.00 | 0.00 | 0.00 | 0.00 | 0.00 | 0.09 | 0.47 | 0.50 | 0.53 | 0.54 |
| | 500 | 0.00 | 0.01 | 0.01 | 0.01 | 0.00 | 0.43 | 0.51 | 0.53 | 0.55 | 0.54 |

$\bar{\nu}_1$

$\bar{\nu}_2$

D DETAILED CLUSTERS OF THE APPLICATION TO STOCKS RETURNS

For each cluster, company names, tickers and sectors (according to nasdaq.com) are given. A more detailed description of the clusters including the industry can be generated with the R-code available online.

```
[1] "#####"
[1] "##### cluster 1 ##### tau.tilde = 0.194 #####"
[1] "#####"
```

| | Symbol | Name | Sector |
|----|--------|---------------------------------|-----------------------|
| 1: | AAL | American Airlines Group, Inc. | Transportation |
| 2: | ADP | Automatic Data Processing, Inc. | Technology |
| 3: | ESRX | Express Scripts Holding Company | Health Care |
| 4: | HAS | Hasbro, Inc. | Consumer Non-Durables |
| 5: | PAYX | Paychex, Inc. | Consumer Services |
| 6: | SBUX | Starbucks Corporation | Consumer Services |
| 7: | XRAY | DENTSPLY SIRONA Inc. | Health Care |

```
[1] ""
```

```
[1] ""
```

```
[1] "#####"
[1] "##### cluster 2 ##### tau.tilde = 0.246 #####"
[1] "#####"
```

| | Symbol | Name | Sector |
|----|--------|--------------------------|------------|
| 1: | AAPL | Apple Inc. | Technology |
| 2: | ATVI | Activision Blizzard, Inc | Technology |
| 3: | CERN | Cerner Corporation | Technology |

| | | | |
|-----|------|--|-------------------|
| 4: | CHKP | Check Point Software Technologies Ltd. | Technology |
| 5: | EA | Electronic Arts Inc. | Technology |
| 6: | EBAY | eBay Inc. | Miscellaneous |
| 7: | EXPE | Expedia, Inc. | Consumer Services |
| 8: | HOLX | Hologic, Inc. | Health Care |
| 9: | ISRG | Intuitive Surgical, Inc. | Health Care |
| 10: | MU | Micron Technology, Inc. | Technology |
| 11: | NVDA | NVIDIA Corporation | Technology |
| 12: | IDXX | IDEXX Laboratories, Inc. | Health Care |

[1] ""

[1] ""

[1] "#####"

[1] "##### cluster 3 ##### tau.tilde = 0.376 #####"

[1] "#####"

| | Symbol | Name | Sector |
|----|--------|----------------------------|-------------------|
| 1: | ADBE | Adobe Systems Incorporated | Technology |
| 2: | AMZN | Amazon.com, Inc. | Consumer Services |
| 3: | FB | Facebook, Inc. | Technology |
| 4: | MSFT | Microsoft Corporation | Technology |
| 5: | NFLX | Netflix, Inc. | Consumer Services |
| 6: | PCLN | The Priceline Group Inc. | Miscellaneous |

[1] ""

[1] ""

[1] "#####"

[1] "##### cluster 4 ##### tau.tilde = 0.444 #####"

[1] "#####"

| | Symbol | Name | Sector |
|--|--------|------|--------|
|--|--------|------|--------|

| | | | |
|-----|------|-----------------------------------|---------------|
| 1: | ADI | Analog Devices, Inc. | Technology |
| 2: | AMAT | Applied Materials, Inc. | Technology |
| 3: | AVGO | Broadcom Limited | Technology |
| 4: | KLAC | KLA-Tencor Corporation | Capital Goods |
| 5: | MXIM | Maxim Integrated Products, Inc. | Technology |
| 6: | SWKS | Skyworks Solutions, Inc. | Technology |
| 7: | TXN | Texas Instruments Incorporated | Technology |
| 8: | LRCX | Lam Research Corporation | Technology |
| 9: | MCHP | Microchip Technology Incorporated | Technology |
| 10: | XLNX | Xilinx, Inc. | Technology |

[1] ""

[1] ""

[1] "#####"

[1] "##### cluster 5 ##### tau.tilde = 0.27 #####"

[1] "#####"

| | Symbol | Name | Sector |
|-----|--------|--|-----------------------|
| 1: | ADSK | Autodesk, Inc. | Technology |
| 2: | CA | CA Inc. | Technology |
| 3: | CTAS | Cintas Corporation | Consumer Non-Durables |
| 4: | CSCO | Cisco Systems, Inc. | Technology |
| 5: | CTXS | Citrix Systems, Inc. | Technology |
| 6: | CTSH | Cognizant Technology Solutions Corporation | Technology |
| 7: | FISV | Fiserv, Inc. | Technology |
| 8: | HSIC | Henry Schein, Inc. | Health Care |
| 9: | MAR | Marriott International | Consumer Services |
| 10: | PYPL | PayPal Holdings, Inc. | Miscellaneous |
| 11: | QCOM | QUALCOMM Incorporated | Technology |

12: VRSK Verisk Analytics, Inc. Technology

[1] ""

[1] ""

[1] "#####"

[1] "##### cluster 6 ##### tau.tilde = 0.172 #####"

[1] "#####"

| | Symbol | Name | Sector |
|-----|--------|-------------------------------------|-------------------|
| 1: | AKAM | Akamai Technologies, Inc. | Miscellaneous |
| 2: | CSX | CSX Corporation | Transportation |
| 3: | INTC | Intel Corporation | Technology |
| 4: | INTU | Intuit Inc. | Technology |
| 5: | MELI | MercadoLibre, Inc. | Miscellaneous |
| 6: | NCLH | Norwegian Cruise Line Holdings Ltd. | Consumer Services |
| 7: | SIRI | Sirius XM Holdings Inc. | Consumer Services |
| 8: | SYMC | Symantec Corporation | Technology |
| 9: | TMUS | T-Mobile US, Inc. | Public Utilities |
| 10: | WDC | Western Digital Corporation | Technology |
| 11: | STX | Seagate Technology PLC | Technology |
| 12: | WYNN | Wynn Resorts, Limited | Consumer Services |

[1] ""

[1] ""

[1] "#####"

[1] "##### cluster 7 ##### tau.tilde = 0.294 #####"

[1] "#####"

| | Symbol | Name | Sector |
|----|--------|-------------------------------|-------------|
| 1: | ALXN | Alexion Pharmaceuticals, Inc. | Health Care |
| 2: | AMGN | Amgen Inc. | Health Care |

| | | | |
|----|------|-------------------------------------|---------------|
| 3: | BIIB | Biogen Inc. | Health Care |
| 4: | BMRN | BioMarin Pharmaceutical Inc. | Health Care |
| 5: | CELG | Celgene Corporation | Health Care |
| 6: | ILMN | Illumina, Inc. | Capital Goods |
| 7: | INCY | Incyte Corporation | Health Care |
| 8: | REGN | Regeneron Pharmaceuticals, Inc. | Health Care |
| 9: | VRTX | Vertex Pharmaceuticals Incorporated | Health Care |

[1] ""

[1] ""

[1] "#####"

[1] "##### cluster 8 ##### tau.tilde = 0.243 #####"

[1] "#####"

| | Symbol | Name | Sector |
|----|--------|-------------------------------|-------------------|
| 1: | BIDU | Baidu, Inc. | Technology |
| 2: | CTRP | Ctrip.com International, Ltd. | Miscellaneous |
| 3: | JD | JD.com, Inc. | Consumer Services |
| 4: | NTES | NetEase, Inc. | Miscellaneous |
| 5: | TSLA | Tesla, Inc. | Capital Goods |

[1] ""

[1] ""

[1] "#####"

[1] "##### cluster 9 ##### tau.tilde = 0.12 #####"

[1] "#####"

| | Symbol | Name | Sector |
|----|--------|------------------------------|-------------------|
| 1: | CHTR | Charter Communications, Inc. | Consumer Services |
| 2: | CMCSA | Comcast Corporation | Consumer Services |
| 3: | COST | Costco Wholesale Corporation | Consumer Services |

| | | | |
|-----|------|------------------------------------|-----------------------|
| 4: | DISH | DISH Network Corporation | Consumer Services |
| 5: | FAST | Fastenal Company | Consumer Services |
| 6: | JBHT | J.B. Hunt Transport Services, Inc. | Transportation |
| 7: | KHC | The Kraft Heinz Company | Consumer Non-Durables |
| 8: | QVCA | Liberty Interactive Corporation | Consumer Services |
| 9: | MAT | Mattel, Inc. | Consumer Non-Durables |
| 10: | MDLZ | Mondelez International, Inc. | Consumer Non-Durables |
| 11: | MNST | Monster Beverage Corporation | Consumer Non-Durables |
| 12: | ULTA | Ulta Beauty, Inc. | Consumer Services |
| 13: | VIAB | Viacom Inc. | Consumer Services |
| 14: | VOD | Vodafone Group Plc | Public Utilities |
| 15: | WBA | Walgreens Boots Alliance, Inc. | Health Care |
| 16: | PCAR | PACCAR Inc. | Capital Goods |

[1] ""

[1] ""

[1] "#####"

[1] "##### cluster 10 ##### tau.tilde = 0.876 #####"

[1] "#####"

| Symbol | Name | Sector |
|--------|------|--------|
|--------|------|--------|

| | | | |
|----|-------|--------------------------------|-------------------|
| 1: | DISCA | Discovery Communications, Inc. | Consumer Services |
|----|-------|--------------------------------|-------------------|

| | | | |
|----|-------|--------------------------------|-------------------|
| 2: | DISCK | Discovery Communications, Inc. | Consumer Services |
|----|-------|--------------------------------|-------------------|

[1] ""

[1] ""

[1] "#####"

[1] "##### cluster 11 ##### tau.tilde = 0.338 #####"

[1] "#####"

| Symbol | Name | Sector |
|--------|------|--------|
|--------|------|--------|

| | | |
|----|------|---|
| 1: | DLTR | Dollar Tree, Inc. Consumer Services |
| 2: | ROST | Ross Stores, Inc. Consumer Services |
| 3: | TSCO | Tractor Supply Company Consumer Services |
| 4: | ORLY | O'Reilly Automotive, Inc. Consumer Services |

[1] ""

[1] ""

[1] "#####"

[1] "##### cluster 12 ##### tau.tilde = 0.874 #####"

[1] "#####"

| Symbol | Name | Sector |
|--------|------|--------|
|--------|------|--------|

| | | |
|----|-----|--|
| 1: | FOX | Twenty-First Century Fox, Inc. Consumer Services |
|----|-----|--|

| | | |
|----|------|--|
| 2: | FOXA | Twenty-First Century Fox, Inc. Consumer Services |
|----|------|--|

[1] ""

[1] ""

[1] "#####"

[1] "##### cluster 13 ##### tau.tilde = 0.201 #####"

[1] "#####"

| Symbol | Name | Sector |
|--------|------|--------|
|--------|------|--------|

| | | |
|----|------|-----------------------------------|
| 1: | GILD | Gilead Sciences, Inc. Health Care |
|----|------|-----------------------------------|

| | | |
|----|-----|------------------------|
| 2: | MYL | Mylan N.V. Health Care |
|----|-----|------------------------|

| | | |
|----|------|-----------------------|
| 3: | SHPG | Shire plc Health Care |
|----|------|-----------------------|

[1] ""

[1] ""

[1] "#####"

[1] "##### cluster 14 ##### tau.tilde = 0.893 #####"

[1] "#####"

| Symbol | Name | Sector |
|--------|------|--------|
|--------|------|--------|

1: GOOG Alphabet Inc. Technology

2: GOOGL Alphabet Inc. Technology

[1] ""

[1] ""

[1] "#####"

[1] "##### cluster 15 ##### tau.tilde = 0.85 #####"

[1] "#####"

| Symbol | Name | Sector |
|--------|------|--------|
|--------|------|--------|

| | | |
|----------|--------------------|-------------------|
| 1: LBTYK | Liberty Global plc | Consumer Services |
|----------|--------------------|-------------------|

| | | |
|----------|--------------------|-------------------|
| 2: LBTYA | Liberty Global plc | Consumer Services |
|----------|--------------------|-------------------|

[1] ""

[1] ""

[1] "#####"

[1] "##### cluster 16 ##### tau.tilde = 0.757 #####"

[1] "#####"

| Symbol | Name | Sector |
|--------|------|--------|
|--------|------|--------|

| | | |
|---------|--------------------|-------------------|
| 1: LILA | Liberty Global plc | Consumer Services |
|---------|--------------------|-------------------|

| | | |
|----------|--------------------|-------------------|
| 2: LILAK | Liberty Global plc | Consumer Services |
|----------|--------------------|-------------------|

References

- Agarwal, A., Negahban, S., and Wainwright, M. J. (2012). Noisy matrix decomposition via convex relaxation: Optimal rates in high dimensions. *The Annals of Statistics*, pages 1171–1197.
- Ben Ghorbal, N., Genest, C., and Nešlehová, J. (2009). On the Ghoudi, Khoudraji, and Rivest test for extreme-value dependence. *Canadian Journal of Statistics*, 37:534–552.
- Borkowf, C. B. (2002). Computing the nonnull asymptotic variance and the asymptotic relative efficiency of Spearman’s rank correlation. *Comput. Statist. Data Anal.*, 39:271–286.
- Brechmann, E. C. (2014). Hierarchical Kendall copulas: Properties and inference. *Canadian Journal of Statistics*, 42:78–108.
- Cai, T. T. and Zhang, L. (2017). High-dimensional Gaussian copula regression: Adaptive estimation and statistical inference. *Statistica Sinica*, forthcoming.
- Chandrasekaran, V., Parrilo, P. A., and Willsky, A. S. (2010). Latent variable graphical model selection via convex optimization. In *Communication, Control, and Computing (Allerton), 2010 48th Annual Allerton Conference on*, pages 1610–1613. IEEE.
- Datta, A. and Zou, H. (2017). Cocolasso for high-dimensional error-in-variables regression. *Ann. Statist.*, forthcoming.
- Devlin, S. J., Gnanadesikan, R., and Kettenring, J. R. (1975). Robust estimation and outlier detection with correlation coefficients. *Biometrika*, 62(3):531–545.
- Ehrenberg, A. (1952). On sampling from a population of rankers. *Biometrika*, 39:82–87.

- El Maache, H. and Lepage, Y. (2003). Spearman's rho and Kendall's tau for multivariate data sets. In *Mathematical statistics and applications: Festschrift for Constance van Eeden*, volume 42 of *IMS Lecture Notes Monogr. Ser.*, pages 113–130. Institute of Mathematical Statistics, Beachwood, OH.
- Elton, E. J. and Gruber, M. J. (1973). Estimating the dependence structure of share prices —implications for portfolio selection. *The Journal of Finance*, 28:1203–1232.
- Embrechts, P., McNeil, A. J., and Straumann, D. (2002). Correlation and dependence in risk management: Properties and pitfalls. In *Risk Management: Value at Risk and Beyond (Cambridge, 1998)*, pages 176–223. Cambridge University Press, Cambridge.
- Engle, R. and Kelly, B. (2012). Dynamic equicorrelation. *Journal of Business & Economic Statistics*, 30(2):212–228.
- Fang, H.-B., Fang, K.-T., and Kotz, S. (2002). The meta-elliptical distributions with given marginals. *Journal of Multivariate Analysis*, 82:1 – 16.
- Fang, K.-T., Kotz, S., and Ng, K. W. (1990). *Symmetric Multivariate and Related Distributions*. Chapman & Hall, London.
- Fang, K.-T. and Zhang, Y.-T. (1990). *Generalized Multivariate Analysis*. Springer Verlag & Science Press, Beijing.
- Genest, C. and Nešlehová, J. (2012). Copulas and copula models. In El-Shaarawi, A. H. and Piegorsch, W. W., editors, *Encyclopedia of Environmetrics*. Wiley, Chichester, 2nd edition.
- Genest, C., Nešlehová, J., and Ben Ghorbal, N. (2011). Estimators based on Kendall's

- tau in multivariate copula models. *Australian & New Zealand Journal of Statistics*, 53:157–177.
- Gregory, J. and Laurent, J.-P. (2004). In the core of correlation. *Risk*, 17:87–91.
- Harville, D. A. (2008). *Matrix Algebra From a Statistician’s Perspective*. Springer Science & Business Media.
- Hoeffding, W. (1947). On the distribution of the rank correlation coefficient τ when the variates are not independent. *Biometrika*, 34:183–196.
- Hoeffding, W. (1948). A class of statistics with asymptotically normal distribution. *The Annals of Mathematical Statistics*, 19:293–325.
- Hua, L. and Joe, H. (2017). Multivariate dependence modeling based on comonotonic factors. *Journal of Multivariate Analysis*, 155:317–333.
- Hult, H. and Lindskog, F. (2002). Multivariate extremes, aggregation and dependence in elliptical distributions. *Advances in Applied Probability*, 34:587–608.
- Joe, H. (2015). *Dependence Modeling With Copulas*. CRC Press, Boca Raton, FL.
- Krupskii, P. and Joe, H. (2013). Factor copula models for multivariate data. *Journal of Multivariate Analysis*, 120:85–101.
- Krupskii, P. and Joe, H. (2015). Structured factor copula models: Theory, inference and computation. *Journal of Multivariate Analysis*, 138(Supplement C):53 – 73. High-Dimensional Dependence and Copulas.
- Kurowicka, D. and Joe, H., editors (2011). *Dependence Modeling: Handbook on Vine Copulae*. World Scientific Publishing, Hackensack, NJ.

- Ledoit, O. and Wolf, M. (2003a). Honey, I shrunk the sample covariance matrix. *UPF economics and business working paper*.
- Ledoit, O. and Wolf, M. (2003b). Improved estimation of the covariance matrix of stock returns with an application to portfolio selection. *Journal of Empirical Finance*, 10:603–621.
- Ledoit, O. and Wolf, M. (2004). A well-conditioned estimator for large-dimensional covariance matrices. *Journal of Multivariate Analysis*, 88:365–411.
- Lindeberg, J. (1927). Über die korrelation. In *Den VI skandinaviske Matematikerkongres i København*, pages 437–446, Copenhagen, Denmark. J. Gjellerup.
- Lindeberg, J. (1929). Some remarks on the mean error of the percentage of correlation. *Nordic Statistical Journal*, 1:137–141.
- Lindskog, F., McNeil, A. J., and Schmock, U. (2002). Kendall’s tau for elliptical distributions. In Bol, G., Nakhaeizadeh, G., Rachev, S. T., Ridder, T., and Vollmer, K.-H., editors, *Credit Risk: Measurement, Evaluation and Management*, pages 149–156. Springer.
- Liu, H., Han, F., Yuan, M., Lafferty, J., and Wasserman, L. (2012). High-dimensional semiparametric gaussian copula graphical models. *The Annals of Statistics*, 40:2293–2326.
- Ma, S., Xue, L., and Zou, H. (2013). Alternating direction methods for latent variable gaussian graphical model selection. *Neural Computation*, 25(8):2172–2198.
- Mai, J.-F. and Scherer, M. (2012). H-extendible copulas. *Journal of Multivariate Analysis*, 110:151–160.

- McNeil, A. J., Frey, R., and Embrechts, P. (2015). *Quantitative risk management*. Princeton Series in Finance. Princeton University Press, Princeton, NJ, revised edition. Concepts, techniques and tools.
- Nelsen, R. B. (2006). *An Introduction to Copulas*. Springer, New York, 2nd edition.
- Patton, A. J. (2006). Modelling asymmetric exchange rate dependence. *Internat. Econom. Rev.*, 47:527–556.
- Patton, A. J. (2012). A review of copula models for economic time series. *Journal of Multivariate Analysis*, 110(Supplement C):4 – 18. Special Issue on Copula Modeling and Dependence.
- Rémillard, B. (2013). *Statistical methods for financial engineering*. CRC Press, Boca Raton, FL.
- Rémillard, B. (2017). Goodness-of-fit tests for copulas of multivariate time series. *Econometrics*, 5:13.
- Rousseeuw, P. J. and Molenberghs, G. (1993). Transformation of non positive semidefinite correlation matrices. *Communications in Statistics - Theory and Methods*, 22:965–984.
- Schäfer, J. and Strimmer, K. (2005). A shrinkage approach to large-scale covariance matrix estimation and implications for functional genomics. *Statistical applications in genetics and molecular biology*, 4:32.
- Severini, T. A. (2005). *Elements of Distribution Theory*. Cambridge University Press.
- Sklar, A. (1959). Fonctions de répartition à n dimensions et leurs marges. *Publications de l’Institut de Statistique de l’Université de Paris*, 8:229–231.

- Stewart, G. W. (1969). On the continuity of the generalized inverse. *SIAM Journal on Applied Mathematics*, 17:33–45.
- Xue, L. and Zou, H. (2012). Regularized rank-based estimation of high-dimensional non-paranormal graphical models. *The Annals of Statistics*, 40(5):2541–2571.
- Zhao, Y. and Genest, C. (2017). Inference for elliptical copula multivariate response regression. Technical report, McGill University, Montréal, Canada.

NOTATION INDEX

d – number of random variables considered: X_1, \dots, X_d ;

\mathbf{T} – $d \times d$ Kendall τ matrix of X_1, \dots, X_d ;

$\boldsymbol{\tau}$ – vectorized version of \mathbf{T} ;

p – dimension of $\boldsymbol{\tau}$, $p := d(d-1)/2$;

$\hat{\boldsymbol{\tau}}$ – usual estimator of $\boldsymbol{\tau}$;

\mathcal{G} – partition of $\{1, \dots, d\}$ defining the block structure of \mathbf{T} or, equivalently, the clustering of X_1, \dots, X_d ;

K – number of clusters: $K = |\mathcal{G}|$;

\mathcal{G}_k – clusters forming the partition \mathcal{G} , that is $\mathcal{G} = \{\mathcal{G}_k, \dots, \mathcal{G}_K\}$;

$\mathcal{B}_{\mathcal{G}}$ – partition of $\boldsymbol{\tau}$ defining the blocks of \mathbf{T} ;

L – number of distinct blocks in \mathbf{T} , $L = |\mathcal{B}_{\mathcal{G}}| \leq K(K+1)/2$;

\mathcal{B}_k – blocks forming the partition $\mathcal{B}_{\mathcal{G}}$, that is $\mathcal{B}_{\mathcal{G}} = \{\mathcal{B}_1, \dots, \mathcal{B}_L\}$;

$\mathcal{T}_{\mathcal{G}}$ – space of matrices clustered according to $\mathcal{B}_{\mathcal{G}}$, in particular $\mathbf{T} \in \mathcal{T}_{\mathcal{G}}$;

Σ – covariance matrix of $\hat{\boldsymbol{\tau}}$;

$\hat{\Sigma}$ – basic estimator of Σ ;

$\mathcal{C}_{\mathcal{G}}$ – partition of Σ ;

$\mathcal{S}_{\mathcal{G}}$ – space of matrices clustered according to $\mathcal{C}_{\mathcal{G}}$, in particular $\Sigma \in \mathcal{S}_{\mathcal{G}}$.